Nucleic Acid Chaperone Activity of HIV-1 Nucleocapsid Protein: Critical Role in Reverse Transcription and Molecular Mechanism

JUDITH G. LEVIN,[*] JIANHUI GUO,[*‡] IOULIA ROUZINA,[†] AND KARIN MUSIER-FORSYTH[†]

[*]*Laboratory of Molecular Genetics, National Institute of Child Health and Human Development, National Institutes of Health, Bethesda, Maryland 20892*

[†]*Department of Chemistry, University of Minnesota, Minneapolis, Minnesota 55455*

[‡]Present Address: Shanghai Allist Pharmaceuticals, Zhangjiang, Shanghai 201203, People's Republic of China

Progress in Nucleic Acid Research and Molecular Biology, Vol. 80
DOI: 10.1016/S0079-6603(05)80006-6

0079-6603/05 $35.00

The HIV-1 nucleocapsid protein (NC) is a short, basic, nucleic-acid binding protein with two zinc finger domains, each containing the invariant CCHC metal ion binding motif. The mature protein (55 amino acid residues) is produced by proteolytic cleavage of the Gag precursor and is found in the interior of the virus particle, where it is tightly associated with genomic RNA. NC or the NC domain in Gag has multiple functions during the virus replication cycle, including genomic RNA packaging and virus assembly, primer placement on viral RNA, reverse transcription, and integration. Many of these functions rely on the nucleic acid chaperone activity of NC, i.e., the ability to catalyze nucleic acid conformational rearrangements that lead to the most thermodynamically stable structure.

In this chapter, we focus on recent biochemical and biophysical studies that examine the nucleic acid chaperone function of HIV-1 NC and its critical role in facilitating specific and efficient reverse transcription. We describe the effect of NC on individual steps in viral DNA synthesis and summarize what is known about NC structure, NC nucleic acid binding properties, and the contribution of the zinc fingers to chaperone activity. In addition, we discuss new evidence that provides a model to explain the mechanism of NC's nucleic acid chaperone activity at the molecular level.

I. Introduction

Retroviral nucleocapsid (NC) proteins are short, basic proteins containing one or two highly conserved zinc-finger domains, each having a common sequence motif $CX_2CX_4HX_4C$ (referred to as CCHC) (*1–4*). The basic residues and zinc fingers are both required for virus replication (reviewed in (*5–7*)). NC is an abundant component of the HIV-1 retrovirus and is associated with the two copies of genomic RNA in the interior of the mature virus particle (*7*). It is first synthesized as part of the Gag polyprotein precursor and then processed to its mature 55-amino acid form via site-specific proteolysis during virus maturation (*7–10*).

NC is a multifunctional nucleic acid binding protein, which plays a role in essentially every step of the retroviral replication cycle, from packaging and assembly to reverse transcription and DNA integration. NC (or the NC domain of the Gag precursor protein) is involved in dimerization of the RNA genome and stabilization of the dimer (*11–15*), genomic RNA packaging (*16*), tRNA primer placement (*17–24*), the initiation step (*25–27*), and minus- (reviewed in Refs. (*5, 6, 28*); for more recent references, see following text) and plus-strand (*29–32*) transfer events during reverse transcription. NC was also shown to alleviate pausing during reverse transcription (*33–37*) and to stimulate integration *in vitro* into a model target DNA (*38–41*).

While some NC functions such as genomic RNA packaging are believed to involve sequence-specific binding to nucleic acids (*16*); see also (*42–45*), NC

also displays more general nucleic acid binding properties. In addition, NC is a nucleic acid "chaperone" protein, catalyzing the rearrangement of nucleic acids into thermodynamically more stable structures (*6, 28, 46–48*). The chaperone activity of NC is critical to reverse transcription, a fact that has become evident as a result of the concerted effort of many researchers over the past decade (*5, 6, 28, 49*). However, the physical mechanism of NC's chaperone function remained unclear until recently.

During the past few years, detailed quantitative information has accumulated on the effect of NC on nucleic acid annealing and strand transfer both *in vitro* and during virus replication. As a result, an understanding of NC's chaperone activity at the molecular level is beginning to emerge. In particular, it now seems clear that the chaperone function of NC is determined by two independent activities: its abilities to destabilize nucleic acid secondary structure and to aggregate nucleic acids. Both activities are related to NC's nonspecific nucleic acid-binding capability. In addition, neither of these two NC activities relies on ATP hydrolysis. These properties of NC determine its main features as an ATP-independent stoichiometrically binding nucleic acid chaperone (*47, 50, 51*).

This chapter focuses on recent biochemical and biophysical studies examining the nucleic acid chaperone function of HIV-1 NC (also referred to as NCp7) in reverse transcription. Some of these studies were carried out with different forms of NC, including an extended 71- or 72-amino acid protein (NC71, which consists of NCp7 plus the spacer peptide SP2 or NC72, which is like NC71, but has one additional amino acid at its C-terminus, respectively; both forms are also termed NCp9) and truncated 42- and 44-amino acid versions [(12-53)NC and (12-55)NC]. We first describe what is known about HIV-1 NC's structure and nucleic acid binding properties. Next, we describe the steps in reverse transcription and discuss NC's effect on these events. In addition, the contribution of the zinc fingers to NC's nucleic acid chaperone activity will be extensively discussed. We will then summarize the current evidence for both components of NC's chaperone activity (i.e., nucleic acid destabilization and aggregation), and show how they may work together to yield an efficient mechanism for annealing complementary structured nucleic acids. This chapter will not cover NC's role in other steps of the retrovirus replication cycle, including RNA packaging (*16*), virus assembly (*7, 52*), integration (*38–41*), and recombination (*53*).

II. Structure and Nucleic Acid Binding Properties of HIV-1 NC

To understand NC's chaperone function in reverse transcription, it is important to review more generally what is known about NC's structure and nucleic acid binding properties. Much of the information on structure and

nucleic acid binding obtained to date has focused on NC binding to nucleic acids that are part of the Ψ packaging signal in the RNA genome (*16*). Thus, although not directly related to NC's role in reverse transcription, these studies will be included in the following discussion.

A. Specific and Nonspecific Nucleic Acid Binding

NC demonstrates complex, ionic strength-dependent nucleic acid binding properties (*20,54*). Although NC binds to many different nucleic acid sequences with varying affinity, sequence-specific binding was also observed (*16*); see also (*42–45*). In particular, NC appears to display specific, high-affinity binding to single-stranded UG- or TG-rich sequences (*44, 55, 56*). As will be described in more detail, GNG sequences within single-stranded loops are another preferred binding site (*57, 58*).

By contrast, binding of NC to some nucleic acids, such as primer $tRNA_3^{Lys}$, did not appear to be specific, as similar binding parameters were obtained for binding to $tRNA^{Phe}$ (*54*). The presence of base modifications also had little effect on the binding interaction (*54*). These results are consistent with the lack of a direct role of NC (or the NC domain of Gag) in specific selection of the tRNA primer from the pool of host cell tRNAs.

Early work using circular dichroism spectroscopy and Trp fluorescence quenching made it possible to monitor the binding of HIV-1 NC71 to poly(A) (*50*). These studies suggested that the extended 71-amino acid form of NC is capable of binding to poly(A) via at least two distinguishable binding modes that differ in site size. The occluded apparent site sizes (n_{app}) of $n = 8$ and $n = 14$ were measured under conditions of high and low protein:nt ratios, respectively. Interestingly, proteolytic cleavage of the COOH-terminal 14 amino acids from NC71 removed the apparent binding site size heterogeneity. The n_{app} for NC57 was found to be 6 to 7 and was independent of the protein:nt ratio (*59*). There is general agreement in the literature that the binding site size of the mature form of NC is 5 to 8 nucleotides (nt) (*10, 44, 50, 54, 59–62*).

The ability of NC to adapt to different nucleic acid structures and to bind them stoichiometrically suggests that the protein is likely to be highly flexible and mobile in the bound state. The latter conclusion is supported by numerous biophysical studies (*31, 63–67*) (R. J. Fisher *et al.*, personal communication). The substantial polyelectrolyte contribution to NC-nucleic acid binding suggested that the binding is driven to a significant extent by the release of Na^+ counterions (or other cations). This conclusion is supported by the strong salt dependence of NC binding to both DNA and RNA (*44, 45, 54, 62, 68*). These features of NC resemble nucleic acid binding by mobile nonspecific multivalent cationic ligands, such as polyamines, Mg^{2+} or Ca^{2+} ions, cobalt hexamine^{3+}, or polyLysine (*69, 70*). These nonspecific cationic ligands are known to be very efficient nucleic acid aggregating agents (*71*). Therefore, it is not

surprising that NC also displays efficient and nonspecific nucleic acid aggregating ability (*50, 72–74*). The implications of the aggregating activity of NC for the kinetics of annealing will be discussed in Section V.

B. Structural Studies

1. Zinc Finger Structures

HIV-1 NC is only 55 amino acids in length. It consists of a flexible polypeptide chain and two rigid CCHC-type zinc-binding domains, also referred to as zinc fingers or zinc "knuckles," which are connected by a four-amino acid basic peptide linker (*5, 6*) (Fig. 1). The structures of the individual zinc finger domains (*75–77*), as well as that of the full-length NC protein (*78, 79*) free in solution were determined by nuclear magnetic resonance (NMR) spectroscopy (for a more complete summary of early structural work, see (*80*)). Structures of the individual domains showed that the overall folds were very similar, although the C-terminal finger was shown to be conformationally more labile than the N-terminal finger (*75*), in accord with chemical probing experiments (*81*).

NMR studies of the full-length protein also showed that the zinc finger domains adopt similar three-dimensional folds (*78, 79*). Evidence for the existence of weak NOEs (nuclear Overhauser effect) between residues of the two fingers was also obtained by NMR, leading to the proposal that the zinc binding domains are proximal to each other (*78, 82*).

Fluorescence resonance energy transfer (FRET) data were also consistent with close spatial proximity of the two finger motifs (*83*). More recent NMR studies confirmed weak interfinger NOEs, but showed that the structure is very dynamic and suggested that the interactions are transitory (*84*). This conformational flexibility is consistent with NCs ability to recognize and interact with numerous nucleic acid structures, as will be discussed in more detail.

Among other interactions of NC zinc fingers with nucleic acids are the particularly strong stacking interactions of the bases with hydrophobic residues located in the second position of each zinc finger (*85–87*). More specifically,

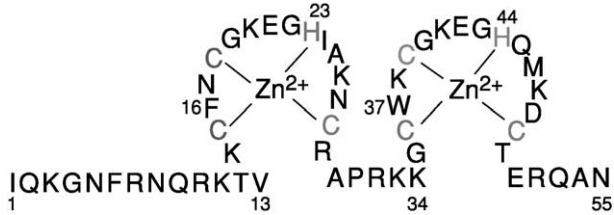

FIG. 1. Primary sequence of HIV-1 NC (NL4-3 isolate). The cysteine and histidine residues that chelate zinc are shown in gray.

stacking interactions between Phe16 in the N-terminal finger and Trp37 in the C-terminal zinc finger and nucleic acid bases have been detected by fluorescence spectroscopy and have been proposed to be a major driving force for NC-nucleic acid interactions (*45, 87*). This stacking was shown to be most efficient with G bases, especially when preceded by T (*42, 44, 45*). NMR data were also consistent with close interactions between Phe16 and Trp37 and purine residues (especially G) in single-stranded regions of SL2 and SL3 RNA hairpins derived from the HIV-1 genomic Ψ packaging signal (*57, 58*). In summary, based on both the fluorescence and structural studies performed to date, it appears that the CCHC-type zinc knuckle domains containing specifically positioned hydrophobic residues form an ideal binding surface for exposed G residues within nucleic acid sequences.

2. Binding of NC to the Ψ RNA Packaging Signal

Binding of NC to various stem-loop sequences (SL1, SL2, SL3, and SL4) that constitute the Ψ genomic RNA packaging signal was extensively investigated by a number of groups using a variety of biophysical techniques (*45, 55, 57, 58, 68, 88–93*). The reported K_d values and binding stoichiometries varied widely and appeared to be strongly dependent on the buffer conditions, the analytical technique used for the measurement, and the form of NC used in the study (see (*68*) for a comparison and thorough discussion of literature K_d values). Binding to SL2 and SL3 occurs with the highest affinity (K_d = 20–30 nM at physiological ionic strength), with weaker binding generally observed to SL1 and SL4 (K_d = 100–320 nM) (*68*). Another general conclusion was that DNA analogs of the RNA stem-loops bound less tightly to NC than the corresponding RNA (*45, 89, 91, 93*).

As has been mentioned, NMR structures of NC bound to the genomic packaging signals SL2 and SL3 were determined. Genomic RNA packaging involves the entire Gag protein *in vivo* and other regions of the RNA genome also contribute to packaging (*16*). Nevertheless, much insight into NC–nucleic acid interactions was derived from these structures (*57, 58*). Isothermal titration calorimetry established similar binding affinities between NC and these two stem-loops (100 nM and 170 nM for SL2 and SL3, respectively) (*57*), and under the conditions of the NMR studies, 1:1 binding stoichiometries were observed (*57, 58*). Although some features of NC binding are conserved between the two structures, other features of the complexes differ.

Substantial differences between the structures include the relative orientations of the N- and C-terminal zinc fingers and the mode of N-terminal helix binding, highlighting NC's adaptive RNA binding capability (*57*). In the SL3 RNA-NC complex, the N-terminal 3_{10} helix of NC, the structure of which is induced upon RNA binding, is packed against the N-terminal zinc knuckle and is therefore able to penetrate the widened major groove near the top of the

stem-loop. In contrast, the 3_{10} helix along with the N-terminal zinc knuckle interacts with a A-U-A base triple in the minor groove of SL2 RNA (*57, 58, 94*).

Common features of both NC-RNA complexes were also observed in the NMR structures. In both structures, the basic residues participate in the formation of intramolecular salt bridges that stabilize the folding of the zinc fingers and are also involved in forming electrostatic interactions with the RNA backbone (*57, 58*). Additional common features include the preferential binding of NC's zinc fingers to the single-stranded hairpin loop regions and the binding of the cationic N-terminal domain to the double-stranded stem of the hairpin. The binding and folding of this domain is most likely driven by the optimization of electrostatic interactions between the 3_{10} helix and the phosphate strands of the duplex.

C. Computational Studies

In addition to the experimental approaches already described, computational tools were also applied to gain insights into NC's nucleic acid binding properties, as well as to investigate the propensity of NC's zinc coordinating Cys residues to undergo electrophilic attack (*95, 96*). The results suggested that Cys residues of finger 2 were more reactive than those found in finger 1. In particular, Cys49 of finger 2 was predicted to be the NC site most labile to electrophilic attack, in good agreement with experimental observations (*81, 97*).

Computational methods that took into account the effect of the full protein environment, solvation, and nucleic acid binding were also used to gain insights into the SL2/SL3 RNA binding properties of HIV NC (*96*). These studies concluded that different basic residues make the most important contributions to the binding energy in each complex. Whereas Lys26 appeared to be the most important to the electrostatic binding of NC to SL2, a number of Lys and Arg residues in the N-terminal helix and finger were found to be critical for binding to SL3 (*96*). Future experimental studies will be needed to investigate these predictions further.

III. NC Function in Reverse Transcription

As has been mentioned, NC is a nucleic acid chaperone protein, which catalyzes the rearrangement of nucleic acids into thermodynamically more stable structures (*5, 6, 28, 46, 47, 49*). The chaperone activity of NC is critical for reverse transcription. Although the details of how NC facilitates nucleic acid rearrangement are not completely understood, a combination of biochemical assays and biophysical approaches by researchers studying a variety of oligonucleotide systems has led to our current understanding of

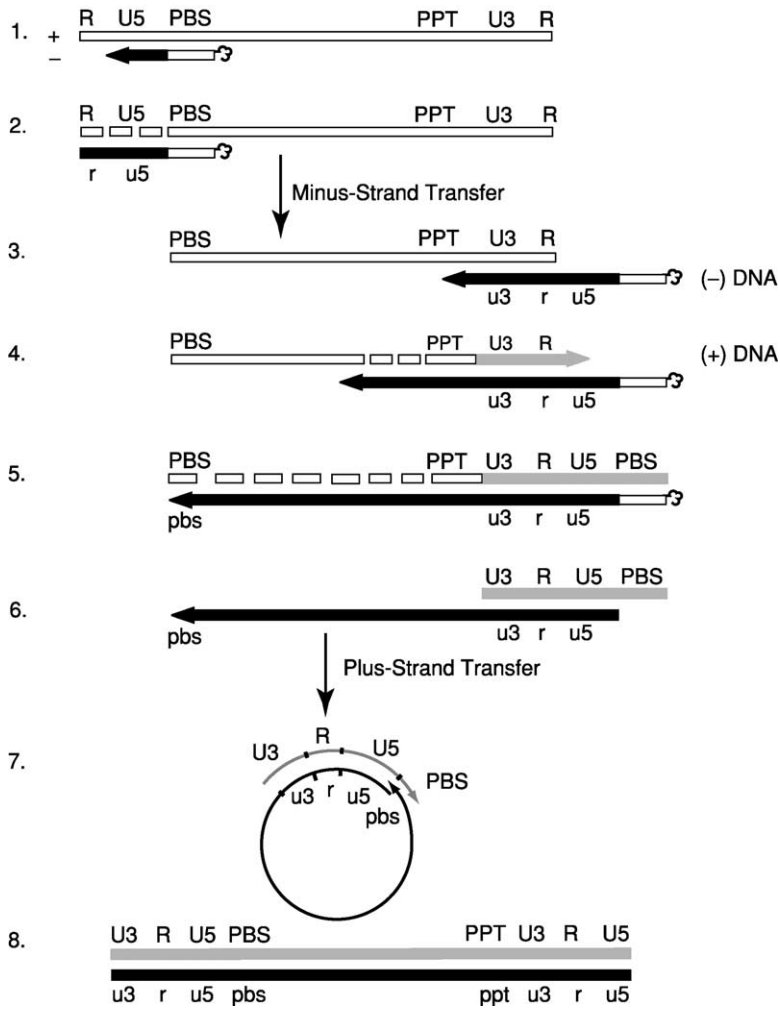

FIG. 2. Schematic diagram of the events in reverse transcription. *Step 1.* Reverse transcription is initiated by a cellular tRNA primer ($tRNA_3^{Lys}$, in the case of HIV-1), following annealing of the 3′ 18 nt of the tRNA to the 18-nt PBS near the 5′ end of the genome. RT catalyzes synthesis of (−) SSDNA, which contains copies of the R sequence and the unique 5′ genomic sequence (U5). *Step 2.* As the primer is extended, the RNase H activity of RT degrades the genomic RNA sequences that have been reverse transcribed. *Step 3.* (−) SSDNA is transferred to the 3′ end of viral RNA (minus-strand transfer). *Step 4.* Elongation of minus-strand DNA and RNase H degradation continue. Plus-strand synthesis is initiated by the 15-nt polypurine tract (PPT) immediately upstream of the unique 3′ genomic sequence (U3). (See text, (Section III. E–G for discussion of the role of a second PPT (i.e., the central PPT) in HIV-1 plus-strand synthesis. *Step 5.* RT copies the u3, u5, and r regions in minus-strand DNA, as well as the 3′ 18 nt of the

the mechanism of NC's chaperone activity, which will be described in Section V. In this section, we focus on NC's effect on specific steps in reverse transcription.

A. Overview

Reverse transcription consists of a complex series of events that culminates in the synthesis of a linear double-stranded DNA copy of the viral RNA genome (Fig. 2). This process is catalyzed by the virus-encoded enzyme, reverse transcriptase (RT), which, in the case of HIV-1, is a heterodimeric protein consisting of two subunits, p66 and p51 (*98, 99*) that are derived by proteolytic cleavage of the Gag-Pol precursor (*7, 100*). The catalytic sites reside in the larger subunit (N-terminal domain, RNA- and DNA-dependent polymerase activities; C-terminal domain, RNase H activity, which degrades the RNA moiety in an RNA–DNA hybrid), whereas the p51 subunit has a structural role only. The organization of the p66 polymerase domain has been described in relation to a right hand with fingers, palm, and thumb subdomains; in addition, there is a fourth element known as the "connection" subdomain (*98, 99*).

B. Initiation of Reverse Transcription

1. Primer Placement and Synthesis of Minus-Strand DNA

Before reverse transcription can begin, the 3′ 18 nt of a cellular tRNA must be annealed to the complementary 18-nt primer binding site (PBS) near the 5′ end of the viral RNA genome (Fig. 2, step 1). Each retrovirus uses a specific tRNA as primer: e.g., avian retroviruses, $tRNA^{Trp}$; murine leukemia virus (MuLV), $tRNA^{Pro}$; and lentiviruses such as HIV-1, HIV-2, simian immunodeficiency virus (SIV), equine infectious anemia virus (EIAV), and feline immunodeficiency virus (FIV), $tRNA_3^{Lys}$ (reviewed in (*101–103*)). Primer tRNAs were selectively incorporated into virions by interaction with the RT sequences

tRNA primer, thereby reconstituting the PBS. The product formed is termed (+) SSDNA. *Step 6*. RNase H removal of the tRNA and PPT primers from minus- and plus-strand DNAs, respectively. *Step 7*. Plus-strand transfer, facilitated by annealing of the complementary PBS sequences at the 3′ ends of (+) SSDNA and minus-strand DNA, is followed by circularization of the two DNA strands and displacement synthesis. *Step 8*. Minus- and plus-strand DNAs are elongated, resulting in a linear double-stranded DNA with a long terminal repeat (LTR) at each end. Viral RNA is shown by an open rectangle and minus- and plus-strand DNAs are shown by black and gray rectangles, respectively. The tRNA primer is represented by a short open rectangle (3′ 18 nt of the tRNA) attached to a "clover-leaf" (remaining tRNA bases). Minus- and plus-strand sequences are depicted in lower and upper case, respectively. The very short white rectangles represent fragments produced by RNase H cleavage of genomic RNA. (Adapted, with permission, from 262).

(*104–109*) in Gag-Pol (*109*). Recent findings demonstrated that for HIV-1 and Rous sarcoma virus (RSV) (but not MuLV), the cognate aminoacyl-tRNA synthetases were also encapsidated (*110–112*) through an interaction with Gag (*113*). It is now thought that select packaging of $tRNA_3^{Lys}$ involves formation of a complex consisting of Gag, Gag-Pol, and genomic RNA, which interacts with the tRNA primer and lysyl-tRNA synthetase, although the detailed mechanism is still not known (*113*) (also reviewed in (*102, 114*)).

Based on data from an early study of MuLV tRNA packaging, it was proposed that the NC protein (p10) or the NC domain in the Gag precursor, $Pr65^{Gag}$, was responsible for $tRNA^{Pro}$ placement on genomic RNA (*106*). Results of subsequent studies demonstrated that the annealing reaction was promoted by the NC domain in Gag *in vivo* (*23, 24*), although the mature NC protein also had this activity *in vitro* (*17, 18, 20, 22, 23, 63, 65, 115–117*). It was also reported that a functional initiation complex was formed *in vitro* only if NC catalyzed the annealing reaction (*25, 26*). However, two other groups subsequently found that complexes formed by NC or heat annealing were functionally equivalent (*27, 118*). The reason for this apparent contradiction is not clear.

Following primer placement, RT catalyzes extension of the tRNA primer until the 5′ terminus of genomic RNA is copied. This reaction generates the first product of reverse transcription, termed (−) strong-stop DNA ((−) SSDNA) (Fig. 2, step 2). Once template RNA sequences are reverse transcribed, they are degraded by the RNase H activity of RT (Fig. 2, step 2). Kinetic analysis showed that in the presence of the $tRNA_3^{Lys}$ primer, initiation involved two different modes of DNA synthesis: an initiation mode (distributive synthesis) followed by an elongation mode (processive synthesis) (*119–123*) (reviewed in (*124*)).

2. NC-induced Structural Changes in Primer tRNA

During tRNA primer/template annealing, significant structural changes in both RNAs were shown to occur (*125, 126*), and these will be discussed in more detail in the following text. The extent of tRNA unwinding that occurs upon NC binding in the absence of the HIV genome was also investigated (*22, 63, 117, 127, 128*). FRET experiments showed that NC binding to tRNA alone did not result in global acceptor-TΨC stem unwinding or strand separation (*22*). Heteronuclear NMR studies conducted with a truncated form of NC [(12–53)NC] and partially modified ^{15}N-$tRNA_3^{Lys}$ were also consistent with the lack of global $tRNA_3^{Lys}$ unwinding by NC (*63*). The imino groups are good probes of base pair (bp) melting and only small shifts were observed in some bp within the helical domains upon NC binding (e.g., G6:U67 near the base of the acceptor stem). The NMR studies were also consistent with slight destabilization of the tertiary core region of the tRNA (e.g., T54:A58 in the TΨC loop).

Lanthanide metals such as terbium have been shown to be excellent probes of metal binding sites in RNA and are also useful for probing conformational changes (see (*117*) and references therein). Terbium probing experiments of $tRNA_3^{Lys}$, in the absence and presence of NC, showed that disruption of the D-TΨC tertiary interaction occurred upon NC binding at low concentrations, followed by slight destabilization of the acceptor-TΨC minihelix at saturating NC (*117*). Thus, the lanthanide metal probing results were in excellent agreement with the NMR studies previously described. Taken together, these recent studies of $tRNA_3^{Lys}$, along with earlier one-dimensional NMR and Pb^{2+} cleavage studies conducted with yeast $tRNA^{Phe}$ (*129*), showed that in the absence of the genome, NC binding only slightly perturbs bp in the acceptor stem and core region of the tRNA.

In contrast to the studies already described, which were carried out in the absence of the genome, in the presence of the RNA genome and NC, the tRNA undergoes global acceptor stem unwinding and annealing to the complementary PBS sequence. During this process, significant structural changes in both RNAs were shown to occur, as will be described.

3. Extended Interactions between the Viral RNA Template and the tRNA Primer

Mutational analysis as well as enzymatic and chemical probing led to the proposal that an interaction between bases in the anticodon loop of $tRNA_3^{Lys}$ with an A-rich loop in HIV-1 RNA, approximately 10 nt upstream of the PBS, contributed to efficient minus-strand initiation (*119, 122, 125, 126, 130–137*). However, deletion of the four A residues in HXB2 RNA resulted in slightly reduced or similar amounts of (−) SSDNA synthesis over time (*21, 122, 134*). In addition, in the presence of NC, (−) SSDNA synthesis was stimulated by ~1.5- to 3-fold with a mutant NL4-3 template having a change of four A residues to four U residues (*27*), presumably because NC reduced RT pausing at this site (*122, 131, 134*).

Results from chemical probing *in vitro* and *in situ* (i.e., treatment of cells and virus with dimethyl sulfate prior to RNA extraction) revealed that the A-rich loop in the viral RNA of the HIV-1 HXB2 and NL4-3 strains does not have a stable interaction with the anticodon loop of $tRNA_3^{Lys}$ and, in fact, only the interaction between the PBS and the 3′ 18 nt of $tRNA_3^{Lys}$ could be detected (*138*). Nuclease mapping studies also concluded that the loop–loop interaction is less stable on the HIV-1 HXB2 genome than on the HIV-1 MAL isolate (*139*). In the latter case, the A-rich loop interaction was important for efficient initiation of reverse transcription (*119, 130, 138, 140*).

Other types of extended interactions between the tRNA primer and viral RNA were also reported. For example, interactions between U5 sequences (including the U5-inverted repeat (IR) stem) upstream of the PBS and the

TΨC loop in $tRNA^{Trp}$ were shown to enhance initiation of RSV DNA synthesis (*141–143*). An unusual interaction between the U5-IR loop of FIV RNA and the 5′ end of $tRNA_3^{Lys}$ was described as well (*144*). In addition, it was proposed that an interaction between the TΨC loop in $tRNA_3^{Lys}$ and a conserved 8-nt sequence downstream of the PBS (termed the "primer activation signal" or PAS) promotes efficient initiation of (−) SSDNA synthesis (*145, 146*). Data from other studies appeared to be at variance with this proposal (*27, 138, 140, 147*). Interestingly, after long passage in culture, a mutant with changes in the PAS motif and the PBS to allow recognition of $tRNA_{1,2}^{Lys}$, eventually reverted to a virus that retained the mutant PBS sequence and apparently optimized the PAS motif for interaction with the nonself primer. During passage, this virus also acquired a single change in a conserved residue in the RNase H domain of RT (*148*).

The initiation reaction is sensitive to the helical conformation of the nucleic acid duplexes (*149, 150*) that react with RT. For example, when an 18-nt DNA complementary to the PBS (D18) was used instead of $tRNA_3^{Lys}$, synthesis of (−) SSDNA bypassed the initiation mode entirely and proceeded exclusively in the elongation mode (*119, 120, 123, 151*). In the absence of NC, efficient (−) SSDNA synthesis *in vitro* required the presence of at least 24 nt downstream of the PBS in template RNA, when the primer was $tRNA_3^{Lys}$ or an 18-nt RNA complementary to the PBS (R18), but not D18; chimeric 18-nt RNA–DNA primers behaved like R18 or D18, depending on the identity of the sugar in bases contained in the 3′ segment of the oligonucleotide (*27*). Results obtained from melting studies and circular dichroism spectra of 18-nt primer:PBS duplexes indicated that priming efficiency was correlated with duplex conformation and thermostability. These findings in conjunction with *m*Fold analysis also suggested that the additional 24 bases might allow the template to assume a more favorable conformation for annealing to the RNA primers (*27*).

Interestingly, NC abrogated the requirement for the 24-nt downstream element only in $tRNA_3^{Lys}$-primed (−) SSDNA synthesis, but not in reactions primed by R18. This suggested that NC might stabilize extended interactions between the tRNA primer and the viral RNA template that are not possible with an 18-nt oligonucleotide primer. Mutational analysis of template RNA in regions upstream of the PBS supported the possibility that NC promotes an interaction between $tRNA_3^{Lys}$ (in particular, the 3′ arm of the anticodon stem and part of the variable loop) and nt 143–149 in NL4-3 viral RNA (*27*).

In earlier work (in the absence of NC), it was proposed that such an interaction would facilitate RT binding to the substrate by preventing steric clashes between RT and the nucleic acid duplex (*125, 152*). However, gel-shift experiments showed that in the absence of dNTPs, NC did not affect RT binding to complexes constituted with either wild-type RNA or mutant

templates having changes in nt 143–149. In contrast, in a similar assay in which there was also a +1 extension of the tRNA primer, NC stimulated incorporation with the wild-type, but not with the mutant templates (Y. Iwatani, J. Guo, R. J. Gorelick, and J. G. Levin, unpublished observations). Thus, it would appear that the NC stimulation was dependent on RT binding to the substrate and extension of the primer by at least 1 nt.

C. Minus-Strand Transfer

1. Properties of Reconstituted Minus-Strand Transfer Systems

Minus-strand transfer is required for elongation of (−) SSDNA and generation of a full-length minus-strand DNA copy of the RNA genome. During this step (Fig. 2, step 3), (−) SSDNA is translocated to the 3′ end of viral RNA in a reaction facilitated by base pairing of the complementary repeat (R) regions present at the 3′ ends of the DNA and RNA reactants (*153–155*) (reviewed in (*156*)). The R region contains the highly structured trans-activation response element (TAR) (Fig. 3A) and a portion of the poly(A)-signal hairpin (*157, 158*). Strand transfer during virus replication was originally thought to be intermolecular (i.e., transfer of (−) SSDNA to the other genomic RNA copy in the virion) (*159*), but subsequent work showed that it could also be intramolecular (i.e., transfer to the original RNA template) (*160–162*). In addition, minus-strand transfer was found to be highly efficient *in vivo*, since significant amounts of (−) SSDNA did not accumulate in infected cells (*163*) (D. C. Thomas and V. K. Pathak, personal communication).

The first studies on minus-strand transfer *in vivo* were performed with systems containing relatively unstructured viral donor and acceptor RNA templates (5′ and 3′ ends of the genome, respectively) and no NC (*154, 155, 164*). This work demonstrated that during (−) SSDNA synthesis, the 5′ end of the template must be degraded by the RNase H activity of RT to allow subsequent strand transfer (*154, 155, 165*) and was in accord with the conclusion reached from *in vivo* replication studies with MuLV RNase H-minus mutants (*166–169*). (More detailed discussion of the RNase H requirement will be given.) In addition, it was reported that strand transfer was more efficient as the homology region of the two templates was lengthened (*154*) (see also (*169a*) and following text).

2. NC Promotes the Specificity and Efficiency of Minus-Strand Transfer

Using reconstituted systems, many laboratories showed that NC increases the efficiency of retroviral minus-strand transfer: HIV-1 (*170–185*); FIV (*186*); MuLV (*187–189*); and RSV (*190*). Formation of stable nucleoprotein

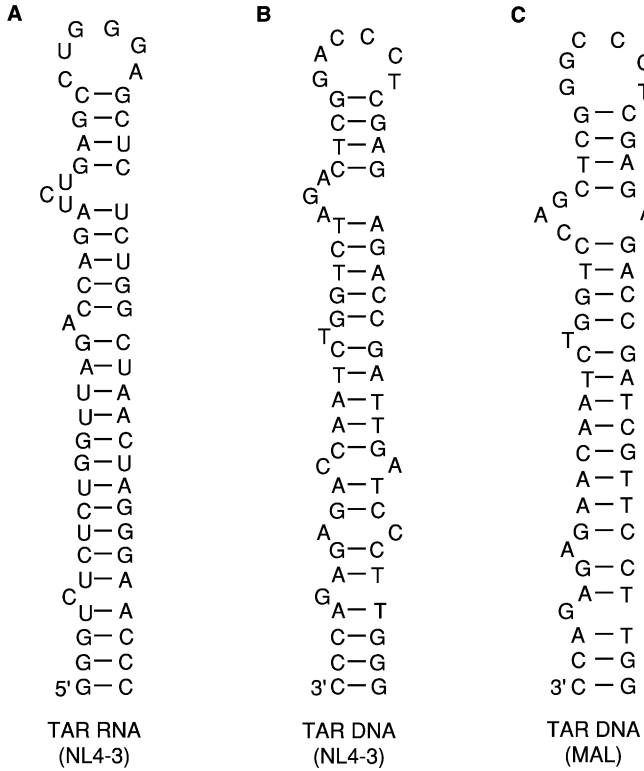

FIG. 3. Structures of TAR RNA and TAR DNA. The NL4-3 TAR RNA structure (A) is based on the RNA structures given in (*157, 158*). The TAR DNA structure (B) is shown as the complement of NL4-3 TAR RNA, although other conformers are also formed ((*185*) and references therein). The TAR DNA from the MAL isolate (C) is shown as drawn in (*202*).

complexes *in vitro*, consisting of RT, NC, and donor and acceptor RNA templates, promoted HIV-1 minus-strand transfer, but only if both RNAs were present during formation of the complex (*191*).

NC plays a major role in minus-strand transfer by facilitating annealing of the complementary R regions (*20, 46, 177–179, 192–196*) and accelerates this reaction by as much as 3000-fold (*193*). Since highly structured RNA and DNA molecules must be annealed in the case of HIV-1 (i.e., the TAR RNA and DNA stem-loops comprising 2/3 of R) (Fig. 3), the reaction is dependent on the ability of NC to destabilize secondary structures that might interfere with the intermolecular reaction (*178, 179, 193, 196–199*). In fact, unfolding of these structures was thought to be rate-limiting in annealing reactions with DNA

and RNA molecules containing most of R, i.e., all of TAR plus an additional 22 nt (*193*).

The destabilizing activity of NC makes it possible for NC to perform another function in minus-strand transfer, i.e., inhibition of a competing, nonspecific self-priming reaction (*21, 175, 176, 178–181, 185, 189, 195, 200, 201*). Thus, NC also increases the specificity of minus-strand transfer. In HIV-1 reactions, self-priming resulted from intramolecular formation of TAR-induced fold-back structures at the 3′ end of (−) SSDNA, which were elongated in the presence of RT. Isolation of self-priming products (SP products or SP DNAs) from polyacrylamide gels, followed by cloning and sequence analysis, demonstrated that these products were minus-strand DNAs with plus-strand extensions (*176*). Self-priming occurred only with (−) SSDNAs that had a 5′ overhang as well as a base-paired 3′ end and was not detected if there was a truncation of TAR DNA (*176, 185, 201*).

It was reported that self-priming in the absence of acceptor could be blocked by NC alone (*175*), possibly because under the conditions used, increasing amounts of NC inhibited overall reverse transcription. Other investigators found that NC had little effect on self-priming in the absence of the acceptor (*181, 185, 195, 201*). However, if acceptor RNA and NC were *both* present, self-priming was dramatically reduced (*21, 175, 176, 178–181, 185, 188, 195, 200, 201*) and a concomitant increase in strand transfer resulted. This is the expected outcome when the hybrid formed by (−) SSDNA and acceptor RNA is more stable than either of the nucleic acid reactants and any SP DNAs that might be formed ((*185*); see also following text).

Interestingly, if NC was added together with a 70-fold excess of short DNA oligonucleotides complementary to the 3′ end of (−) SSDNA, self-priming was effectively blocked even in the absence of acceptor RNA (*181, 201*). These short DNAs mimic the small RNA fragments generated during RNase H degradation of sequences at the 5′ end of the viral genome (*180, 181, 201*).

More recently, both absorbance (*202*) and fluorescence spectroscopy (*195, 202*) were used to directly examine NC's effect on the structure of the TAR DNA hairpin (Fig. 3). The absorbance measurements showed that NC had a greater effect on melting of TAR DNA than on melting of TAR RNA (*202*). This result was consistent with the greater stability of the RNA hairpin. Using a TAR DNA hairpin doubly-labeled at the 3′ and 5′ ends with an appropriate donor/acceptor pair, steady-state and time-resolved FRET measurements were also performed (*195, 202, 203*). In the absence of acceptor RNA, three populations of TAR DNA hairpin conformations were observed in solution. NC binding enhanced fraying of the ends of TAR DNA and shifted the distribution of hairpin conformations toward the more open structures, but did not completely unfold the hairpin. This result was consistent with the almost complete inability of NC to inhibit self-priming under these conditions.

In contrast, in the presence of the complementary TAR RNA, the majority of the TAR DNA molecules were present in an unfolded state (i.e., the annealed state) (*195*). These biophysical studies help to explain why significant inhibition of self-priming was only observed in the presence of acceptor RNA (*181, 185, 195, 201*).

3. Influence of NC on RNase H Cleavage of Viral RNA during (−) SSDNA Synthesis and Removal of 5′ Terminal Donor RNA Fragments

During minus-strand DNA synthesis, RT encounters three types of substrates, which are bound to RT in different binding modes and have different RNase H cleavage patterns: (i) DNA primer recessed on long viral RNA template (polymerase-dependent cleavage); (ii) RNA fragment recessed on long minus-strand DNA (polymerase-independent cleavage); and (iii) a blunt-end RNA–DNA hybrid containing the 5′ RNA terminal fragment (14 to 18 nt), formed when RT reaches the 5′ end of the genome and completes synthesis of (−) SSDNA (a special case of polymerase-independent cleavage).

In the polymerase-dependent mode, the polymerase active site of RT is positioned over the 3′ OH of the replicating DNA primer and cleavage is coupled to DNA synthesis. The spatial separation (18 nt) between the polymerase and RNase H active sites (*98, 99*) determines the initial site of cleavage (*154, 155, 164, 204–214*). This type of cleavage is sometimes referred to as a "−18 cut" or "primary RNase H cleavage."

Polymerase-dependent cleavages are not sufficient to completely degrade the genomic RNA template ((*211, 215*); reviewed in (*216*)). Rather, to facilitate further degradation of the template, RT binds in the polymerase-independent mode. In this case, cleavage is not coupled to DNA synthesis and RT is repositioned away from the 3′ terminus of the DNA (*155, 207, 209–211, 215, 217–221*), resulting in the alignment of the polymerase active site with the 5′ terminus of viral RNA (*212, 221–227*).

An ordered series of cleavages occurred during this process (*222, 223*), but each cleavage event was independent of the others and had its own characteristic rate (*224*). The products of polymerase-independent cleavages (also termed "secondary cleavages" or "secondary cuts") ranged in size from 8 to 10 nt, but could also be as small as 5 nt (*155, 177, 180, 207–209, 217, 219, 222–224, 226, 228*). Thus, this activity ensures that large fragments produced during minus-strand DNA synthesis are further degraded and ultimately dissociated from the DNA strand (reviewed in (*216*)).

Although RNase H cleavages remove most of the genomic RNA fragments generated during minus-strand DNA synthesis, initially, 5′ terminal RNAs ranging in size from 14 to 18 nt remain annealed to the 3′ end of (−) SSDNA. This creates a blunt-end substrate, which is cleaved with low efficiency by

RNase H (*155, 164, 180, 209, 212, 224, 228*). In addition, the terminal hybrids have high melting point temperature (T_m) values that are above 37°C (ranging from 40.5 (14 nt) to 50.3°C (18 nt)), yet the RNAs must be removed to allow minus-strand transfer to occur. Since NC destabilizes secondary structures, a possible role for NC in terminal fragment removal was investigated by several laboratories.

In an early study conducted in the absence of NC and acceptor RNA, a substrate consisting of a 3′ terminal 65-nt DNA, complementary to the 5′ end of viral RNA, was annealed to a long 5′ HIV-1 RNA template. RNase H cleavage yielded terminal fragments predominantly 17 to 18 nt in size, but also included a smaller amount of 12- to 16-nt fragments; these fragments were not dissociated from the DNA (*Escherichia coli* RNase H was able to cleave the remaining hybrid) (*212*). Another group reported that in reactions lacking acceptor RNA and NC, a terminal 14-nt fragment was dissociated from (−) SSDNA (further cleavage by *E. coli* RNase H was not observed after reactions were first treated with heparin to block additional HIV-1 RNase H activity); it was suggested that the kinetic advantage of hairpin formation resulted in destabilization of the terminal hybrid. When NC was added, these investigators found that the 14-nt RNA remained annealed to (−) SSDNA, suggesting that NC stabilized the terminal hybrid (*180*). It was also reported that with blunt-end substrates, NC stimulated overall RNase H activity and had its greatest effect on secondary cleavages, generating products of 8 to 10 nt (*183, 224*). The apparent discrepancies in some of these results could be due to differences in experimental conditions, which can affect the extent of secondary RNase H cleavage (J. Guo and J. G. Levin, unpublished observations).

In strand transfer reactions (in the presence of NC and acceptor RNA), it was found that if the R region was 19 or 20 nt, overall cleavage of donor RNA as well as secondary cuts were increased (*171, 183, 229*) and the secondary cleavages occurred with a greater efficiency than strand transfer (*183*). In fact, RNase H secondary cleavage was found to be the rate-limiting step for strand transfer in the presence or absence of NC (*155, 171*). With a substrate having a homology of 45 nt, secondary cleavage products accumulated more rapidly than did transfer products in the absence of NC. In contrast, in reactions with NC, strand transfer occurred before the secondary cleavages at the 5′ end of the donor were initiated. These observations supported the proposal that in the presence of NC, 5′ terminal fragments are displaced by acceptor RNA through an acceptor-initiated invasion mechanism (*182, 183*) (see following text).

To directly address the issue of fragment removal in the context of minus-strand transfer, reactions in which the substrate consisted of a small 5′ terminal RNA heat-annealed to a 128-nt (−) SSDNA were performed (J. Guo, T. Wu, Y. Iwatani, R. J. Gorelick, and J. G. Levin, in preparation). The presence of a

terminal RNA fragment did not have any effect on the efficiency of minus-strand transfer, indicating that the RNA had to have been removed under the conditions of the assay. Results obtained from RNase H cleavage assays suggested that in the presence of acceptor RNA, NC destabilized the RNA-(−) SSDNA hybrid, resulting in dissociation of the RNA. The data also led to the prediction that NC might mediate removal of the terminal RNA fragments in the absence of RNase H activity. Indeed, when this was tested, the rates and extents of minus-strand transfer were found to be very similar in assays with RNase H-minus or wild-type RTs.

These results were in accord with observations previously cited using a complete minus-strand transfer system in which donor RNA was included (*182, 183*). The data also directly demonstrated that secondary RNase H cleavage is not absolutely required for 5′ terminal RNA removal: NC nucleic acid chaperone activity alone is sufficient to catalyze this reaction (J. Guo, T. Wu, Y. Iwatani, R. J. Gorelick, and J. G. Levin, in preparation).

To explain the effects of NC on secondary RNase H cleavage of template RNA, it was proposed that RT and NC form a complex (*171, 229–231*), possibly through a zinc-finger dependent interaction (*231*) of NC with the RNase H domain of RT (*171, 229, 231*). The exact nature of such interactions has not been established. Alternatively, the data suggest a possible explanation based on NC function as a nucleic acid chaperone, which would not require a direct interaction of NC with RT, but would be mediated by NC–nucleic acid interactions.

In this case, NC would either stabilize or destabilize the RNA–DNA hybrid, depending on which activity could lead to a more stable nucleic acid conformation. Thus, it appears likely that as RNase H degrades the donor RNA template to relatively large or even moderately sized fragments during (−) SSDNA synthesis, NC stimulates annealing of these fragments to minus-strand DNA, thereby providing additional substrates for further cleavage. This would occur as long as the RNA–DNA hybrid had a high T_m value and was more thermodynamically stable than either of the nucleic acids alone. As a consequence, secondary RNase H cleavage would increase, as was found experimentally. However, when the RNA fragments annealed to (−) SSDNA are relatively short (as is the case for the 5′ terminal hybrids) and acceptor RNA is present, NC destabilization of these hybrids is sufficient to dissociate the RNA, without participation of RNase H. Here, the hybrid formed by (−) SSDNA and acceptor RNA is more stable (97-bp homology) than small hybrids with homologies of 25 bp or less.

4. Nucleic Acid Structural Determinants in Minus-Strand Transfer

To understand NC function in minus-strand transfer, there are several questions that one may ask. For example, is the length of the homology region (R) a major determinant for efficient strand transfer? How is the ability of NC

to facilitate strand transfer influenced by the secondary structure and thermostability of (−) SSDNA and acceptor RNA? What effect, if any, does NC have if these nucleic acid intermediates lack significant secondary structure?

As has been mentioned, the extent of homology between minus-strand DNA and acceptor RNA was initially considered to be a crucial factor for ensuring the success of strand transfer, since a more stable hybrid is presumably formed when there is a high degree of complementarity (*154*). For example, in an *in vitro* HIV-1 system, the presence of the entire R region in both (−) SSDNA and acceptor RNA appeared to be responsible, at least in part, for the observed high level of strand transfer, compared with levels obtained when the complementarity consisted of only a portion of R (*185*). Mutational analysis of genomic RNA performed *in vivo* demonstrated that most of the minus-strand transfers occurred after completion of (−) SSDNA synthesis (i.e., transfer is facilitated by base pairing of the full-length R regions, resulting in the inheritance of the 5′ R region by progeny virus); only a small percentage of the transfers occurred before full-length DNA was made (*232–238*).

Additionally, the rates of annealing of DNA oligonucleotides with sequences from the HIV-1 R region were increased if longer regions of homology were present, although complementarity of at least 12 to 14 bases was sufficient for specific and efficient annealing to occur (*196*). Similarly, studies with MuLV replication systems demonstrated that strand transfer was more efficient when the homology consisted of the entire R sequence (*239*), or a long region of complementarity at or near a defined site in an internal region of the genome (*240*). However, at least 12 (*239*) or 14 (*240*) bases of homology were sufficient to obtain a positive result in these assays. Other *in vitro* and *in vivo* studies with HIV-1 (*162, 176, 182, 183, 185, 232*) or with EIAV (*241*) also showed that although the size of the complementary region could play some role, it was not always a primary determinant of efficient minus-strand transfer or recombination.

Instead, what turned out to be critical in most cases is the relationship between nucleic acid structure/thermostability and NC nucleic acid chaperone activity. In one study, this issue was systematically investigated by designing a series of truncated (−) SSDNA and acceptor RNA constructs, which were used to measure minus-strand transfer and self-priming in an HIV-1 reconstituted system. In this system, full-length (−) SSDNA was 128 nt and contained all of R and 31 nt from the 5′ end of U5; full-length acceptor RNA was 148 nt and contained 94 nt from R and 54 nt from the 3′ end of U3 (*176, 185, 195*). The experimental findings were correlated with enzymatic mapping and *m*Fold analysis (*185*).

(−) SSDNAs with truncations in U5 and the 3′ bases of R were quite stable and, in reactions with and without NC, these DNAs were able to undergo high levels of self-priming; as expected (see preceding text), this led to low levels of

minus-strand transfer. When truncations were extended to bases within the TAR region (*176, 185*), little or no self-priming occurred, but the lack of self-priming did not necessarily result in efficient strand transfer. The stability of acceptor RNA was also a major determinant (*185*). Thus, if the RNA had a high ΔG value, NC was unable to catalyze formation of the RNA–DNA duplex, regardless of whether (−) SSDNA had a low ΔG value. These findings demonstrated that NC nucleic acid chaperone activity was most effective when both (−) SSDNA and acceptor RNA were only moderately structured. If the reactants were relatively unstructured, NC had little or no effect on the reaction. Taken together, the results led to the conclusion that NC-mediated efficient strand transfer depends on a delicate thermodynamic balance between structures in (−) SSDNA and acceptor RNA and the stability of the strand transfer duplex (*185*).

Although NC exerts its effect on both RNA and DNA secondary structures, minus-strand transfer appeared to be especially sensitive to RNA structure and, to a somewhat lesser extent, to the structure of (−) SSDNA. This is consistent with the observation that NC catalyzes limited melting of the TAR RNA stem-loop compared with destabilization of TAR DNA ((*202*); see also preceding text). Other studies also showed that RNA structure is a crucial determinant of efficient minus-strand transfer. For example, the activity of RNA constructs composed of sequences from several regions within the HIV-1 genome were tested in an assay for internal strand transfer. The results showed that NC significantly stimulated the rate and extent of internal strand transfer with sequences from more structured regions such as *gag-pol*, but had little effect when sequences were derived from the relatively unstructured *env* region (*184, 242*).

Similar conclusions were reached from *in vitro* and *in vivo* studies of recombination with HIV-1 (*243–245*), EIAV (*241, 246*), and MuLV (*37*) systems. In other work, stabilizing mutations in the poly(A) hairpin (consisting of sequences at the 3′ end of R and the 5′ end of U5) and mutations in the loop sequence in TAR were reported to inhibit efficient HIV-1 minus-strand transfer in the presence of NC (*247*). Moreover, it was proposed that base-pairing interactions between the complementary loop sequences in (−) SSDNA and acceptor RNA might enhance minus-strand transfer (*247*).

The issue of secondary structure was also examined in studies of HIV-1 NC's effect on annealing. In one approach to addressing this question, a series of model RNAs with increasing ΔG values was designed and the kinetics of annealing to complementary DNAs was determined. NC had its greatest effect when structured RNAs were used in the assay (*199*). Another group investigated the rate of annealing of a series of short complementary DNA oligonucleotides containing sequences from the R region (see preceding text). In the absence of significant secondary structure and low thermodynamic stability,

NC had little effect on annealing, whereas when the reactants were structured, annealing was stimulated by NC. Interestingly, when the DNAs shared very limited homology, NC reduced the rate of annealing and it was suggested that, as a consequence, this behavior might serve as a mechanism to increase the fidelity of recombination (*196*). Additionally, in a study of NC-mediated strand exchange (*46*), the structure of acceptor RNA as well as the length of a single-stranded DNA region abutting an RNA–DNA hybrid (containing the donor RNA to be displaced) were found to affect the efficiency of the reaction (*247a*).

In one of the studies that addressed the influence of HIV-1 acceptor RNA structure on the efficiency of minus-strand transfer, there was an apparent discrepancy that turned out to be of unusual interest (*185*). Two similar RNAs with part of the TAR sequence, one having 70 nt (RNA70, $\Delta G = -22.9$ kcal/mol) and the other having 50 nt (RNA50, $\Delta G = -14.9$ kcal/mol), were assayed for their activity in a strand transfer assay with the same 50-nt (−) SSDNA. Paradoxically, RNA70 had significantly more activity, despite the fact that its overall thermodynamic stability was greater than that of the smaller RNA50.

Closer examination of the structures predicted by *m*Fold (*248, 249*) showed that local structure at favorable NC binding sites (a run of G or UG residues) (*31, 44, 45, 58, 250, 251*) appeared to differ. In the case of RNA70, the presumptive binding site contained a relatively weak helix with three G-U wobble pairs and only two G-C bp, whereas the analogous site in RNA50 contained three G-C bp as well as a destabilizing G-G mismatch. It was suggested that the weak stem-loop in RNA70 provided a more favorable site for initiation of annealing than the more stable stem-loop in RNA50. These findings led to the proposal that stability of local structure, rather than overall thermodynamic stability, is a primary determinant of NC nucleic acid chaperone activity. This concept is in accord with conclusions reached in a kinetic study of $tRNA_3^{Lys}$ annealing to the 18-nt PBS in an HIV-1 genomic RNA transcript ((*116*); see also following text) and also in another study of recombination *in vivo* (*245*).

5. Mechanisms of Minus-Strand Transfer

As has been discussed, the mechanism originally proposed to explain the minus-strand transfer step in reverse transcription envisioned end terminal transfer from the 3′ end of full-length (−) SSDNA to the 3′ end of genomic RNA (acceptor RNA), in a reaction involving base pairing of the complementary R regions (Fig. 2; (*153–155*); reviewed in (*156*)). Evidence was also presented indicating that a major pathway for *in vitro* minus-strand transfer is through an NC-stimulated acceptor-initiated invasion mechanism, which was favored in cases where the RNA and DNA reactants shared a long R homology region (*182, 183*).

It was proposed that (i) primary RNase H cleavages at internal sites in the donor RNA create gaps, which allow the acceptor RNA to displace the donor

fragments and anneal to the complementary region in (−) SSDNA, upstream of its 3′ end; and (ii) DNA synthesis proceeds by a branch migration mechanism, which ultimately leads to terminus transfer, in the absence of secondary RNase H cleavages to remove 5′ terminal RNA fragments annealed to (−) SSDNA (see preceding text) (*182, 183*). This model is based, in part, on experiments with blocking oligonucleotides, which showed that almost normal levels of the full-length transfer product could be formed with substrates having a long region of complementarity, even if the 5′ terminal segment of donor RNA could not be cleaved by RNase H. In contrast, blocking internal cleavage sites strongly reduced strand transfer. The region around the base of the TAR stem-loop was found to be a preferred site for cleavage.

It should be noted that the acceptor-initiated transfer mechanism is a specific version of a more general model for retroviral (HIV, EIAV, MuLV) recombination, which occurs during minus-strand DNA transfer at internal sites in the genome (see review in (*53*) and references therein; for more recent papers, see (*241, 242, 244–246, 252, 253*)).

D. Elongation of Minus-Strand DNA

Following minus-strand transfer, RT catalyzes elongation of (−) SSDNA and continues to degrade viral RNA template sequences that have already been copied (Fig. 2, steps 4 and 5). A major problem that RT must confront during polymerization has to do with the fact that the retroviral RNA genome is a single-stranded RNA. RNAs are known to form stem-loop structures and these have the potential to significantly reduce the rate and extent of polymerization.

In fact, RT pausing at secondary structures in the RNA template was documented in numerous *in vitro* studies of MuLV (*34, 37, 254, 255*) and HIV (*33, 35, 36, 173, 174, 176, 177, 191, 256–262*) RTs. RT overcomes this problem with the help of NC's nucleic acid chaperone activity, which destabilizes secondary structures that might impede enzyme movement across the genome (*33–37*). Pausing on an RNA template was also correlated with homopolymeric rC and rG tracts (*258, 263*). There are conflicting reports as to whether NC has an effect on RT processivity (*173, 230, 258, 259*). However, it is clear that the ability of NC to reduce RT pausing leads to increased efficiency of minus-strand viral DNA synthesis (*33–37*).

E. Plus-Strand DNA Synthesis

1. Initiation of Plus-Strand DNA Synthesis by the Polypurine Tract Primer

As elongation of minus-strand DNA proceeds, RT initiates synthesis of plus-strand DNA (Fig. 2, steps 4 and 5). The primer is a short purine-rich RNA sequence, known as the polypurine tract (PPT) or 3′ PPT, whose 3′ end

abuts the 5′ boundary of U3 in genomic RNA, and is generated by precise RNase H cleavage at the U3 boundary (for references before 1993, see (*216*); also see (*213, 221, 264–269*). Cleavage at the 5′ end of the PPT is less precise (*216*). The template for plus-strand DNA synthesis is minus-strand DNA with the tRNA primer still attached to its 5′ terminus.

As is the case for minus-strand DNA synthesis, the first plus-strand DNA product made is a short DNA, termed (+) strong-stop DNA ((+) SSDNA). In addition, like initiation of minus-strand DNA synthesis (see preceding text), a specific helical conformation of the primer-template hybrid (in this case, the hybrid formed by the PPT RNA-minus-strand DNA template) is required for interaction with RT ((*265, 270–274*); see also (*269*)).

Interestingly, HIV-1 and other lentiviruses have a second PPT priming site, which is located in the central portion of the genome within the integrase coding region. In HIV-1, this PPT, known as the central or cPPT, has the same sequence as the 3′ PPT (*7, 275, 276*). Mutational analysis showed that the cPPT sequence was important for efficient HIV-1 replication (*277, 278*). It was suggested that by having two PPT sites, plus-strand DNA synthesis can proceed before elongation of minus-strand DNA is complete, thereby resulting in more rapid DNA synthesis (*275*). Priming from other upstream sites in the HIV-1 genome was also reported (*279*) (D. C. Thomas and V. K. Pathak, personal communication). (Further discussion of priming by the two PPTs is given in the following text.)

2. Termination of (+) Strong-Stop DNA Synthesis

The major termination site for (+) SSDNA synthesis occurs at the nucleotide preceding the 3′ methyl A at position 58 of the tRNA primer (*153, 280, 281*), thereby reconstituting the PBS sequence in (+) SSDNA. (Note that this tRNA modification is present in all retroviral tRNA primers (*103*).) Unexpectedly, several studies showed that for HIV-1, termination at position 58 is not absolute and also occurs at two other positions: at a position in the anticodon loop of $tRNA_3^{Lys}$, which leads to a dead-end product; and at a pseudouridine at position 55 (*29, 30, 32, 282, 283*). Termination at position 58 and 55 was also detected in an endogenous assay with detergent-treated HIV-1 particles (*30*). This suggested that synthesis beyond the methyl A to position 55 is not an *in vitro* artifact (*30*) and might result from undermodification at this position in some of the molecules in the $tRNA_3^{Lys}$ population (*29, 30, 32*). Results from one study indicated that when the base at position 58 was transcribed, there was a high error rate, resulting in the incorporation of a dA, even in the presence of NC (*29*).

It was originally reported that, for certain HIV-1 strains (e.g., NL4-3 (*284*)), complementarity between nt 56 to 58 in the tRNA primer and the first three bases downstream of the PBS would allow productive plus-strand

transfer beyond position 58 (*30*). Later work supports this possibility and also uncovered a strong consensus sequence, termed the "primer overextension sequence" (POS), which is adjacent to and downstream of the PBS and is found only in the genomes of lentiviruses and spumaviruses (*32*).

F. Plus-Strand Transfer

1. Properties of Reconstituted Plus-Strand Transfer Systems

Synthesis of (+) SSDNA is followed by plus-strand transfer (Fig. 2, step 7), which is required for subsequent elongation of plus-strand DNA. During this step, the complementary PBS sequences at the 3′ ends of minus-strand DNA and (+) SSDNA are annealed and form a circular intermediate.

To investigate the mechanism of plus-strand transfer, *in vitro* systems were designed with a minus-strand DNA template (all of (−) SSDNA or sequences from the 5′ end) covalently attached to $tRNA_3^{Lys}$ or to an 18-nt RNA containing the 3′ 18 nt of the tRNA primer (donor DNA); a DNA primer to direct synthesis of (+) SSDNA and an acceptor DNA having sequences from the 3′ end of minus-strand DNA were also included (*29, 30, 32, 282, 283, 285*). Substitution of an 18-nt DNA PBS primer (*29, 283*), or synthetic $tRNA_3^{Lys}$ (*29, 282, 283, 286*) for the RNA moiety attached to the donor minus-strand DNA failed to support strand transfer. Successful strand transfer was mediated by annealing of the 18-nt complementary PBS sequences at the 3′ termini of (+) SSDNA and the minus-strand DNA acceptor. NC stimulated overall plus-strand transfer (*29, 30, 32*), but in systems where the DNA substrates were mostly unstructured, the effect was only two- to three-fold (*30, 32*) or not detectable at all (*285*).

However, it was possible to demonstrate that NC has a crucial role in two of the individual reactions that contribute to the overall strand transfer process: (i) removal of the tRNA primer attached to the minus-strand DNA donor, and (ii) stimulation of the annealing reaction. Actually, these two reactions are related, since without removal of the primer, annealing of the complementary PBS sequences cannot take place. This is the same strategy that dictates the requirement for removal of the 5′ terminal fragments during minus-strand transfer (see preceding text).

2. NC Requirement for Maximal Removal of the tRNA Primer

Removal of the $tRNA_3^{Lys}$ primer requires the RNase H activity of RT. Analysis of sequences at HIV-1 circle junctions (*287–290*) and identification of degradation products generated in model HIV-1 RNase H assays (*208, 291, 292*) unexpectedly demonstrated that primary cleavage did not occur at the

tRNA–DNA junction. Rather, cleavage occurred between the 3′ terminal rA of the primer and the penultimate rC. This results in covalent attachment of an rA to the 5′ end of the minus-strand DNA donor template and formation of a 17-nt hybrid consisting of 3′ tRNA and (+) SSDNA sequences. Similarly, initial cleavage at the 3′ end of the MuLV $tRNA^{Pro}$ primer also occurred between the terminal rA and rC; however, in this case, the rA was ultimately cleaved away from the 5′ end of minus-strand DNA (*208, 221, 267, 293, 294*). In contrast to the HIV-1 and MuLV primers, the $tRNA^{Trp}$ primer used by the avian retroviruses is removed intact by a single RNase H cleavage at the RNA–DNA junction (*208, 295*).

The RNase H requirement for primer removal was also investigated in the context of *in vitro* HIV-1 plus-strand transfer. Thus, if the RNase H-minus RT mutant E478Q (*296*) was used, plus-strand transfer was markedly reduced (*29*) or completely abolished (*30, 285*), unless *E. coli* RNase H was added *in trans* (*30, 285*). However, several lines of evidence clearly showed that the initial cleavage event alone was not sufficient for successful plus-strand transfer. For example, when the E478Q mutant was incubated in reactions containing Mn^{2+}, initial cleavage could occur, but strand transfer was still not observed (*285*). In addition, kinetic studies demonstrated that the primary cleavage product (17 nt for an 18-nt RNA PBS sequence; 75 nt for $tRNA_3^{Lys}$) appeared at very early times (1 to 3 min), whereas the final cleavage product (8 or 9 nt for the 18-nt RNA; 67 nt for $tRNA_3^{Lys}$) was more prominent at late times (10 to 30 min) (*30, 285*). This lag was correlated with the delay in synthesis of the plus-strand DNA transfer product (*30, 285*). Collectively, these findings indicated that secondary RNase H cleavage is required for plus-strand transfer, presumably because of the high T_m value of the remaining 17-nt RNA–DNA hybrid (*29, 30, 285*).

Retroviral RTs possess RNA displacement activity (MuLV, (*297, 298*); HIV-1, (*282, 298, 299*)), but to date, NC is known to stimulate only the activity of MuLV RT (*297*). In the case of HIV-1, the 17-bp hybrid cannot be removed by HIV-1 RT alone (*29, 30, 285*). The hybrid is expected to dissociate spontaneously, however, if it is shortened by additional RNase, H cleavages to less than 11 bp (*30*). In contrast, removal of the $tRNA^{Trp}$ primer, which does not require secondary RNase H cleavage, is most likely due to an unwinding activity associated with avian retroviral RT (*295*).

Since HIV-1 NC chaperone activity destabilizes RNA–DNA hybrids with moderate stability, a role for NC in tRNA primer removal was considered. Substrates that model the intermediates formed *after* the initial cleavage event has taken place (Fig. 4) were used in an assay having plus-strand transfer as the read-out. It was found that in the absence of RNase H activity, NC could displace the 17-nt hybrid in a dose-dependent manner (*30*). However, the presence of wild-type RT and NC increased the amount of strand transfer

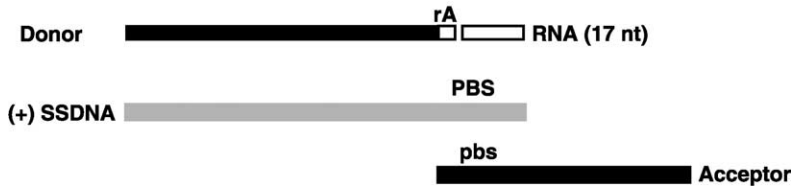

FIG. 4. Nucleic acid plus-strand transfer intermediates used in assay for complete $tRNA_3^{Lys}$ removal following primary RNase H cleavage event. The donor DNA template with a single rA at its 5′ end, a 17-nt RNA representing the 17 bases remaining at the 3′ end of $tRNA_3^{Lys}$ after the initial RNase H cleavage, (+) SSDNA, and minus-strand acceptor DNA template are shown. (+) SSDNA and the minus-strand donor and acceptor DNAs are represented by gray and black rectangles, respectively; the rA attached to the donor DNA and the 17-nt RNA are indicated by open rectangles. (Adapted, with permission, from (*30*)).

achieved with either one alone (*30*). This finding strongly suggested that both secondary RNase H cleavage and NC contribute to successful plus-strand transfer during virus replication.

3. NC Requirement for Efficient Annealing

In addition to its pivotal role in primer removal, NC nucleic acid chaperone activity is critical for facilitating efficient annealing in plus-strand transfer (see preceding text). The ability of NC to promote hybridization of complementary DNA sequences has been known for many years (*20, 46, 50, 192, 194, 196*). Annealing of the complementary 18-nt PBS sequences during plus-strand transfer was investigated in reactions containing a synthetic (+) SSDNA and a short minus-strand DNA acceptor oligonucleotide (*30*). With increasing concentrations of NC, there was a dramatic stimulation of the rate and extent of annealing (e.g., a 20-fold increase in rate at the highest NC concentration used, compared with the rate in the absence of NC). Semi-logarithmic plots of the kinetic data were consistent with the possibility that the reaction follows second-order kinetics, i.e., a bimolecular reaction, with rate-limiting nucleation followed by fast zippering ((*50*) and references therein; also, see following text).

It is of interest that the NC stimulatory effect on the rate of annealing of the complementary R regions (*178, 193*) was ~8-fold greater than the rate of annealing of the complementary PBS regions (*30, 178*). This difference in annealing kinetics reflects the requirement for destabilization of the highly structured TAR sequence within R, as opposed to the more weakly structured 18-nt PBS (*178*). An NMR study of an 18-nt (−) PBS DNA mimic was performed in the absence and presence of HIV NC to investigate the

mechanism of annealing in plus-strand transfer (*31*). The data showed that addition of NC lowered the T_m of the (−) PBS DNA and destabilized a stable hairpin structure formed by the DNA, consistent with NC's function as a nucleic acid chaperone in this reaction.

Studies using fluorescently labeled DNA oligonucleotides derived from the (−) and (+) PBS sequences were consistent with only weak NC-induced transient melting of the hairpins (*300*). The 18-mer (−) PBS hairpin was shown to bind 3 NC molecules. The TGTTC loop sequence appeared to bind one NC, since substitution of the loop with a hexaethyleneglycol tether decreased the number of NC's bound by one. Moreover, substitution of the G residue in the loop with a T resulted in a similar decrease, a finding that is consistent with NC's preference for GT-rich sequences. The double-stranded stem and a single-stranded tetranucleotide extension were proposed to each bind one NC molecule as well. Similar results were obtained for the (+) PBS sequence.

Time-resolved fluorescence spectroscopy, however, showed only a very weak destabilizing effect of NC on these hairpins, much less than was observed for TAR DNA, as has been described. Interestingly, fluorescence correlation spectroscopy (FCS) measurements along with gel electrophoresis analyses suggested that NC promoted the formation of (−) PBS and (+) PBS homodimers, as well as (−) PBS/(+) PBS heterodimers (*300*). The dimerization was proposed to occur via the formation of "kissing" complexes held together by the partial self-complementarity of the loop nucleotides. The appearance of these binary kissing complexes was dependent on the salt concentration, which explains why dimers were not observed in the (−) PBS NMR experiments previously described (*31*).

4. How NC Nucleic Acid Chaperone Activity Affects Plus-Strand Transfer

It is of interest to consider how the relationship between NC nucleic acid chaperone activity in the primer removal and annealing reactions influences the ultimate success of plus-strand transfer. Formation of the DNA duplex is favored over stabilization of the RNA–DNA hybrid. This is to be expected since RT-catalyzed elongation of the plus- and minus-strands in the DNA duplex results in production of an extended duplex with a significantly greater number of bp than is found in the 17-bp hybrid. Thus, as more of the (+) SSDNA is annealed to the minus-strand acceptor, less (+) SSDNA is available to anneal to the tRNA primer, and eventually the 17-bp hybrid will dissociate (*30*). A parallel situation exists during NC-mediated minus-strand transfer: NC removes 5′ terminal RNA fragments initially annealed to (−) SSDNA so that (−) SSDNA can anneal to the acceptor RNA and form a more stable RNA–DNA hybrid (see preceding text).

G. Completion of Reverse Transcription

During extension of plus-strand DNA, RT pauses at sites of secondary structure in the minus-strand DNA template (*177, 255, 256, 258*). NC-mediated destabilization of these structures leads to increased efficiency of plus-strand DNA synthesis (*33*). Pausing also occurs at homopolymeric runs of dA and dT (*256, 258, 301, 303*). The final product of reverse transcription is a linear, double-stranded DNA with a long terminal repeat (LTR) at both ends of each strand (Fig. 2, step 8), which is ultimately integrated into the host genome (*7*). To complete elongation of minus- and plus-strand DNAs and duplication of the LTRs, synthesis must include strand displacement of a relatively large region of duplex DNA (HIV-1, 636 bp (*284, 304*); MuLV, 594 bp (*305*); FIV, 361 bp (*306*); and avian sarcoma virus, 300 bp (*307*)). DNA displacement synthesis is critical for generating a duplex DNA that is integration-competent. In early studies with purified enzymes, it was shown that in addition to an RNA–DNA unwinding activity (*295, 308*), avian myeloblastosis RT can unwind a DNA duplex and catalyze limited strand displacement synthesis (*308, 309*). Strand displacement activity was also detected in melittin-treated avian retrovirus particles (*310*).

Initial work with HIV-1 RT revealed that the enzyme could displace up to 50 nt of DNA (*302, 311*). Maximum activity was obtained with the p66/p51 RT heterodimer (*311*). However, the relatively short length of the DNA displaced in these experiments did not reflect the requirement to displace a much longer region of DNA during virus replication. Subsequently, it was shown that HIV-1 RT could displace 634 nt of DNA containing the natural LTR sequences (*312*). This activity was stimulated several-fold by the *E. coli* single-stranded binding protein and human replication protein A, but surprisingly, not by HIV-1 NC (*312*).

Studies of HIV-1 plus-strand elongation during virus infection showed that priming from both PPTs resulted in formation of unintegrated linear DNA with a single-stranded central flap, indicating that plus-strand DNA synthesis is discontinuous (*275, 276, 279*) (D. C. Thomas and V. K. Pathak, personal communication). This was also reported for EIAV (*313*) and avian retroviral (*314, 315*) plus-strand DNA synthesis (for a more complete discussion, see (*316*) and references therein). Experimental evidence supported the following mechanism for HIV-1 (*275, 317, 318*): Priming from the cPPT begins at the first downstream base and continues to the 3′ end of the linear viral DNA. After plus-strand transfer, the DNA strand generated by priming from the 3′ PPT is elongated past the cPPT and is followed by strand displacement (*319*) of the cPPT-initiated DNA segment over a region of ~99 bases (size of central flap); synthesis is terminated when RT reaches the region known as the central termination sequence (*317*). A more recent study demonstrated that synthesis

of the entire central flap could be achieved *in vitro*. NC increased the rate of synthesis and it was suggested that NC stabilizes structural fluctuations within the flap (*318*).

MuLV RT is also capable of efficient strand displacement activity with nonviral (*320*) and LTR-containing (*321*) DNA templates. Interestingly, using an RNase H-minus MuLV RT and an LTR-containing template, it could be shown that MuLV NC had a small (approximately 2-fold) stimulatory effect on DNA displacement activity compared with activity in the absence of NC (*297*). A mechanistic study of DNA strand displacement catalyzed by HIV-1 or MuLV RT can be found in (*322*).

IV. Role of NC's Zinc Fingers

A. Importance of Zinc Finger Motifs for Virus Replication and RNA Packaging

The strict conservation of the CCHC zinc-binding array in all retroviruses containing NC zinc fingers (the orthoretrovirus class) (*1–4*) and the absence of other common zinc binding motifs, such as the CCCC or CCHH sequences found in steroid hormone receptors and transcription factors (*323*), respectively, strongly suggested a critical functional role for these structures in retrovirus replication. Indeed, this prediction was confirmed in extensive studies on the importance of the retroviral NC zinc finger structures for multiple events during virus replication (*324–332*). Although both retroviral zinc fingers contain the CCHC array, the amino acid sequences between the zinc-coordinating residues are similar, but not identical, and both motifs are required for production of replication-competent virus (*330, 333–335*). The requirement for both zinc fingers was also shown for RSV (*336*) and for SIV (*337*).

The relative importance of the position of each finger was demonstrated by constructing NC proteins with two first fingers (designated NC 1-1), two second fingers (designated NC 2-2), and a finger switch variant (designated NC 2-1) (*333*). The NC 2-2 and NC 2-1 variants were replication-defective. However, the 1-1 mutant reverted to a wild-type phenotype three weeks postinfection, indicating that it was initially able to replicate at a very low level. Thus, only those mutants containing the authentic finger 1 sequence in the N-terminal position were replication-competent, thereby highlighting the importance of the first finger in viral spread as well as the correct context surrounding the zinc-coordinating residues.

More subtle mutations of HIV NC's highly conserved CCHC motif to sequences that do not abolish zinc binding were also made (*82, 332, 338,*

339). These mutants were composed of combinations of CCHC, CCCC, and CCHH. Although these changes did not significantly affect RNA binding *in vitro* (62), they had varying effects on viral RNA packaging and replication. Compared to the wild-type protein (designated CCHC/CCHC), the CCCC/CCCC, CCHH/CCCC, and CCHH/CCHH mutants were the most defective in RNA packaging, containing <15% of the wild-type levels of genomic RNA (332). With respect to virus replication, mutants with modifications in the first (N-terminal) zinc finger were found to be replication-defective even if they had a wild-type second finger (82, 332, 338, 339). In contrast, modifications in the second finger were generally well tolerated as long as the N-terminal finger was wild-type (332). This analysis supports the conclusion that the first finger exerts a greater influence on replication than does the second finger.

Interestingly, some mutations in the CCHC residues conferred a replication-defective phenotype that could not be explained simply by a reduction in RNA packaging alone (324–328, 330–332). These results provided the first clue that the CCHC zinc-coordination center is required for other NC functions in addition to packaging. One of these functions was shown to be viral DNA synthesis (HIV, (332, 338–340); MuLV, (331, 341, 342)). These studies also demonstrated that NC maintains the integrity of viral DNA ends (331, 332, 338, 339, 342), which is required for successful integration. Detailed analysis of zinc finger involvement in reverse transcription reactions is presented in the next section.

B. Role of Zinc Fingers in Reverse Transcription

1. Role of Zinc Fingers in tRNA Primer Annealing

Although the role of the zinc fingers in retroviral replication has been demonstrated, their function in specific nucleic acid chaperone activities is less clear and it is only recently that answers to this critical question are beginning to emerge. In a study of the effect of single, double, or triple NC mutations on $tRNA_3^{Lys}$ placement onto the PBS in the context of the virus, it was concluded that mutations flanking the first zinc finger maximally inhibited primer placement, whereas mutations within the two fingers resulted in only moderate or no inhibition (343). Many of the early studies investigating the importance of the zinc finger motifs in tRNA primer annealing *in vitro* used deletion mutants of NC that also eliminated potentially important basic residues. These studies led to contradictory conclusions regarding the role of the zinc fingers in primer annealing (17, 20, 115, 344).

tRNA annealing studies performed with a mutant form of NC (SSHS NC), wherein all six cysteine residues involved in chelating zinc were changed to serine, showed that the rate of annealing was 3- to 4-fold faster than the rate obtained in the presence of wild-type NC under all conditions tested (116,

117). Although the SSHS mutant is unable to coordinate zinc, this protein maintains all of the basic residues that contribute to electrostatic interactions with nucleic acids. Annealing studies with polyLys confirmed that nonspecific electrostatic interactions were sufficient for annealing tRNA to the PBS *in vitro*, as the same rate enhancement was observed for polyLys as for SSHS NC (*117*).

To understand the lack of a requirement for zinc finger structures in tRNA annealing, a detailed kinetic analysis was carried out. This study showed that 10- to 100-fold of the rate enhancement observed in the NC-catalyzed tRNA annealing reaction was due to NC-induced destabilization (*116*). The remainder of the overall $\sim 10^5$-fold enhancement was a result of NC's ability to facilitate new duplex nucleation, an effect that was related to NC's nucleic acid aggregating activity (discussed in more detail in the following text). Although wild-type NC was more effective than SSHS NC at melting secondary structures, the mutant was predicted to be a better nucleating agent. Thus, the similar rate enhancement observed for the two proteins in the tRNA annealing reaction was most likely due to a fortuitous balance between these two activities.

Although the zinc fingers do not appear to play a major role in facilitating tRNA annealing, both structure-probing and NMR studies showed subtle differences in the tRNA conformational changes induced by wild-type and mutant protein binding. In particular, terbium cleavage assays showed that the A-form helical regions of the tRNA underwent enhanced cleavage due to destabilization by wild-type NC, while SSHS NC did not induce this effect (*117*). As expected, the pattern of terbium cleavage observed with polyLys was similar to that of SSHS NC.

Using NMR spectroscopy, altered effects on tRNA structure upon mutation of NC's N-terminal finger were also observed (*64*). In accordance with the terbium cleavage assays previously described, wild-type NC was shown to shift the imino proton resonances in a manner that was consistent with destabilization of the A-form helical domains of the tRNA. When the zinc-binding His residue in the first finger was mutated to Cys [Cys23 (12–53)NC], fewer variations in imino resonances were observed, especially in the acceptor stem domain.

2. Role of Zinc Fingers in Minus-Strand Transfer

In contrast to the results obtained with tRNA annealing, studies with SSHS NC showed that the zinc finger structures play a critical role in facilitating efficient minus-strand transfer *in vitro* and are essential for blocking TAR-induced self-priming reactions (*178*). SSHS NC had a small stimulatory effect on minus-strand transfer, presumably due to retention of the basic residues in the mutant protein. However, stimulation of strand transfer was

~8-fold greater with wild-type NC than with the mutant. Similar findings were reported for an FIV minus-strand transfer system (*186*). A very small effect of HIV-1 zinc finger mutations on minus-strand transfer was noted in an early study (*170*). However, these experiments were conducted under low salt conditions, which would favor nonspecific ionic protein–nucleic acid interactions and minimize contributions of the hydrophobic zinc fingers (*178*). Identification of an RT reaction dependent on NC zinc finger function provided the first *in vitro* assay system to investigate a role for the zinc fingers in events occurring during the infectious process (*178*).

Minus-strand transfer was also determined in the presence of the CCHH and CCCC series of NC mutants. Mutations exclusively in the first finger were generally more detrimental to minus-strand transfer than mutations exclusively in the C-terminal finger (*179*). Similarly, using mutants 1-1, 2-1, and 2-2 (*333*), it was shown that with 1-1 NC, minus-strand transfer was ~50% of the wild-type level and self-priming was significantly reduced. In constrast, strand transfer was not detectable with the 2-1 and 2-2 mutants (*179*). With a weakly structured Env substrate, 2-1 NC had somewhat greater enhancing activity than 1-1 and wild-type NC's, which displayed the same levels of activity in an assay for internal strand transfer. With a more structured substrate such as Gag-Pol, 1-1 and wild-type were equally efficient in stimulating internal strand transfer and compared with these two NCs, the activity of 2-2 was only slightly reduced (*184*). Collectively, these results demonstrated that the greatest differential effect of the position-switch mutations was observed in assays with reactants having the most stable structure, i.e., containing the TAR RNA or DNA stem-loops.

To gain further insights into zinc finger–TAR RNA interactions, hydroxyl-radical footprinting of NC bound to a 59-nt TAR RNA hairpin was carried out (*345*). These studies showed different patterns of cleavage for wild-type and mutant constructs. Whereas binding of wild-type NC resulted in significant protection from cleavage, binding of SSHS NC and CCCC/CCHC NC resulted primarily in enhanced cleavage of the RNA backbone. These data support an altered mode of binding of the NC variants that is clearly highly dependent on the zinc finger architecture.

In general, the results of biochemical experiments were in good agreement with those observed in virus replication and infectivity assays previously described ((*332, 333, 338, 339*); see discussion of this point in (*179*)). Not surprisingly, virions carrying the SSHS/SSHS mutation in the NC domain of Gag were also noninfectious and had defects in encapsidation of genomic RNA and viral DNA synthesis (*178*). Defects in strand transfer events were shown for HIV-1 virions with the H23C and H44C zinc finger mutations. Interestingly, the effect was more severe with the H23C mutant, which has the change in the N-terminal zinc finger (*339*). (In an earlier study, it was found that the

H44C mutant eventually reverted to the wild-type genotype (*332*).) In contrast, another group reported that minus- and plus-strand transfer were unaffected by the H23C mutation (*338*). However, both studies concluded that the major defect in the H23C virus was the inability of the mutant NC to protect viral DNA ends.

Study of two MuLV zinc finger mutants (Y28S and H34C) demonstrated that mutant virions were unable to replicate and synthesize detectable levels of plus-strand DNA; in addition, accumulation of mutant minus-strand DNA was about 10-fold lower than that of the wild-type control (*341*). Dependence of MuLV replication and viral DNA synthesis on the zinc finger domain was also shown in other work focusing on parameters that affect template switching (internal minus-strand transfer) in a cell-culture assay (*37*).

3. Role of Zinc Fingers in Specific Steps Required for Minus- and Plus-Strand Transfer

As has been discussed, 5′ terminal RNA fragments must be removed so that minus-strand transfer can occur (Fig. 2, step 2). SSHS NC inhibited this reaction, as did other zinc finger mutants; 1-1 NC had close to wild-type activity (J. Guo, T. Wu, Y. Iwatani, R. J. Gorelick, and J. G. Levin, in preparation). In the case of tRNA primer removal during plus-strand transfer (Fig. 2, step 6), experiments with SSHS NC demonstrated that both RNase H activity and zinc coordination were required for *maximal* removal of the tRNA primer. This result is in contrast with the observation that NC alone (with an active N-terminal finger) was sufficient for removal of terminal fragments annealed to (−) SSDNA. Primer removal with the position switch mutants followed the same pattern as that for overall minus-strand transfer ((*179*); see preceding text).

Annealing of the complementary R regions during minus-strand transfer was also dependent on the presence of the zinc fingers. However, this dependence was diminished when reactions were performed in a low salt environment (*20*). Interestingly, SSHS NC could stimulate annealing, but the rate was reduced by ~8-fold (*178*). The CCHH-containing mutants generally catalyzed high rates of annealing, whereas the mutants with CCCC in the first or second finger and mutants 2-1 and 2-2 were inactive; 1-1 NC activity was nearly as high as that of wild-type (*179*). Somewhat similar results were obtained in annealing reactions with model RNAs (ΔG values lower than that of TAR-containing RNAs): wild-type >1-1 ≅ 2-1 > 2-2 ≅ no NC (*199*). Interestingly, annealing in plus-strand transfer did not require the zinc fingers and SSHS NC had the same stimulatory effect as the wild-type protein (*178*). These observations led to the realization that the zinc fingers are critical for transient destabilization of complex nucleic acid structures (e.g., TAR), but not for simpler structures (e.g., 18-nt PBS) (*178*).

4. Role of Zinc Fingers in Elongation of Minus-Strand DNA and Strand Displacement Reactions

Using an HIV-1 RNA template (874 nt), it was found that efficient synthesis of full-length minus-strand DNA required the zinc fingers. However, the small effects of the 1-1, 2-1, and 2-2 NC mutants were equivalent (*35*). Similar results were obtained with an MuLV RNA template containing a 24-nt stem-loop structure ($\Delta G = -8.7$ kcal/mol) that includes sequences from the PPT. HIV-1 NC significantly reduced RT pausing in the vicinity of the stem-loop and this activity was zinc-finger dependent. The position switch mutants had about 2-fold less activity than did wild-type NC, but no differences could be detected among the three mutants, presumably because the structure destabilized by NC had only moderate stability. Deletion of either zinc finger, mutation of the 6 Cys residues to Ala or modification of the last 3 Cys residues with N-ethylmaleimide reduced NC activity even further, but binding of N-ethylmaleimide to all 6 Cys residues had the most detrimental effect (*34*).

It is of interest that NC-stimulated MuLV RNA and DNA displacement activities also require the presence of the zinc fingers. The activity of a zinc-finger deletion mutant was close to that observed in the absence of MuLV NC. However, the rate of displacement was affected to a greater degree than the extent of the reaction (*297*).

C. NMR Studies with NC Zinc Finger Mutants

Solution NMR studies have led to some insights into altered nucleic acid binding and chaperone activity of NC zinc finger variants. For example, the NMR structure of mutant Cys23(13–64)NC showed that the subtle His23 to Cys change altered the conformation of the first finger and changed the spatial proximity of the two fingers, thereby eliminating the interfinger interactions (*82*). This structural change may be responsible for the altered tRNA binding properties of the mutant protein previously described. The effect of another subtle change in the N-terminal finger (Cys28 to His) was also investigated by NMR (*346*). This study suggested that the conformations of His28(12–53)NC were more similar to those of native (12–53)NC than to those of the Cys23 mutant previously described.

The NMR structure of the C-terminal zinc finger peptide, (35–50)NC, containing a single His44 to Ala mutation was also determined (*67*). This change removed one of the zinc-coordinating residues and resulted in a significant decrease in binding to the $(TG)_3$ model oligonucleotide. Although NMR studies showed a similar overall folding pattern to that of the native peptide, the mutation led to increased flexibility of residues close to the mutated position. Moreover, modeling studies suggested that the mutant lacks the hydrophobic cleft found in wild-type NC, which is critical for nucleic acid

binding. This structural data may explain the decrease in viral RNA packaging observed for a His 44 to Ala mutant NC protein *in vivo* (*334*).

V. Mechanism of NC's Nucleic Acid Chaperone Activity

A. Dual Effect of NC on Nucleic Acid Duplex Stability

The two main features of NC–nucleic acid interactions described in Section II (zinc finger binding to single-stranded regions and cationic residue binding to the phosphate backbone) have two distinct and opposite effects on duplex stability. As a cationic ligand binding via nonspecific polyelectrolyte interactions with phosphates, NC has a duplex-*stabilizing* effect. This effect was similar to the effect of increasing solution ionic strength (*347–349*) and resulted from improved screening of duplex strands by high salt or multivalent cations. Duplex stabilization produced by the addition of NC increased as the salt concentration decreased. Thus, for double-stranded nucleic acids in low (~10–20 mM NaCl) salt, addition of NC could result in up to ~0.7 kcal/mol•bp stabilization (*116, 349*).

On the other hand, the preferential binding of the zinc fingers of NC to unpaired bases, resulted in the *destabilization* of nucleic acid duplexes. This effect was salt independent. The maximum destabilization of ~1 kcal/mol•bp was achieved upon saturation with the protein (~8:1 nt:NC). Therefore, the net effect of NC on duplex stability depends strongly on the solution ionic strength. While in low salt, NC-induced duplex destabilization can be very small, in higher salt the effect of NC becomes purely destabilizing (assuming that there is enough NC to bind to the duplex under the high-salt conditions).

1. Thermal Melting Studies of NC's Effect on Duplex Stability

The effect of NC on duplex stability was probed directly using traditional thermal melting studies (*43*). An NC-induced T_m depression of ~10 °C was measured for a 28 base-pair duplex in a solution containing 10 mM NaCl (*43*). These data were used to estimate very weak ($\Delta G = -0.23$ kcal/mol•bp) NC-induced duplex destabilization (*116*). Low-salt conditions were used to avoid two major problems of thermal melting studies. First, the T_m of the duplex at high salt is often above the melting temperature of the protein. Second, addition of saturating NC to the high concentrations of DNA that are required for UV melting studies usually results in nucleic acid aggregation and precipitation, which precludes determination of the T_m. In the next section, a novel strategy will be discussed that allowed determination of the effects of NC on DNA melting using single DNA molecules, thus avoiding the high concentrations required for conventional thermal melting studies.

2. Single-Molecule DNA Stretching Studies of NC's Effect on Duplex Stability

The difficulties with thermal melting studies previously described were overcome by using the novel biophysical technique of single-molecule DNA stretching (*198, 350–354*). In these experiments, a single long double-stranded λ-DNA molecule is stretched by tethering its ends to polystyrene beads, which can be manipulated with optical tweezers (*355*). The optical tweezers instrument allows simultaneous monitoring of the molecular end-to-end extension and the applied force.

In the absence of protein, the double-stranded DNA first extends to the B-DNA contour length and then, at a well-defined force of ~65 pN, it extends to twice its original length without the complete dissociation of the two strands. It was theoretically proposed that this highly cooperative transition corresponded to force-induced melting (*356, 357*). This hypothesis was confirmed by a series of experiments, which showed that the DNA melting force parallels the DNA melting temperature as a function of solution ionic strength (*351*), pH (*354*), and temperature (*353*). In other words, the force in the DNA stretching studies is the thermodynamic equivalent of the temperature in thermal melting studies. However, in contrast to conventional thermal melting, DNA stretching can be performed at room temperature. In addition, since single molecules of stretched DNA are not easily aggregated, force-induced melting measurements can be made even under conditions that would normally lead to nucleic acid aggregation.

This technique was successfully used to study the effect of HIV-1 NC on the force-induced DNA melting transition (*197*). Interestingly, it was shown that saturating levels of NC indeed destabilized double-stranded DNA by up to ~1 kcal/mol•bp at physiological salt conditions, i.e., ~150 mM NaCl, and by ~0.6 kcal/mol•bp at 25 mM NaCl (*197*). These results were in reasonable agreement with the ~0.5 kcal/mol•bp destabilizing effect of NC observed at 20 mM NaCl based on tRNA/PBS annealing rate measurements (*116*) and the ~0.2 kcal/mol•bp destabilization measured at 10 mM NaCl (*43*). Moreover, the small amount of hysteresis (lack of an exact match between the stretch and relax curves) observed upon relaxing the DNA in the presence of wild-type NC suggested that the protein falls off single-stranded DNA very rapidly and facilitates the reannealing of the strands.

The DNA stretching studies showed that the elastic properties of λ-DNA were significantly altered in the presence of saturating NC, a property that is consistent with its chaperone function. In particular, in the presence of NC, the λ-DNA force-extension curve shows a much broader melting transition, which begins at much lower forces. The observed transition broadening can be attributed to at least three effects of NC: (i) specific binding to certain

single-stranded DNA sequences (*44, 45, 55, 56*); (ii) reduced cooperativity of DNA duplex melting (*197*); and (iii) weak intercalation of NC between the bases of stretched ds DNA (M. Cruceanu, I. Rouzina, M. Williams, unpublished observations).

The requirement for a specific zinc-finger architecture for NC's chaperone function was also demonstrated with the single-molecule DNA stretching technique (*197, 198*). Whereas the results of this assay were consistent with wild-type NC's capability to destabilize nucleic acid structures, the transition free energy was increased in the presence of SSHS NC (*197*). Thus, elimination of the zinc finger structures was detrimental to NC's helix destabilization function.

Using this assay, the wild-type protein's ability to alter the force-induced DNA melting profile was also compared to that of 2-1, 1-1, CCHH/CCHC, and CCCC/CCHC NC variants. The results of this study were in excellent agreement with the *in vitro* minus-strand transfer assays described above (*179*), and showed that the first finger is more important for chaperone activity than the second finger. Even subtle changes to the N-terminal finger had dramatic effects on NC's ability to alter the helix-coil transition (*198*). Binding of the CCCC/CCHC variant had essentially no effect on the helix-coil transition, whereas the CCHH/CCHC variant appeared slightly more active. Interestingly, as mentioned in Section IV.C, the NMR structure of the CCHH/CCHC mutant in the context of (12–53)NC showed that the conformation of this mutant is closer to that of wild-type NC than to that of CCCC/CCHC NC (*346*).

B. Studies of NC's Chaperone Activity

1. Early Studies Using Model DNA Oligonucleotides

Using DNA oligonucleotides, significant insights into NC's chaperone activity have been gained. For example, potent renaturation of a 149-bp DNA fragment by NC71 was reported (*50*). The kinetics of annealing of the two complementary strands was enhanced by four orders of magnitude in the presence of saturating NC71 and was shown to be second order in single-stranded DNA concentration and independent of zinc binding.

In other early work, it was shown that HIV NC71 stimulated the annealing of 93-mer complementary DNA strands as well as of shorter DNA oligonucleotides (*46*). NC was shown to form a large coaggregate with DNA, which suggested that the mechanism of DNA strand renaturation might involve aggregation. The results of strand exchange and annealing studies also led to the proposal that NC lowered the kinetic barrier for achievement of the double-strand⟷single-strand equilibrium to favor the lowest energy conformation (*46*).

2. Studies Using Oligonucleotide Systems Derived from the HIV Genome

NC's chaperone activity has also been examined using model oligonucleotides derived from the HIV genome. In particular, tRNA primer annealing to fragments of the RNA genome containing the PBS, as well as NC's effect on minus-strand transfer, have been extensively studied. The effect of NC on these two steps in reverse transcription was described in Sections III.B and III.C. The following sections focus on the mechanistic insights into NC's chaperone function gained from studies of these systems.

a. Primer tRNA Annealing. A detailed kinetic study investigating tRNA primer annealing to a 105-nt fragment of the RNA genome containing the complementary PBS sequence showed that NC enhanced this reaction by five orders of magnitude and that the annealing followed second-order kinetics (*116*). This result, together with the small positive enthalpy measured for the NC-catalyzed process ($\Delta H^{\ddagger} = 13$ kcal/mol), led to the proposal that a rate-limiting nucleation step is preceded by melting of a few bp within the PBS-containing fragment (Fig. 5). Additionally, a mutational analysis using semi-synthetic tRNA constructs containing changes in the acceptor stem domain was consistent with a mechanism wherein the annealing initiated from the single-stranded CCA-3′ end of the acceptor stem.

In particular, mutations that resulted in stabilization of the 3′ single-stranded region through Watson-Crick base pairing significantly reduced the annealing rate. The results suggested that the intermolecular duplex was nucleated by annealing of 4–5 bases at the 3′ end of the tRNA to the complementary bases of the PBS followed by fast zippering of the rest of the 18-nt duplex. In contrast to the effects of mutations that involve the 3′ end of the tRNA, even drastic changes in the stability of the D arm and the tertiary core of the tRNA had only modest effects on annealing. These results were consistent with the fact that NC can catalyze tRNA annealing to the PBS despite its inability to cause global tRNA unwinding (*22, 63*).

NMR spectroscopy was also used to study the formation of the tRNA/PBS complex (*65*). By monitoring imino resonances characteristic of the tRNA/PBS duplex, slow formation of the NC-annealed complex was observed at 15°C. Whereas at 10 h only partial annealing was observed, at 24 h annealing was complete. The authors concluded that annealing was initiated at the bottom of the acceptor/TΨC stem, based on the appearance of imino resonances corresponding to U66 and U67. However, due to technical limitations, the 3′ end of the tRNA could not be observed using this method. Thus, the alternative mechanism, wherein nucleation is initiated at the 3′ single-stranded tRNA end, could not be ruled out and, in fact, this mechanism is strongly supported by the kinetic studies previously described.

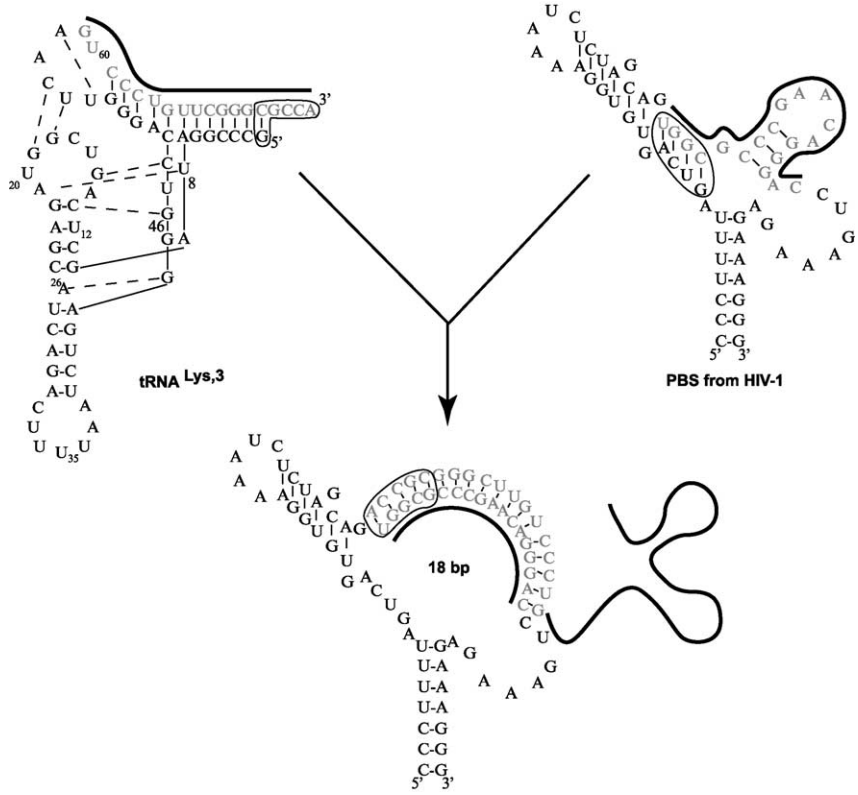

FIG. 5. Secondary structure of the 76-nt $tRNA_3^{Lys}$ (top left) and the 105-nt fragment of the HIV-1 genome containing the primer binding site (top right). The complementary sequences are indicated by a solid line; dashed lines indicate known tertiary contacts in the tRNA core. The nt that are hypothesized to participate in the rate-limiting nucleation step are circled. The product of the annealing reaction is shown schematically at the bottom, with the solid semicircle indicating the 18-bp intermolecular duplex. (Adapted, with permission, from (*116*)).

b. Minus-Strand Transfer. In contrast to the tRNA annealing reaction, both protein-free and NC-assisted minus-strand transfer annealing have been reported to follow first-order kinetics (*193*). Although additional studies are needed, it was hypothesized that the rate-limiting step for annealing in minus-strand transfer is a first-order conformational change of the stable TAR RNA and TAR DNA stem-loop structures (Fig. 3) rather than a bimolecular nucleation step typical of most annealing reactions.

NC's effect on TAR DNA hairpin opening and closing rates was investigated using two-photon FCS (*358*). A truncated form of NC [(12–55)NC]

was used in this work to avoid aggregation. By attaching a fluorophore/quencher couple to the ends of TAR DNA (derived from the MAL isolate) (Fig. 3C), FCS could be used to measure the kinetics of fraying. In this technique, statistical fluctuations in the fluorescence intensity are monitored as the sample flows through a small sample volume. Diffusion both in and out of the focal volume, as well as changes in the dye-to-quencher distance due to hairpin conformational changes, give rise to the observed fluorescence fluctuations.

The opening and closing rate constants for fraying of TAR DNA were deduced in the absence and presence of NC by separating the dynamics due to diffusion from the dynamics due to hairpin opening/closing. Addition of saturating NC increased the opening rate constant by ~6-fold, but had very little effect on the closing rate. The large effect on the opening rate was consistent with NC's chaperone function and demonstrated NC's ability to lower the energy barrier for bp melting. The lack of a large effect on the rate of closing was attributed, in part, to the specific fluorophore/quencher pair used. Indeed, in a follow-up study, using a different donor/acceptor pair, NC was shown to increase both the opening and closing rates by at least 10-fold and 2-fold, respectively (*203*).

NC's ability to destabilize TAR DNA variants containing mutations that stabilize the hairpin was also examined using absorbance spectroscopy and time-resolved fluorescence (*203*). NC-facilitated melting of TAR DNA was shown to be dependent on the presence of the two terminal bulges, which appeared to cooperatively destabilize the lower part of the stem (*203*). In addition, FCS was used to monitor the kinetics of fraying of the bulge variants. In all cases examined, NC increased both the opening (~10-fold) and closing (~2-fold) rates, as has been described for the wild-type system.

In addition to examining the effects of bulges proximal to the 3′ and 5′ ends of the TAR DNA stem (i.e., lower half), the role of structural elements in the top half of TAR DNA in NC's destabilization activity was also investigated (*359*). Variants of the top half of TAR DNA ranging in size from 14 to 26 nt were labeled with a fluorophore/quencher pair. In accord with results with the full-length TAR DNA hairpin, (12-55)NC binding shifted the population of truncated hairpins toward the more open species, although the effects were reduced relative to the native hairpin. When the internal loop was deleted, leaving an 8-bp stem, the effects of NC were almost completely eliminated. In contrast, maintaining the internal loop but altering the sequence (G33A and G35A variants) increased NC's destabilizing activity, whereas substitution of the hairpin loop bases with a non-nucleotide flexible tether had almost no effect. These results, together with previous studies of the full-length TAR DNA already described, suggested that the top half of TAR DNA is more stable than the bottom half and that bulges and internal loops are critical

initiation sites for NC's melting activity. In contrast, the top loop of the hairpin does not appear to serve a similar function.

Single molecule spectroscopy studies were also used to examine the conformational distribution and dynamics of TAR DNA-derived hairpins in the presence of HIV-1 NC (*360*). In these studies, single DNA hairpins containing a biotin linker attached to a dT in the hairpin loop region and FRET donor and acceptor dyes at the 5′ and 3′ ends, respectively, were immobilized on a streptavidin-coated surface. Single molecule fluorescence intensity time trajectories were recorded for various hairpin constructs with different numbers of internal bulges (0 to 4). NC's ability to destabilize the hairpin was found to be directly related to the number of internal bulges present, in good agreement with the bulk-level FCS measurements already described.

Whereas hairpins with two or more internal bulges were found predominantly with the two terminal stems open in the presence of saturating NC (450 nM) and low ionic strength (40 mM NaCl and 0.2 mM $MgCl_2$), smaller donor-acceptor dye separations were observed in the presence of only one internal bulge. A TAR DNA mutant with all four internal loops deleted was characterized by a fully closed conformation in the presence of NC. The predominantly "open" conformation observed under these conditions in the presence of two terminal bulges was proposed to be a key intermediate in the NC-induced annealing of TAR RNA to TAR DNA (*360*). However, it is unlikely that NC binding to TAR DNA under physiological conditions results in an exclusively open conformation. Indeed, when studies were carried out in the presence of increasing $MgCl_2$ concentrations, a reduction in the frequency of transitions from closed to open states was observed (G. Cosa, Y. Zeng, H.-W. Liu, C. F. Landes, D. E. Makarov, K. Musier-Forsyth, and P. Barbara, submitted).

Cross-correlation analyses of single-molecule time trajectories revealed dynamics in the milliseconds time domain for TAR DNA hairpins with at least one internal bulge in equilibrium with NC (*360*). This is in contrast to the results of the FCS studies already described, which reported that NC-induced conformational fluctuations for a related TAR DNA hairpin occurred on the microsecond timescale (*203, 358*). These differences likely reflect, at least in part, DNA sequence differences (see Fig. 3), as well as differences in the NC protein used (NCp7 was used in (*360*) whereas NC(11-55) was used in Ref. (*358*)). In addition, the difference in the observed time scales of duplex opening–closing may result from technical limitations of the FCS method. In particular, for the single-molecule studies, the hairpins are immobilized so diffusion does not preclude the observation of slow time-scale events, as is the case for conventional FCS measurements (*358, 361*). Thus, the FCS method can only monitor end-fraying, whereas the single molecule spectroscopy approach can additionally monitor slow dynamics associated with larger conformational changes.

C. NC is a Weak Duplex Destabilizer

1. Weak Destabilizing Activity of NC is Key to Its Chaperone Function in Reverse Transcription

The NC-induced nucleic acid duplex destabilization of ~0.5–1 kcal/mol·bp appears quite weak when compared to the average stability per bp of polymeric double-stranded DNA (~1.5 kcal/mol) or of dsRNA (~3 kcal/mol) (*70*). It is also much weaker than duplex destabilization by other single-stranded binding proteins such as gp32 and *E. coli* SSB, which are capable of complete destabilization of dsDNA (*362–365*). Indeed, as previously described, many studies showed that long fully base-paired nucleic acid helices were not destabilized by NC. By contrast, short fully base paired regions of 4 to 8 bp bordered by unpaired regions (duplex ends, loops, bulges, or mismatches) can be significantly destabilized by NC.

Why is NC such a weak duplex destabilizer? Wouldn't it be more efficient for retroviruses to have a much stronger single-stranded binding protein as their nucleic acid chaperone? Understanding the mechanism of NC's chaperone activity allows us to answer this question. Indeed, melting of relatively short fragments of secondary structure is, in most cases, sufficient for providing the complementary single-stranded regions that can nucleate new duplex formation. Moreover, since the weak destabilization activity of NC has very little effect on the stability of longer helices, it does not interfere with the nucleation and zippering of the final annealed state. Thus, the weak duplex destabilizing activity of NC proteins appears to be ideally suited to optimize the annealing rate of complementary structured nucleic acids as well as the restructuring of single nucleic acid molecules.

The destabilization of nucleic acid bp by NC resulted in at most a 10- to 100-fold rate enhancement of the annealing reaction. Since NC is such a weak duplex destabilizer, why is its effect on the rate of annealing so strong? As will be discussed in greater detail, the remainder of the rate enhancement is due to the nucleic acid aggregating ability of NC.

2. The Nucleation-Limited Mechanism of Nucleic Acid Annealing by NC

The duplex destabilizing activity of NC (*5, 6, 178, 179, 197, 198, 202, 203, 358, 359*) was mapped to its zinc finger structures (*178, 179, 197, 198, 202*). The physical reason for duplex destabilization appears to be the preferential binding of NC's zinc fingers to unpaired bases of nucleic acids (*45, 56–58, 92, 94*). Addition of NC to most annealing and strand-transfer reactions studied to date caused significant (10- to 10^5-fold) rate enhancements that depended on the solution ionic strength and, to a lesser extent, on the identity of the annealing molecules.

Interestingly, while the annealing and strand transfer reaction rates of various reactions that have been investigated both with and without NC were quite different in the absence of NC, in the presence of NC similar reaction rate constants ($k \sim 10^5$–10^6 $M^{-1}\bullet s^{-1}$) were observed. In addition, by measuring the dependence of the annealing rate on nucleic acid concentration, the reactions generally appeared bimolecular, in both the absence and presence of NC (*50, 116, 196*) (M. Vo, I. Rouzina, and K. Musier-Forsyth, in preparation). This result was in accord with previous studies of nucleic acid annealing both in the absence of chaperones (*69, 366–369*) and in the presence of several other nucleic acid chaperone proteins (*370–376*).

The importance of secondary structure stability within the annealing molecules was quantitatively assessed in a study of minus-strand transfer (*185*). Surprisingly, in one case, the strand transfer efficiency did not correlate with net nucleic acid stability. As discussed previously in more detail, the authors hypothesized that it is not the stability of the entire molecule, but rather the stability of a small portion, that is critical for the annealing.

Why is the reaction rate only sensitive to the stability of a small portion of the secondary structure? This mechanistic question was addressed in the case of tRNA annealing to the PBS (*116*). The bimolecular nature of this annealing reaction both with and without NC suggested that the reaction is nucleation-limited. In other words, the slowest step in the annealing process is the formation of the first few bp of the new intermolecular duplex, followed by much faster zippering of the rest of the structure. The positive value of the enthalpy (ΔH) of the annealing reaction measured in the presence and the absence of NC suggested that the breaking of 4–5 bp precedes the rate-limiting nucleation step (*116*). Comparable annealing enthalpies were observed in several other studies of NC annealing (*193, 377*) (M. Vo, I. Rouzina, and K. Musier-Forsyth, in preparation).

In the case of tRNA annealing to the PBS, mutational analysis identified a "critical site" within the PBS-containing RNA genome that must be destabilized by NC prior to the rate-limiting nucleation step (*116*) (Fig. 5). More generally, NC's ability to facilitate destabilization of weak structural elements located in one or both of the annealing molecules creates the single-stranded complementary regions necessary for the subsequent rate-limiting nucleation of the intermolecular duplex. The magnitude of the rate enhancement due to NC-induced duplex destabilization (typically, 10- to 100-fold) depends on the sequence and the structure of the annealing molecules. More specifically, it is determined by the stability of the critical site(s) in the original structure(s) that NC destabilizes.

Based on this mechanism of NC-facilitated annealing, the variable effects on the annealing rates of different reactions observed upon mutation of NC's zinc finger structures can be readily explained. In particular, the much weaker

effect of mutating the zinc fingers on the annealing of tRNA to the PBS (*116, 117*) as compared to the effect on the annealing of TAR DNA to TAR RNA (*178, 179*) is likely due to the higher stability of the critical site within the TAR molecules that must be destabilized prior to the annealing reaction. Interestingly, in the viral RNA genome, even the most structured regions, such as TAR, contain short helical segments separated by loops, bulges, and mismatches. These "interruptions" in the base-paired helices provide NC with the choice of "weak spots" for facilitating nucleation of thermodynamically more stable duplexes.

D. NC-Induced Aggregation of Nucleic Acids

1. Studies of NC-Induced Nucleic Acid Aggregation

The NC72-induced aggregation of single-stranded RNA was studied using quasielastic dynamic light scattering and optical density measurements (*73*) as well as with electron microscopy (*72*). The ordered growth of a monodisperse population of large nucleic acid–NC aggregates was observed, independent of the length and sequence of RNA molecules. The kinetics of growth was that of the so-called Ostwald ripening mechanism, limited by transfer of NC-covered single-stranded RNA complexes from small to large aggregates. This growth mechanism is described by the power dependence of the average aggregate size over time, with the power close to 1/3. The aggregate growth rate was optimal for a nt:protein (r) ratio close to 8. The growth became slower as r became significantly smaller or larger then 8. Additionally, the nt:protein ratio within the aggregates was always close to 8, even when this ratio in solution was varied ~1300-fold. In addition, the growth rate was optimal at physiological concentrations of Na^+ and Mg^{2+}. All of these features were reminiscent of the kinetics of growth of the polyelectrolyte aggregates induced by multivalent cations (*378, 379*). Similar kinetics was observed in NC-facilitated annealing reactions carried out with hairpins that mimic the top part of TAR DNA/RNA, suggesting that aggregation may dominate the annealing kinetics (M. Vo, I. Rouzina, and K. Musier-Forsyth, in preparation).

2. NC-Induced Aggregation Facilitates the Nucleation Step of Strand Annealing

In addition to the duplex destabilizing activity of NC's zinc fingers already described, the ability of NC to aggregate nucleic acids nonspecifically facilitates the nucleation step of the annealing reaction. Nucleation is a diffusion-limited association, which is slowed down by the electrostatic repulsion between the annealing strands as well as by the low probability of the correct positioning of nucleotides for annealing. The rate of nucleation of structured

nucleic acids is also reduced by the low probability of melting of the weakest element of their secondary structure.

It is well known that high salt greatly facilitates the rate of strand renaturation by up to 10^4-fold (*366, 368, 380, 381*). Moreover, moderately high temperatures, which are high enough to melt relatively weak intramolecular interactions but unable to melt more stable interactions present in annealed complexes, are known to increase annealing rates up to ~100-fold (*366, 368, 382*). However, the nucleic acid annealing rate in the presence of NC exceeds the optimum annealing rate observed at 1 M NaCl and 68°C by almost ~10^3-fold (*50*). This suggests that NC possesses an activity in addition to simply melting nucleic acid structures and reducing interstrand repulsion. Indeed, an important component of NC's chaperone activity is its ability to aggregate nucleic acids, thus facilitating the attraction between nucleic acid strands (*50, 72–74, 192*). This effect is expected to greatly accelerate the rate of nucleation-limited annealing, since complementary sequences, if mobile, can search for each other within the aggregate.

These expectations are in good agreement with the observed rate enhancement of annealing and strand transfer reactions by NC. The rate enhancement is generally greater (~10^3–10^5-fold) for reactions carried out in low salt buffer (~10–30 mM ionic strength) (*20, 46, 116, 193*) than for reactions performed in higher salt (~100 mM ionic strength) (*178, 179, 184, 185, 199*). The weaker effect of NC on annealing under these latter conditions is likely due to the more efficient uncatalyzed rate (i.e., rate measured in the absence of a chaperone protein) of duplex nucleation observed in the presence of high salt.

3. Nonspecific Nucleic Acid Aggregating Agents are Good Nucleic Acid Chaperones

If protein-induced aggregation of nucleic acids is indeed a major component of NC's chaperone function, then any nucleic acid aggregating agent can be expected to facilitate annealing and strand-transfer reactions. Indeed, a rate enhancement comparable to that induced by NC was observed in annealing reactions carried out with the nonspecific multivalent cations cobalt hexamine ($CoHex^{3+}$) or spermidine (Spd^{3+}) (*383*), polyamines (*363*), polyLysine (*116, 117*) (M. Vo, unpublished observations), several cationic detergents (*371, 374, 376*), the p53 protein (*375*), and the human prion protein (*384, 385*). Interestingly, despite the fact that all of the agents mentioned are known to be effective duplex stabilizers (with the exception of the human prion protein), they have been shown to enhance annealing rates by 10^2- to 10^5-fold, due primarily to nucleic acid aggregation.

In order for nucleic acid aggregation to lead to annealing rate enhancement, nucleic acids must remain highly mobile within the aggregate. High mobility allows for the rapid search of complementary single-stranded regions.

If this were not the case, nucleation of the new duplex would be impeded and the reaction slowed down rather than facilitated. This capability requires a special kind of aggregating agent, one that attracts nucleic acids nonspecifically, but that does not result in rigid crosslinks. As an example, cationic detergents are aliphatic amines that bind nucleic acids via their cationic polar head groups and induce aggregation via the association of their hydrophobic tails, which are bound to different nucleic acid strands (*370–372, 386, 387*).

NC most likely uses a related but different mechanism for aggregating nucleic acids. NC is highly cationic, with 15 positive amino acids distributed throughout its sequence. Therefore, in contrast to aliphatic amines, it is highly soluble, and in the absence of nucleic acids does not self-aggregate even in high salt buffers and at high protein concentrations. In addition, when bound to RNA, it appeared to be closely associated with the nucleic acid, with no hydrophobic domains protruding into solution (*57, 58, 94*).

Multiple studies suggested that NC remains highly mobile when bound to nucleic acids (*31, 63–67*) (R. J. Fisher *et al.*, personal communication). As has been discussed, high mobility of multivalent cationic ligands in their nucleic acid-bound state (*378, 388–392*) is a key feature of efficient aggregating or condensing agents (*71, 388–392*). Attraction within such aggregates is mediated by electrostatic interaction of the opposite charges of nucleic acids and cations that self-organize quasi-periodically (*388, 389, 392*). This is not a simple charge neutralization effect, as even high concentrations of monovalent salt do not induce nucleic acid aggregation (*71, 388–392*).

This is also in contrast to the proposal that protein–protein interactions between NC molecules drive nucleic acid aggregation (*5, 20, 28*). Indeed, there is significant experimental evidence that NC molecules do not interact with each other in solution even at very high concentrations. In addition, NCp7 is known to bind nucleic acids noncooperatively (*44, 45, 54, 59, 89, 90, 127, 129, 171*), suggesting the absence of any significant protein–protein interactions in the bound state. This is in contrast to NCp9, which appears to have an additional moderately cooperative binding mode characterized by a larger binding site size of ~15 nt (*59*). However, even for NCp9, it is its noncooperative binding mode with a site size of ~8 nt that was shown to induce nucleic acid aggregation and to be required for its chaperone activity (*50, 59*).

4. Role of Zinc Fingers in Nucleic Acid Aggregation

Although the main aggregating ability of NC was mapped to its N-terminal 3_{10} helix (*5, 20, 72, 73, 192*), the effect of deleting the zinc fingers on NC's ability to condense plasmid DNA was also investigated (*74*). In this study, a $(Gly)_2$ linker was substituted for the zinc-binding domains in the context of NC72 [$NC(1\text{-}72)_{dd}$]. The bis-intercalating fluorescent dye YOYO-1 was used as

a reporter of DNA condensation. Binding of NC to DNA resulted in a decrease in YOYO-1 fluorescence due to DNA condensation. Efficient condensation required the zinc fingers since NC(1-72)$_{dd}$ was only effective at high concentrations of DNA. The fingerless deletion variant studied in this work also lacked numerous basic residues as well as Trp37, which is known to be involved in stacking interactions with G residues. Therefore, the reduced DNA condensation capability of NC(1-72)$_{dd}$ may, in part, be attributed to these differences, which were likely to reduce the binding affinity and increase the critical concentration of the fingerless NC required for nucleic acid aggregation.

VI. Concluding Remarks

NC is a multifunctional protein present in all retroviruses. It is synthesized as a domain of the Gag precursor protein, but following virus maturation, the mature protein (55 amino acid residues in the case of HIV-1 NC) is generated. Unlike any other retroviral protein, NC, in either its mature or immature form, functions in practically every step of the replication cycle. This chapter focuses on developments related to NC's nucleic acid chaperone activity and its critical role in ensuring specific and efficient reverse transcription.

A wide variety of biochemical and biophysical techniques, including single-molecule studies, have led to a molecular description of how HIV-1 NC performs its nucleic acid chaperone function. The chaperone activity consists of two main components: duplex destabilization activity by the zinc fingers and nucleic acid aggregation activity, which resides primarily in the basic N-terminal domain. This domain is unstructured in free NC, but forms a 3_{10} helix upon nucleic acid binding. Although NC preferentially binds to single-stranded G-rich sequences through stacking interactions via hydrophobic residues, NC's nonspecific nucleic acid binding and aggregating ability are an essential part of its chaperone function.

NC binds nucleic acids stoichiometrically, with an nt:NC ratio of about 8:1 being required for optimal chaperone activity under physiological salt conditions. Although this threshold concentration of NC is sufficient for duplex destabilization and annealing, further increases in protein concentration up to a large (~10-fold) excess do not interfere with its chaperone function. The reason for this behavior appears to be that the duplex destabilizing ability of NC is very limited, even at saturating levels. This weak duplex destabilization is sufficient for providing the single-stranded complementary regions necessary for nucleation of new duplex structures.

Since NC does not unwind relatively stable nucleic acid duplexes, it also does not interfere with strand interaction and annealing of more stable

complementary structures, even when present at saturating levels. Additionally, NC is highly flexible and mobile when bound to nucleic acids and rapidly switches between single-stranded and double-stranded binding modes, on the time scale of duplex opening-closing. This is in accord with NC's ability to increase the opening and closing rates of DNA stem-loop structures.

NC binds nucleic acids noncooperatively and does not rely on protein–protein interactions to drive aggregation and annealing. Instead, NC-induced nucleic acid aggregation appears to be facilitated by simple polyelectrolyte attraction, similar to that observed for many multivalent cations.

Characterization of the mechanism of NC's chaperone activity in molecular terms has been invaluable for understanding NC's effect on specific steps in reverse transcription. For example, NC's aggregation ability is responsible for stimulating the annealing of primer tRNA to the PBS in viral RNA. Destabilization activity allows NC to catalyze removal of 5′ terminal genomic RNA fragments after synthesis of (−) SSDNA without a requirement for secondary RNase H cleavage and also to enhance RNase H-mediated removal of the tRNA primer from minus-strand DNA. In addition, transient destabilization of secondary structures in the viral RNA and minus-strand DNA templates results in more efficient minus- and plus-strand DNA synthesis. Moreover, because NC is a weak duplex destabilizer, the success of minus-strand transfer depends on a delicate thermodynamic balance between the (−) SSDNA and acceptor RNA structures and the stability of the RNA–DNA strand transfer duplex.

Recent work has also revealed the important role of the zinc finger structures (especially the N-terminal finger) in NC's chaperone function in reverse transcription. The presence of the intact zinc fingers is essential for destabilization of long, complex structures, such as the TAR DNA and RNA hairpins, which are contained within the complementary R regions that are annealed during minus-strand transfer. This destabilization activity also blocks RT-catalyzed self-priming reactions induced by TAR DNA that have the potential to severely inhibit the strand transfer reaction. Interestingly, even subtle changes to the N-terminal finger dramatically reduce chaperone function as assayed by a variety of biochemical and biophysical techniques. These results are in general agreement with cell culture-based replication assays using the same zinc finger mutants. In contrast, NC's aggregating activity is sufficient to anneal less structured nucleic acids, including the 18-nt RNA duplex formed during the initiation step and the 18-nt (−) and (+) PBS DNA duplexes that are annealed during plus-strand transfer. Thus, the zinc fingers are dispensable for these reactions, at least under *in vitro* assay conditions.

The remarkable biological properties of NC and its central role in retrovirus replication make NC an attractive target for new HIV therapeutics. In several studies, an anticancer agent, actinomycin D, was shown to strongly

inhibit NC's chaperone activity in HIV-1 minus-strand transfer (*177, 194, 393*) by binding to (−) SSDNA and blocking the ability of NC to catalyze the annealing reaction between (−) SSDNA and acceptor RNA (*177, 194*). However, use of this drug in patients is excluded due to its high toxicity (*394*). Other agents, such as chemicals that target the Cys residues in the zinc finger structures (*395*), RNase H inhibitors (*396, 397*), and NC-based vaccines (*398*), represent some of the alternative approaches that are currently being considered. The detailed understanding of NC's nucleic acid binding and chaperone activities that is now beginning to emerge augurs well for the development of effective and safe anti-AIDS therapeutic strategies.

Acknowledgments

We are very grateful to Drs. Gonzalo Cosa, Robert Gorelick, Alan Rein, and Mark Williams for critical reading of the manuscript and stimulating discussion. We also thank Dr. Wei-Shau Hu for helpful comments, Drs. Jeffrey DeStefano, Robert Fisher and Alan Rein, and Vinay Pathak for communicating results prior to publication; Mr. Mithun Mitra, Ms. Klara Post, and Dr. Tiyun Wu for help with references; and Mr. Mithun Mitra for assistance with figures. Work on NC in the K.M.-F. lab is supported by NIH Grant GM65056.

References

1. Green, L. M., and Berg, J. M. (1990). Retroviral nucleocapsid protein-metal ion interactions: Folding and sequence variants. *Proc. Natl. Acad. Sci. USA* **87,** 6403–6407.
2. Henderson, L. E., Copeland, T. D., Sowder, R. C., Smythers, G. W., and Oroszlan, S. (1981). Primary structure of the low molecular weight nucleic acid-binding proteins of murine leukemia viruses. *J. Biol. Chem.* **256,** 8400–8406.
3. Berg, J. M. (1986). Potential metal-binding domains in nucleic acid binding proteins. *Science* **232,** 485–487.
4. Covey, S. N. (1986). Amino acid sequence homology in gag region of reverse transcribing elements and the coat protein gene of cauliflower mosaic virus. *Nucleic Acids Res.* **14,** 623–633.
5. Darlix, J.-L., Lapadat-Tapolsky, M., de Rocquigny, H., and Roques, B. P. (1995). First glimpses at structure–function relationships of the nucleocapsid protein of retroviruses. *J. Mol. Biol.* **254,** 523–537.
6. Rein, A., Henderson, L. E., and Levin, J. G. (1998). Nucleic-acid-chaperone activity of retroviral nucleocapsid proteins: Significance for viral replication. *Trends Biochem. Sci.* **23,** 297–301.
7. Coffin, J. M., Hughes, S. H., and Varmus, H. E. (1997). "Retroviruses." Cold Spring Harbor Laboratory Press, Cold Spring Harbor, New York.
8. Mervis, R. J. *et al.* (1988). The gag gene products of human immunodeficiency virus type 1: Alignment within the gag open reading frame, identification of posttranslational modifications, and evidence for alternative gag precursors. *J. Virol.* **62,** 3993–4002.

9. Wondrak, E. M., Louis, J. M., de Rocquigny, H., Chermann, J. C., and Roques, B. P. (1993). The gag precursor contains a specific HIV-1 protease cleavage site between the NC (P7) and P1 proteins. *FEBS Lett.* **333,** 21–24.
10. Henderson, L. E. *et al.* (1992). Gag proteins of the highly replicative MN strain of human immunodeficiency virus type 1: Posttranslational modifications, proteolytic processings, and complete amino acid sequences. *J. Virol.* **66,** 1856–1865.
11. Darlix, J.-L., Gabus, C., Nugeyre, M. T., Clavel, F., and Barré-Sinoussi, F. (1990). *Cis* elements and *trans*-acting factors involved in the RNA dimerization of the human immunodeficiency virus HIV-1. *J. Mol. Biol.* **216,** 689–699.
12. Feng, Y. X. *et al.* (1996). HIV-1 nucleocapsid protein induces "maturation" of dimeric retroviral RNA *in vitro*. *Proc. Natl. Acad. Sci. USA* **93,** 7577–7581.
12a. Baba, S. *et al.* (2003). Role of the zinc fingers of HIV-1 nucleocapsid protein in maturation of genomic RNA. *J. Biochem.* **134,** 637–639.
13. Sakaguchi, K. *et al.* (1993). Identification of a binding site for the human immunodeficiency virus type 1 nucleocapsid protein. *Proc. Natl. Acad. Sci. USA* **90,** 5219–5223.
14. Fu, W., Gorelick, R. J., and Rein, A. (1994). Characterization of human immunodeficiency virus type 1 dimeric RNA from wild-type and protease-defective virions. *J. Virol.* **68,** 5013–5018.
15. Muriaux, D., De Rocquigny, H., Roques, B. P., and Paoletti, J. (1996). NCp7 activates HIV-1 Lai RNA dimerization by converting a transient loop–loop complex into a stable dimer. *J. Biol. Chem.* **271,** 33686–33692.
16. Berkowitz, R., Fisher, J., and Goff, S. P. (1996). RNA packaging. *Curr. Top. Microbiol. Immunol.* **214,** 177–218.
17. De Rocquigny, H. *et al.* (1992). Viral RNA annealing activities of human immunodeficiency virus type 1 nucleocapsid protein require only peptide domains outside the zinc fingers. *Proc. Natl. Acad. Sci. USA* **89,** 6472–6476.
18. Prats, A. C. *et al.* (1988). Small finger protein of avian and murine retroviruses has nucleic acid annealing activity and positions the replication primer tRNA onto genomic RNA. *EMBO J.* **7,** 1777–1783.
19. Barat, C. *et al.* (1989). HIV-1 reverse transcriptase specifically interacts with the anticodon domain of its cognate primer tRNA. *EMBO J.* **8,** 3279–3285.
20. Lapadat-Tapolsky, M., Pernelle, C., Borie, C., and Darlix, J.-L. (1995). Analysis of the nucleic acid annealing activities of nucleocapsid protein from HIV-1. *Nucleic Acids Res.* **23,** 2434–2441.
21. Li, X. *et al.* (1996). Human immunodeficiency virus type 1 nucleocapsid protein (NCp7) directs specific initiation of minus-strand DNA synthesis primed by human $tRNA_3^{Lys}$ *in vitro*: Studies of viral RNA molecules mutated in regions that flank the primer binding site. *J. Virol.* **70,** 4996–5004.
22. Chan, B., Weidemaier, K., Yip, W. T., Barbara, P. F., and Musier-Forsyth, K. (1999). Intra-tRNA distance measurements for nucleocapsid protein-dependent tRNA unwinding during priming of HIV reverse transcription. *Proc. Natl. Acad. Sci. USA* **96,** 459–464.
23. Feng, Y. X. *et al.* (1999). The human immunodeficiency virus type 1 Gag polyprotein has nucleic acid chaperone activity: Possible role in dimerization of genomic RNA and placement of tRNA on the primer binding site. *J. Virol.* **73,** 4251–4256.
24. Cen, S. *et al.* (1999). The role of $Pr55^{gag}$ in the annealing of $tRNA_3^{Lys}$ to human immunodeficiency virus type 1 genomic RNA. *J. Virol.* **73,** 4485–4488.
25. Rong, L. *et al.* (2001). HIV-1 nucleocapsid protein and the secondary structure of the binary complex formed between $tRNA^{Lys,3}$ and viral RNA template play different roles during initiation of (−) strand DNA reverse transcription. *J. Biol. Chem.* **276,** 47725–47732.
26. Rong, L. *et al.* (1998). Roles of the human immunodeficiency virus type 1 nucleocapsid protein in annealing and initiation versus elongation in reverse transcription of viral negative-strand strong-stop DNA. *J. Virol.* **72,** 9353–9358.

27. Iwatani, Y., Rosen, A. E., Guo, J., Musier-Forsyth, K., and Levin, J. G. (2003). Efficient initiation of HIV-1 reverse transcription *in vitro*. Requirement for RNA sequences downstream of the primer binding site abrogated by nucleocapsid protein-dependent primer-template interactions. *J. Biol. Chem.* **278,** 14185–14195.
28. Cristofari, G., and Darlix, J.-L. (2002). The ubiquitous nature of RNA chaperone proteins. *Prog. Nucleic Acid Res. Mol. Biol.* **72,** 223–268.
29. Auxilien, S., Keith, G., Le Grice, S. F. J., and Darlix, J.-L. (1999). Role of post-transcriptional modifications of primer $tRNA^{Lys,3}$ in the fidelity and efficacy of plus strand DNA transfer during HIV-1 reverse transcription. *J. Biol. Chem.* **274,** 4412–4420.
30. Wu, T., Guo, J., Bess, J., Henderson, L. E., and Levin, J. G. (1999). Molecular requirements for human immunodeficiency virus type 1 plus-strand transfer: Analysis in reconstituted and endogenous reverse transcription systems. *J. Virol.* **73,** 4794–4805.
31. Johnson, P. E. *et al*. (2000). A mechanism for plus-strand transfer enhancement by the HIV-1 nucleocapsid protein during reverse transcription. *Biochemistry* **39,** 9084–9091.
32. Muthuswami, R. *et al*. (2002). The HIV plus-strand transfer reaction: Determination of replication-competent intermediates and identification of a novel lentiviral element, the primer over-extension sequence. *J. Mol. Biol.* **315,** 311–323.
33. Ji, X., Klarmann, G. J., and Preston, B. D. (1996). Effect of human immunodeficiency virus type 1 (HIV-1) nucleocapsid protein on HIV-1 reverse transcriptase activity *in vitro*. *Biochemistry* **35,** 132–143.
34. Wu, W. *et al*. (1996). Human immunodeficiency virus type 1 nucleocapsid protein reduces reverse transcriptase pausing at a secondary structure near the murine leukemia virus polypurine tract. *J. Virol.* **70,** 7132–7142.
35. Drummond, J. E. *et al*. (1997). Wild-type and mutant HIV type 1 nucleocapsid proteins increase the proportion of long cDNA transcripts by viral reverse transcriptase. *AIDS Res. Hum. Retrovir.* **13,** 533–543.
36. Klasens, B. I., Huthoff, H. T., Das, A. T., Jeeninga, R. E., and Berkhout, B. (1999). The effect of template RNA structure on elongation by HIV-1 reverse transcriptase. *Biochim. Biophys. Acta* **1444,** 355–370.
37. Zhang, W. H., Hwang, C. K., Hu, W. S., Gorelick, R. J., and Pathak, V. K. (2002). Zinc finger domain of murine leukemia virus nucleocapsid protein enhances the rate of viral DNA synthesis *in vivo*. *J. Virol.* **76,** 7473–7484.
38. Carteau, S., Gorelick, R. J., and Bushman, F. D. (1999). Coupled integration of human immunodeficiency virus type 1 cDNA ends by purified integrase *in vitro*: Stimulation by the viral nucleocapsid protein. *J. Virol.* **73,** 6670–6679.
39. Carteau, S. *et al*. (1997). Human immunodeficiency virus type 1 nucleocapsid protein specifically stimulates Mg^{2+}-dependent DNA integration *in vitro*. *J. Virol.* **71,** 6225–6229.
40. Gao, K., Gorelick, R. J., Johnson, D. G., and Bushman, F. (2003). Cofactors for human immunodeficiency virus type 1 cDNA integration *in vitro*. *J. Virol.* **77,** 1598–1603.
41. Poljak, L. *et al*. (2003). Analysis of NCp7-dependent activation of HIV-1 cDNA integration and its conservation among retroviral nucleocapsid proteins. *J. Mol. Biol.* **329,** 411–421.
42. Wu, J. Q. *et al*. (1997). Binding of the nucleocapsid protein of type 1 human immunodeficiency virus to nucleic acids studied using phosphorescence and optically detected magnetic resonance. *Biochemistry* **36,** 12506–12518.
43. Urbaneja, M. A., Wu, M., Casas-Finet, J. R., and Karpel, R. L. (2002). HIV-1 nucleocapsid protein as a nucleic acid chaperone: Spectroscopic study of its helix-destabilizing properties, structural binding specificity, and annealing activity. *J. Mol. Biol.* **318,** 749–764.
44. Fisher, R. J. *et al*. (1998). Sequence-specific binding of human immunodeficiency virus type 1 nucleocapsid protein to short oligonucleotides. *J. Virol.* **72,** 1902–1909.

45. Vuilleumier, C. *et al*. (1999). Nucleic acid sequence discrimination by the HIV-1 nucleocapsid protein NCp7: A fluorescence study. *Biochemistry* **38,** 16816–16825.
46. Tsuchihashi, Z., and Brown, P. O. (1994). DNA strand exchange and selective DNA annealing promoted by the human immunodeficiency virus type 1 nucleocapsid protein. *J. Virol.* **68,** 5863–5870.
47. Herschlag, D. (1995). RNA chaperones and the RNA folding problem. *J. Biol. Chem.* **270,** 20871–20874.
48. Schroeder, R., Barta, A., and Semrad, K. (2004). Strategies for RNA folding and assembly. *Nat. Rev. Mol. Cell. Biol.* **5,** 908–919.
49. Bampi, C., Jacquenet, S., Lener, D., Decimo, D., and Darlix, J. L. (2004). The chaperoning and assistance roles of the HIV-1 nucleocapsid protein in proviral DNA synthesis and maintenance. *Curr. HIV Res.* **2,** 79–92.
50. Dib-Hajj, F., Khan, R., and Giedroc, D. P. (1993). Retroviral nucleocapsid proteins possess potent nucleic acid strand renaturation activity. *Protein Sci.* **2,** 231–243.
51. Lorsch, J. R. (2002). RNA chaperones exist and DEAD box proteins get a life. *Cell* **109,** 797–800.
52. Wills, J. W., and Craven, R. C. (1991). Form, function, and use of retroviral Gag proteins. *AIDS* **5,** 639–654.
53. Negroni, M., and Buc, H. (2001). Mechanisms of retroviral recombination. *Annu. Rev. Genet.* **35,** 275–302.
54. Mély, Y. *et al*. (1995). Binding of the HIV-1 nucleocapsid protein to the primer $tRNA_3^{Lys}$ *in vitro* is essentially not specific. *J. Biol. Chem.* **270,** 1650–1656.
55. Berglund, J. A., Charpentier, B., and Rosbash, M. (1997). A high affinity binding site for the HIV-1 nucleocapsid protein. *Nucleic Acids Res.* **25,** 1042–1049.
56. D'Souza, V., and Summers, M. F. (2004). Structural basis for packaging the dimeric genome of Moloney murine leukemia virus. *Nature* **431,** 586–590.
57. Amarasinghe, G. K. *et al*. (2000). NMR structure of the HIV-1 nucleocapsid protein bound to stem-loop SL2 of the psi-RNA packaging signal. Implications for genome recognition. *J. Mol. Biol.* **301,** 491–511.
58. De Guzman, R. N. *et al*. (1998). Structure of the HIV-1 nucleocapsid protein bound to the SL3 Ψ-RNA recognition element. *Science* **279,** 384–388.
59. Khan, R., and Giedroc, D. P. (1994). Nucleic acid binding properties of recombinant Zn^{2+} HIV-1 nucleocapsid protein are modulated by COOH-terminal processing. *J. Biol. Chem.* **269,** 22538–22546.
60. Karpel, R. L., Henderson, L. E., and Oroszlan, S. (1987). Interactions of retroviral structural proteins with single-stranded nucleic acids. *J. Biol. Chem.* **262,** 4961–4967.
61. You, J. C., and McHenry, C. S. (1993). HIV nucleocapsid protein. Expression in *Escherichia coli*, purification, and characterization. *J. Biol. Chem.* **268,** 16519–16527.
62. Urbaneja, M. A. *et al*. (1999). Binding properties of the human immunodeficiency virus type 1 nucleocapsid protein p7 to a model RNA: Elucidation of the structural determinants for function. *J. Mol. Biol.* **287,** 59–75.
63. Tisné, C., Roques, B. P., and Dardel, F. (2001). Heteronuclear NMR studies of the interaction of $tRNA_3^{Lys}$ with HIV-1 nucleocapsid protein. *J. Mol. Biol.* **306,** 443–454.
64. Tisné, C., Roques, B. P., and Dardel, F. (2003). Specific recognition of primer $tRNA_3^{Lys}$ by HIV-1 nucleocapsid protein: Involvement of the zinc fingers and the N-terminal basic extension. *Biochimie* **85,** 557–561.
65. Tisné, C., Roques, B. P., and Dardel, F. (2004). The annealing mechanism of HIV-1 reverse transcription primer onto the viral genome. *J. Biol. Chem.* **279,** 3588–3595.
66. Ramboarina, S. *et al*. (2002). Effects of temperature on the dynamic behavior of the HIV-1 nucleocapsid NCp7 and its DNA complex. *J. Mol. Biol.* **316,** 611–627.

67. Stote, R. H. *et al*. (2004). Structure of the His44 → Ala single point mutant of the distal finger motif of HIV-1 nucleocapsid protein: A combined NMR, molecular dynamics simulation, and fluorescence study. *Biochemistry* **43,** 7687–7697.
68. Shubsda, M. F., Paoletti, A. C., Hudson, B. S., and Borer, P. N. (2002). Affinities of packaging domain loops in HIV-1 RNA for the nucleocapsid protein. *Biochemistry* **41,** 5276–5282.
69. Cantor, C. R., and Schimmel, P. R. (1980). "Biophysical Chemistry. Part III. The Behavior of Biological Macromolecules," W. H. Freeman & Co., San Francisco, California.
70. Bloomfield, V. A., Crothers, D. M., and Tinoco, I., Jr. (1998). "Nucleic Acids: Structures, Properties and Functions." University Science Press, Mill Valley, California.
71. Bloomfield, V. A. (1996). DNA condensation. *Curr. Opinion Struct. Biol.* **6,** 334–341.
72. Le Cam, E. *et al*. (1998). Properties and growth mechanism of the ordered aggregation of a model RNA by the HIV-1 nucleocapsid protein: An electron microscopy investigation. *Biopolymers* **45,** 217–229.
73. Stoylov, S. P. *et al*. (1997). Ordered aggregation of ribonucleic acids by the human immunodeficiency virus type 1 nucleocapsid protein. *Biopolymers* **41,** 301–312.
74. Krishnamoorthy, G., Roques, B., Darlix, J.-L., and Mély, Y. (2003). DNA condensation by the nucleocapsid protein of HIV-1: A mechanism ensuring DNA protection. *Nucleic Acids Res.* **31,** 5425–5432.
75. South, T. L., Blake, P. R., Hare, D. R., and Summers, M. F. (1991). C-terminal retroviral-type zinc finger domain from the HIV-1 nucleocapsid protein is structurally similar to the N-terminal zinc finger domain. *Biochemistry* **30,** 6342–6349.
76. Summers, M. F., South, T. L., Kim, B., and Hare, D. R. (1990). High-resolution structure of an HIV zinc fingerlike domain via a new NMR-based distance geometry approach. *Biochemistry* **29,** 329–340.
77. Omichinski, J. G., Clore, G. M., Sakaguchi, K., Appella, E., and Gronenborn, A. M. (1991). Structural characterization of a 39-residue synthetic peptide containing the two zinc binding domains from the HIV-1 p7 nucleocapsid protein by CD and NMR spectroscopy. *FEBS Lett.* **292,** 25–30.
78. Morellet, N. *et al*. (1992). Determination of the structure of the nucleocapsid protein NCp7 from the human immunodeficiency virus type 1 by 1H NMR. *EMBO J.* **11,** 3059–3065.
79. Summers, M. F. *et al*. (1992). Nucleocapsid zinc fingers detected in retroviruses: EXAFS studies of intact viruses and the solution-state structure of the nucleocapsid protein from HIV-1. *Protein Sci.* **1,** 563–574.
80. Turner, B. G., and Summers, M. F. (1999). Structural biology of HIV. *J. Mol. Biol.* **285,** 1–32.
81. Chertova, E. N. *et al*. (1998). Probing the topography of HIV-1 nucleocapsid protein with the alkylating agent N-ethylmaleimide. *Biochemistry* **37,** 17890–17897.
82. Déméné, H. *et al*. (1994). 1H NMR structure and biological studies of the His^{23} → Cys mutant nucleocapsid protein of HIV-1 indicate that the conformation of the first zinc finger is critical for virus infectivity. *Biochemistry* **33,** 11707–11716.
83. Mély, Y. *et al*. (1994). Spatial proximity of the HIV-1 nucleocapsid protein zinc fingers investigated by time-resolved fluorescence and fluorescence resonance energy transfer. *Biochemistry* **33,** 12085–12091.
84. Lee, B. M., De Guzman, R. N., Turner, B. G., Tjandra, N., and Summers, M. F. (1998). Dynamical behavior of the HIV-1 nucleocapsid protein. *J. Mol. Biol.* **279,** 633–649.
85. Lam, W. C. *et al*. (1994). Phosphorescence and optically detected magnetic resonance investigation of the binding of the nucleocapsid protein of the human immunodeficiency virus type 1 and related peptides to RNA. *Biochemistry* **33,** 10693–10700.
86. Lam, W. C. *et al*. (1993). Evidence for stacking interactions between 5-mercurated polyuridylic acid and HIV-1 p7 nucleocapsid protein obtained by phosphorescence and optically detected magnetic resonance (ODMR). *FEBS Lett.* **328,** 45–48.

87. Mély, Y. *et al*. (1993). Influence of the N- and C-terminal chains on the zinc-binding and conformational properties of the central zinc-finger structure of Moloney murine leukemia virus nucleocapsid protein: A steady-state and time-resolved fluorescence study. *Biochim. Biophys. Acta* **1161,** 6–18.
88. Clever, J., Sassetti, C., and Parslow, T. G. (1995). RNA secondary structure and binding sites for gag gene products in the 5′ packaging signal of human immunodeficiency virus type 1. *J. Virol.* **69,** 2101–2109.
89. Paoletti, A. C., Shubsda, M. F., Hudson, B. S., and Borer, P. N. (2002). Affinities of the nucleocapsid protein for variants of SL3 RNA in HIV-1. *Biochemistry* **41,** 15423–15428.
90. Yuan, Y., Kerwood, D. J., Paoletti, A. C., Shubsda, M. F., and Borer, P. N. (2003). Stem of SL1 RNA in HIV-1: Structure and nucleocapsid protein binding for a 1 × 3 internal loop. *Biochemistry* **42,** 5259–5269.
91. Maki, A. H., Ozarowski, A., Misra, A., Urbaneja, M. A., and Casas-Finet, J. R. (2001). Phosphorescence and optically detected magnetic resonance of HIV-1 nucleocapsid protein complexes with stem-loop sequences of the genomic Ψ-recognition element. *Biochemistry* **40,** 1403–1412.
92. Amarasinghe, G. K. *et al*. (2001). Stem-loop SL4 of the HIV-1 Ψ RNA packaging signal exhibits weak affinity for the nucleocapsid protein. Structural studies and implications for genome recognition. *J. Mol. Biol.* **314,** 961–970.
93. Hagan, N., and Fabris, D. (2003). Direct mass spectrometric determination of the stoichiometry and binding affinity of the complexes between nucleocapsid protein and RNA stem-loop hairpins of the HIV-1 Ψ-recognition element. *Biochemistry* **42,** 10736–10745.
94. Amarasinghe, G. K., De Guzman, R. N., Turner, R. B., and Summers, M. F. (2000). NMR structure of stem-loop SL2 of the HIV-1 Ψ RNA packaging signal reveals a novel A-U-A base-triple platform. *J. Mol. Biol.* **299,** 145–156.
95. Maynard, A. T., Huang, M., Rice, W. G., and Covell, D. G. (1998). Reactivity of the HIV-1 nucleocapsid protein p7 zinc finger domains from the perspective of density-functional theory. *Proc. Natl. Acad. Sci. USA* **95,** 11578–11583.
96. Khandogin, J., Musier-Forsyth, K., and York, D. M. (2003). Insights into the regioselectivity and RNA-binding affinity of HIV-1 nucleocapsid protein from linear-scaling quantum methods. *J. Mol. Biol.* **330,** 993–1004.
97. Basrur, V. *et al*. (2000). Inactivation of HIV-1 nucleocapsid protein P7 by pyridinioalkanoyl thioesters. Characterization of reaction products and proposed mechanism of action. *J. Biol. Chem.* **275,** 14890–14897.
98. Kohlstaedt, L. A., Wang, J., Friedman, J. M., Rice, P. A., and Steitz, T. A. (1992). Crystal structure at 3.5 Å resolution of HIV-1 reverse transcriptase complexed with an inhibitor. *Science* **256,** 1783–1790.
99. Jacobo-Molina, A. *et al*. (1993). Crystal structure of human immunodeficiency virus type 1 reverse transcriptase complexed with double-stranded DNA at 3.0 Å resolution shows bent DNA. *Proc. Natl. Acad. Sci. USA* **90,** 6320–6324.
100. Skalka, A. M., and Goff, S. P. (1993). "Reverse Transcriptase." Cold Spring Harbor Laboratory Press, Cold Spring Harbor, New York.
101. Waters, L. C., and Mullin, B. C. (1977). Transfer RNA in RNA tumor viruses. *Prog. Nucleic. Acid. Res. Mol. Biol.* **20,** 131–160.
102. Kleiman, L., Halwani, R., and Javanbakht, H. (2004). The selective packaging and annealing of primer $tRNA^{Lys3}$ in HIV-1. *Curr. HIV Res.* **2,** 163–175.
103. Marquet, R., Isel, C., Ehresmann, C., and Ehresmann, B. (1995). tRNAs as primer of reverse transcriptases. *Biochimie* **77,** 113–124.

104. Sawyer, R. C., and Hanafusa, H. (1979). Comparison of the small RNAs of polymerase-deficient and polymerase-positive Rous sarcoma virus and another species of avian retrovirus. *J. Virol.* **29,** 863–871.
105. Peters, G. G., and Hu, J. (1980). Reverse transcriptase as the major determinant for selective packaging of tRNA's into avian sarcoma virus particles. *J. Virol.* **36,** 692–700.
106. Levin, J. G., and Seidman, J. G. (1981). Effect of polymerase mutations on packaging of primer $tRNA^{Pro}$ during murine leukemia virus assembly. *J. Virol.* **38,** 403–408.
107. Panet, A. *et al.* (1975). Specific binding of tryptophan transfer RNA to avian myeloblastosis virus RNA-dependent DNA polymerase reverse transcriptase. *Proc. Natl. Acad. Sci. USA* **72,** 2535–2539.
108. Panet, A., Weil, G., and Friis, R. R. (1978). Binding of tryptophanyl-tRNA to the reverse transcriptase of replication-defective avian sarcoma viruses. *J. Virol.* **28,** 434–443.
109. Mak, J. *et al.* (1994). Role of $Pr160^{gag\text{-}pol}$ in mediating the selective incorporation of $tRNA^{Lys}$ into human immunodeficiency virus type 1 particles. *J. Virol.* **68,** 2065–2072.
110. Cen, S. *et al.* (2001). Incorporation of lysyl-tRNA synthetase into human immunodeficiency virus type 1. *J. Virol.* **75,** 5043–5048.
111. Cen, S. *et al.* (2002). Retrovirus-specific packaging of aminoacyl-tRNA synthetases with cognate primer tRNAs. *J. Virol.* **76,** 13111–13115.
112. Javanbakht, H., Cen, S., Musier-Forsyth, K., and Kleiman, L. (2002). Correlation between $tRNA^{Lys3}$ aminoacylation and its incorporation into HIV-1. *J. Biol. Chem.* **277,** 17389–17396.
113. Javanbakht, H. *et al.* (2003). The interaction between HIV-1 Gag and human lysyl-tRNA synthetase during viral assembly. *J. Biol. Chem.* **278,** 27644–27651.
114. Kleiman, L., and Cen, S. (2004). The $tRNA^{Lys}$ packaging complex in HIV-1. *Int. J. Biochem. Cell Biol.* **36,** 1776–1786.
115. Prats, A. C. *et al.* (1991). Viral RNA annealing activities of the nucleocapsid protein of Moloney murine leukemia virus are zinc independent. *Nucleic Acids Res.* **19,** 3533–3541.
116. Hargittai, M. R., Gorelick, R. J., Rouzina, I., and Musier-Forsyth, K. (2004). Mechanistic insights into the kinetics of HIV-1 nucleocapsid protein-facilitated tRNA annealing to the primer binding site. *J. Mol. Biol.* **337,** 951–968.
117. Hargittai, M. R. S., Mangla, A. T., Gorelick, R. J., and Musier-Forsyth, K. (2001). HIV-1 nucleocapsid protein zinc finger structures induce $tRNA^{Lys,3}$ structural changes but are not critical for primer/template annealing. *J. Mol. Biol.* **312,** 985–997.
118. Brulé, F. *et al.* (2002). Structural and functional properties of the HIV-1 RNA-$tRNA_3^{Lys}$ primer complex annealed by the nucleocapsid protein: Comparison with the heat-annealed complex. *RNA* **8,** 8–15.
119. Isel, C. *et al.* (1996). Specific initiation and switch to elongation of human immunodeficiency virus type 1 reverse transcription require the post-transcriptional modifications of primer $tRNA_3^{Lys}$. *EMBO J.* **15,** 917–924.
120. Lanchy, J. M., Ehresmann, C., Le Grice, S. F. J., Ehresmann, B., and Marquet, R. (1996). Binding and kinetic properties of HIV-1 reverse transcriptase markedly differ during initiation and elongation of reverse transcription. *EMBO J.* **15,** 7178–7187.
121. Lanchy, J. M. *et al.* (1998). Contacts between reverse transcriptase and the primer strand govern the transition from initiation to elongation of HIV-1 reverse transcription. *J. Biol. Chem.* **273,** 24425–24432.
122. Liang, C. *et al.* (1998). Mechanistic studies of early pausing events during initiation of HIV-1 reverse transcription. *J. Biol. Chem.* **273,** 21309–21315.
123. Thrall, S. H. *et al.* (1998). Pre-steady-state kinetic characterization of RNA-primed initiation of transcription by HIV-1 reverse transcriptase and analysis of the transition to a processive DNA-primed polymerization mode. *Biochemistry* **37,** 13349–13358.

124. Le Grice, S. F. J. (2003). In the beginning: Initiation of minus strand DNA synthesis in retroviruses and LTR-containing retrotransposons. *Biochemistry* **42,** 14349–14355.

125. Isel, C., Ehresmann, C., Keith, G., Ehresmann, B., and Marquet, R. (1995). Initiation of reverse transcription of HIV-1: Secondary structure of the HIV-1 RNA/$tRNA_3^{Lys}$ (template/primer). *J. Mol. Biol.* **247,** 236–250.

126. Skripkin, E., Isel, C., Marquet, R., Ehresmann, B., and Ehresmann, C. (1996). Psoralen crosslinking between human immunodeficiency virus type 1 RNA and primer $tRNA_3^{Lys}$. *Nucleic Acids Res.* **24,** 509–514.

127. Khan, R., and Giedroc, D. P. (1992). Recombinant human immunodeficiency virus type 1 nucleocapsid (NCp7) protein unwinds tRNA. *J. Biol. Chem.* **267,** 6689–6695.

128. Gregoire, C. J., Gautheret, D., and Loret, E. P. (1997). No $tRNA_3^{Lys}$ unwinding in a complex with HIV NCp7. *J. Biol. Chem.* **272,** 25143–25148.

129. Khan, R., Chang, H. O., Kaluarachchi, K., and Giedroc, D. P. (1996). Interaction of retroviral nucleocapsid proteins with transfer RNA^{Phe}: A lead ribozyme and 1H NMR study. *Nucleic Acids Res.* **24,** 3568–3575.

130. Isel, C., Marquet, R., Keith, G., Ehresmann, C., and Ehresmann, B. (1993). Modified nucleotides of $tRNA_3^{Lys}$ modulate primer/template loop–loop interaction in the initiation complex of HIV-1 reverse transcription. *J. Biol. Chem.* **268,** 25269–25272.

131. Arts, E. J. *et al.* (1996). Initiation of (−) strand DNA synthesis from $tRNA_3^{Lys}$ on lentiviral RNAs: Implications of specific HIV-1 RNA-$tRNA_3^{Lys}$ interactions inhibiting primer utilization by retroviral reverse transcriptases. *Proc. Natl. Acad. Sci. USA* **93,** 10063–10068.

132. Wakefield, J. K., Kang, S. M., and Morrow, C. D. (1996). Construction of a type 1 human immunodeficiency virus that maintains a primer binding site complementary to $tRNA^{His}$. *J. Virol.* **70,** 966–975.

133. Isel, C., Keith, G., Ehresmann, B., Ehresmann, C., and Marquet, R. (1998). Mutational analysis of the $tRNA_3^{Lys}$/HIV-1 RNA (primer/template) complex. *Nucleic Acids Res.* **26,** 1198–1204.

134. Liang, C. *et al.* (1997). The importance of the A-rich loop in human immunodeficiency virus type 1 reverse transcription and infectivity. *J. Virol.* **71,** 5750–5757.

135. Huang, Y. *et al.* (1996). Effects of modifying the $tRNA_3^{Lys}$ anticodon on the initiation of human immunodeficiency virus type 1 reverse transcription. *J. Virol.* **70,** 4700–4706.

136. Kang, S. M., Zhang, Z., and Morrow, C. D. (1997). Identification of a sequence within U5 required for human immunodeficiency virus type 1 to stably maintain a primer binding site complementary to $tRNA^{Met}$. *J. Virol.* **71,** 207–217.

137. Puglisi, E. V., and Puglisi, J. D. (1998). HIV-1 A-rich RNA loop mimics the tRNA anticodon structure. *Nat. Struct. Biol.* **5,** 1033–1036.

138. Goldschmidt, V. *et al.* (2004). Structural variability of the initiation complex of HIV-1 reverse transcription. *J. Biol. Chem.* **279,** 35923–35931.

139. Miller, J. T., Khvorova, A., Scaringe, S. A., and Le Grice, S. F. J. (2004). Synthetic $tRNA^{Lys,3}$ as the replication primer for the $HIV\text{-}1_{HXB2}$ and $HIV\text{-}1_{Mal}$ genomes. *Nucleic Acids Res.* **32,** 4687–4695.

140. Goldschmidt, V. *et al.* (2002). Direct and indirect contributions of RNA secondary structure elements to the initiation of HIV-1 reverse transcription. *J. Biol. Chem.* **277,** 43233–43242.

141. Aiyar, A., Cobrinik, D., Ge, Z., Kung, H. J., and Leis, J. (1992). Interaction between retroviral U5 RNA and the TΨC loop of the $tRNA^{Trp}$ primer is required for efficient initiation of reverse transcription. *J. Virol.* **66,** 2464–2472.

142. Leis, J., Aiyar, A., and Cobrinik, D. (1993). Regulation of initiation of reverse transcription of retroviruses. *In* "Reverse Transcriptase" (A. M. Skalka and S. P. Goff, Eds.), pp. 33–47. Cold Spring Harbor Laboratory Press, Cold Spring Harbor, New York.

143. Morris, S., Johnson, M., Stavnezer, E., and Leis, J. (2002). Replication of avian sarcoma virus *in vivo* requires an interaction between the viral RNA and the TΨC loop of the $tRNA^{Trp}$ primer. *J. Virol.* **76,** 7571–7577.
144. Miller, J. T., Ehresmann, B., Hübscher, U., and Le Grice, S. F. J. (2001). A novel interaction of $tRNA^{Lys,3}$ with the feline immunodeficiency virus RNA genome governs initiation of minus strand DNA synthesis. *J. Biol. Chem.* **276,** 27721–27730.
145. Beerens, N., and Berkhout, B. (2002). The tRNA primer activation signal in the human immunodeficiency virus type 1 genome is important for initiation and processive elongation of reverse transcription. *J. Virol.* **76,** 2329–2339.
146. Beerens, N., Groot, F., and Berkhout, B. (2001). Initiation of HIV-1 reverse transcription is regulated by a primer activation signal. *J. Biol. Chem.* **276,** 31247–31256.
147. Goldschmidt, V., Ehresmann, C., Ehresmann, B., and Marquet, R. (2003). Does the HIV-1 primer activation signal interact with $tRNA_3^{Lys}$ during the initiation of reverse transcription? *Nucleic Acids Res.* **31,** 850–859.
148. Abbink, T. E., Beerens, N., and Berkhout, B. (2004). Forced selection of a human immunodeficiency virus type 1 variant that uses a non-self tRNA primer for reverse transcription: Involvement of viral RNA sequences and the reverse transcriptase enzyme. *J. Virol.* **78,** 10706–10714.
149. Arnott, S., Chandrasekaran, R., Millane, R. P., and Park, H. S. (1986). DNA–RNA hybrid secondary structures. *J. Mol. Biol.* **188,** 631–640.
150. Szyperski, T. *et al*. (1999). NMR structure of the chimeric hybrid duplex r(gcaguggc).r(gcca) d(CTGC) comprising the tRNA–DNA junction formed during initiation of HIV-1 reverse transcription. *J. Biomol. NMR* **13,** 343–355.
151. Lanchy, J. M. *et al*. (2000). Dynamics of the HIV-1 reverse transcription complex during initiation of DNA synthesis. *J. Biol. Chem.* **275,** 12306–12312.
152. Isel, C. *et al*. (1999). Structural basis for the specificity of the initiation of HIV-1 reverse transcription. *EMBO J.* **18,** 1038–1048.
153. Gilboa, E., Mitra, S. W., Goff, S., and Baltimore, D. (1979). A detailed model of reverse transcription and tests of crucial aspects. *Cell* **18,** 93–100.
154. Luo, G. X., and Taylor, J. (1990). Template switching by reverse transcriptase during DNA synthesis. *J. Virol.* **64,** 4321–4328.
155. Peliska, J. A., and Benkovic, S. J. (1992). Mechanism of DNA strand transfer reactions catalyzed by HIV-1 reverse transcriptase. *Science* **258,** 1112–1118.
156. Telesnitsky, A., and Goff, S. P. (1993). Strong-stop strand transfer during reverse transcription of retroviruses. *In* "Reverse Transcriptase" (A. M. Skalka and S. P. Goff, Eds.), pp. 49–83. Cold Spring Harbor Laboratory Press, Cold Spring Harbor, New York.
157. Berkhout, B., and Jeang, K.-T. (1991). Detailed mutational analysis of TAR RNA: Critical spacing between the bulge and loop recognition domains. *Nucleic Acids Res.* **19,** 6169–6176.
158. Baudin, F. *et al*. (1993). Functional sites in the 5′ region of human immunodeficiency virus type 1 RNA form defined structural domains. *J. Mol. Biol.* **229,** 382–397.
159. Panganiban, A. T., and Fiore, D. (1988). Ordered interstrand and intrastrand DNA transfer during reverse transcription. *Science* **241,** 1064–1069.
160. Hu, W. S., and Temin, H. M. (1990). Retroviral recombination and reverse transcription. *Science* **250,** 1227–1233.
161. Jones, J. S., Allan, R. W., and Temin, H. M. (1994). One retroviral RNA is sufficient for synthesis of viral DNA. *J. Virol.* **68,** 207–216.
162. van Wamel, J. L., and Berkhout, B. (1998). The first strand transfer during HIV-1 reverse transcription can occur either intramolecularly or intermolecularly. *Virology* **244,** 245–251.
163. Varmus, H. E. *et al*. (1978). Kinetics of synthesis, structure, and purification of avian sarcoma virus-specific DNA made in the cytoplasm of acutely infected cells. *J. Mol. Biol.* **120,** 55–82.

164. Fu, T. B., and Taylor, J. (1992). When retroviral reverse transcriptases reach the end of their RNA templates. *J. Virol.* **66,** 4271–4278.
165. Garces, J., and Wittek, R. (1991). Reverse-transcriptase-associated RNaseH activity mediates template switching during reverse transcription *in vitro*. *Proc. R. Soc. Lond. B Biol. Sci.* **243,** 235–239.
166. Tanese, N., Telesnitsky, A., and Goff, S. P. (1991). Abortive reverse transcription by mutants of Moloney murine leukemia virus deficient in the reverse transcriptase-associated RNase H function. *J. Virol.* **65,** 4387–4397.
166a. Repaske, R., Hartley, J. W., Kavlick, M. F., O'Neill, R. R., and Austin, J. B. (1989). Inhibition of RNase H activity and viral replication by single mutations in the 3′ region of Moloney murine leukemia virus reverse transcriptase. *J. Virol.* **63,** 1460–1464.
167. Svarovskaia, E. S., Delviks, K. A., Hwang, C. K., and Pathak, V. K. (2000). Structural determinants of murine leukemia virus reverse transcriptase that affect the frequency of template switching. *J. Virol.* **74,** 7171–7178.
168. Hwang, C. K., Svarovskaia, E. S., and Pathak, V. K. (2001). Dynamic copy choice: Steady state between murine leukemia virus polymerase and polymerase-dependent RNase H activity determines frequency of *in vivo* template switching. *Proc. Natl. Acad. Sci. USA* **98,** 12209–12214.
169. Blain, S. W., and Goff, S. P. (1995). Effects on DNA synthesis and translocation caused by mutations in the RNase H domain of Moloney murine leukemia virus reverse transcriptase. *J. Virol.* **69,** 4440–4452.
169a. Andersen, E. S., Jeeninga, R., Damgaard, E. C. K., Berkhout, B., and Kjems, J. (2003). Dimerization and template switching in the 5′ untranslated region between various subtypes of human immunodeficiency virus type 1. *J. Virol.* **77,** 3020–3030.
170. Darlix, J.-L., Vincent, A., Gabus, C., de Rocquigny, H., and Roques, B. (1993). Transactivation of the 5′ to 3′ viral DNA strand transfer by nucleocapsid protein during reverse transcription of HIV-1 RNA. *C. R. Acad. Sci. Paris Life Sciences* **316,** 763–771.
171. Peliska, J. A., Balasubramanian, S., Giedroc, D. P., and Benkovic, S. J. (1994). Recombinant HIV-1 nucleocapsid protein accelerates HIV-1 reverse transcriptase catalyzed DNA strand transfer reactions and modulates RNase H activity. *Biochemistry* **33,** 13817–13823.
172. DeStefano, J. J. (1995). Human immunodeficiency virus nucleocapsid protein stimulates strand transfer from internal regions of heteropolymeric RNA templates. *Arch. Virol.* **140,** 1775–1789.
173. Rodríguez-Rodríguez, L., Tsuchihashi, Z., Fuentes, G. M., Bambara, R. A., and Fay, P. J. (1995). Influence of human immunodeficiency virus nucleocapsid protein on synthesis and strand transfer by the reverse transcriptase *in vitro*. *J. Biol. Chem.* **270,** 15005–15011.
174. Kim, J. K., Palaniappan, C., Wu, W., Fay, P. J., and Bambara, R. A. (1997). Evidence for a unique mechanism of strand transfer from the transactivation response region of HIV-1. *J. Biol. Chem.* **272,** 16769–16777.
175. Lapadat-Tapolsky, M., Gabus, C., Rau, M., and Darlix, J.-L. (1997). Possible roles of HIV-1 nucleocapsid protein in the specificity of proviral DNA synthesis and in its variability. *J. Mol. Biol.* **268,** 250–260.
176. Guo, J., Henderson, L. E., Bess, J., Kane, B., and Levin, J. G. (1997). Human immunodeficiency virus type 1 nucleocapsid protein promotes efficient strand transfer and specific viral DNA synthesis by inhibiting TAR-dependent self-priming from minus-strand strong-stop DNA. *J. Virol.* **71,** 5178–5188.
177. Guo, J., Wu, T., Bess, J., Henderson, L. E., and Levin, J. G. (1998). Actinomycin D inhibits human immunodeficiency virus type 1 minus-strand transfer in *in vitro* and endogenous reverse transcriptase assays. *J. Virol.* **72,** 6716–6724.

178. Guo, J. *et al.* (2000). Zinc finger structures in the human immunodeficiency virus type 1 nucleocapsid protein facilitate efficient minus- and plus-strand transfer. *J. Virol.* **74,** 8980–8988.
179. Guo, J. *et al.* (2002). Subtle alterations of the native zinc finger structures have dramatic effects on the nucleic acid chaperone activity of human immunodeficiency virus type 1 nucleocapsid protein. *J. Virol.* **76,** 4370–4378.
180. Driscoll, M. D., Golinelli, M.-P., and Hughes, S. H. (2001). *In vitro* analysis of human immunodeficiency virus type 1 minus-strand strong-stop DNA synthesis and genomic RNA processing. *J. Virol.* **75,** 672–686.
181. Driscoll, M. D., and Hughes, S. H. (2000). Human immunodeficiency virus type 1 nucleocapsid protein can prevent self-priming of minus-strand strong stop DNA by promoting the annealing of short oligonucleotides to hairpin sequences. *J. Virol.* **74,** 8785–8792.
182. Chen, Y., Balakrishnan, M., Roques, B. P., and Bambara, R. A. (2003). Steps of the acceptor invasion mechanism for HIV-1 minus strand strong stop transfer. *J. Biol. Chem.* **278,** 38368–38375.
183. Chen, Y., Balakrishnan, M., Roques, B. P., Fay, P. J., and Bambara, R. A. (2003). Mechanism of minus strand strong stop transfer in HIV-1 reverse transcription. *J. Biol. Chem.* **278,** 8006–8017.
184. Derebail, S. S., Heath, M. J., and DeStefano, J. J. (2003). Evidence for the differential effects of nucleocapsid protein on strand transfer in various regions of the HIV genome. *J. Biol. Chem.* **278,** 15702–15712.
185. Heilman-Miller, S. L., Wu, T., and Levin, J. G. (2004). Alteration of nucleic acid structure and stability modulates the efficiency of minus-strand transfer mediated by the HIV-1 nucleocapsid protein. *J. Biol. Chem.* **279,** 44154–44165.
186. Moscardini, M. *et al.* (2002). Functional interactions of nucleocapsid protein of feline immunodeficiency virus and cellular prion protein with the viral RNA. *J. Mol. Biol.* **318,** 149–159.
187. Allain, B., Lapadat-Tapolsky, M., Berlioz, C., and Darlix, J.-L. (1994). Transactivation of the minus-strand DNA transfer by nucleocapsid protein during reverse transcription of the retroviral genome. *EMBO J.* **13,** 973–981.
188. Allain, B., Rascle, J. B., de Rocquigny, H., Roques, B., and Darlix, J.-L. (1998). *CIS* elements and *trans*-acting factors required for minus strand DNA transfer during reverse transcription of the genomic RNA of murine leukemia virus. *J. Mol. Biol.* **277,** 225–235.
189. Rascle, J. B., Ficheux, D., and Darlix, J.-L. (1998). Possible roles of nucleocapsid protein of MoMuLV in the specificity of proviral DNA synthesis and in the genetic variability of the virus. *J. Mol. Biol.* **280,** 215–225.
190. Werner, S., Vogel-Bachmayr, K., Hollinderbaumer, B., and Wöhrl, B. M. (2001). Requirements for minus-strand transfer catalyzed by Rous sarcoma virus reverse transcriptase. *J. Virol.* **75,** 10132–10138.
191. Tanchou, V., Gabus, C., Rogemond, V., and Darlix, J.-L. (1995). Formation of stable and functional HIV-1 nucleoprotein complexes *in vitro*. *J. Mol. Biol.* **252,** 563–571.
192. Lapadat-Tapolsky, M. *et al.* (1993). Interactions between HIV-1 nucleocapsid protein and viral DNA may have important functions in the viral life cycle. *Nucleic Acids Res.* **21,** 831–839.
193. You, J. C., and McHenry, C. S. (1994). Human immunodeficiency virus nucleocapsid protein accelerates strand transfer of the terminally redundant sequences involved in reverse transcription. *J. Biol. Chem.* **269,** 31491–31495.
194. Davis, W. R., Gabbara, S., Hupe, D., and Peliska, J. A. (1998). Actinomycin D inhibition of DNA strand transfer reactions catalyzed by HIV-1 reverse transcriptase and nucleocapsid protein. *Biochemistry* **37,** 14213–14221.

195. Hong, M. K. *et al.* (2003). Nucleic acid conformational changes essential for HIV-1 nucleocapsid protein-mediated inhibition of self-priming in minus-strand transfer. *J. Mol. Biol.* **325,** 1–10.
196. Golinelli, M.-P., and Hughes, S. H. (2003). Secondary structure in the nucleic acid affects the rate of HIV-1 nucleocapsid-mediated strand annealing. *Biochemistry* **42,** 8153–8162.
197. Williams, M. C. *et al.* (2001). Mechanism for nucleic acid chaperone activity of HIV-1 nucleocapsid protein revealed by single molecule stretching. *Proc. Natl. Acad. Sci. USA* **98,** 6121–6126.
198. Williams, M. C., Gorelick, R. J., and Musier-Forsyth, K. (2002). Specific zinc-finger architecture required for HIV-1 nucleocapsid protein's nucleic acid chaperone function. *Proc. Natl. Acad. Sci. USA* **99,** 8614–8619.
199. Heath, M. J., Derebail, S. S., Gorelick, R. J., and DeStefano, J. J. (2003). Differing roles of the N- and C-terminal zinc fingers in human immunodeficiency virus nucleocapsid protein-enhanced nucleic acid annealing. *J. Biol. Chem.* **278,** 30755–30763.
200. Brulé, F. *et al.* (2000). *In vitro* evidence for the interaction of $tRNA_3^{Lys}$ with U3 during the first strand transfer of HIV-1 reverse transcription. *Nucleic Acids Res.* **28,** 634–640.
201. Golinelli, M.-P., and Hughes, S. H. (2001). Self-priming of retroviral minus-strand strong-stop DNAs. *Virology* **285,** 278–290.
202. Bernacchi, S. *et al.* (2002). HIV-1 nucleocapsid protein activates transient melting of least stable parts of the secondary structure of TAR and its complementary sequence. *J. Mol. Biol.* **317,** 385–399.
203. Beltz, H. *et al.* (2003). Impact of the terminal bulges of HIV-1 cTAR DNA on its stability and the destabilizing activity of the nucleocapsid protein NCp7. *J. Mol. Biol.* **328,** 95–108.
204. Oyama, F., Kikuchi, R., Crouch, R. J., and Uchida, T. (1989). Intrinsic properties of reverse transcriptase in reverse transcription. Associated RNase H is essentially regarded as an endonuclease. *J. Biol. Chem.* **264,** 18808–18817.
205. Schatz, O., Mous, J., and Le Grice, S. F. J. (1990). HIV-1 RT-associated ribonuclease H displays both endonuclease and 3′ → 5′ exonuclease activity. *EMBO J.* **9,** 1171–1176.
206. Wöhrl, B. M., and Moelling, K. (1990). Interaction of HIV-1 ribonuclease H with polypurine tract containing RNA–DNA hybrids. *Biochemistry* **29,** 10141–10147.
207. Furfine, E. S., and Reardon, J. E. (1991). Reverse transcriptase•RNase H from the human immunodeficiency virus. Relationship of the DNA polymerase and RNA hydrolysis activities. *J. Biol. Chem.* **266,** 406–412.
208. Furfine, E. S., and Reardon, J. E. (1991). Human immunodeficiency virus reverse transcriptase ribonuclease H: Specificity of $tRNA^{Lys3}$-primer excision. *Biochemistry* **30,** 7041–7046.
209. Gopalakrishnan, V., Peliska, J. A., and Benkovic, S. J. (1992). Human immunodeficiency virus type 1 reverse transcriptase: Spatial and temporal relationship between the polymerase and RNase H activities. *Proc. Natl. Acad. Sci. USA* **89,** 10763–10767.
210. Post, K. *et al.* (1993). A large deletion in the connection subdomain of murine leukemia virus reverse transcriptase or replacement of the RNase H domain with *Escherichia coli* RNase H results in altered polymerase and RNase H activities. *Biochemistry* **32,** 5508–5517.
211. DeStefano, J. J. *et al.* (1991). Polymerization and RNase H activities of the reverse transcriptases from avian myeloblastosis, human immunodeficiency, and Moloney murine leukemia viruses are functionally uncoupled. *J. Biol. Chem.* **266,** 7423–7431.
212. Ben-Artzi, H. *et al.* (1993). RNase H activity of reverse transcriptases on substrates derived from the 5′ end of retroviral genome. *J. Biol. Chem.* **268,** 16465–16471.
213. Randolph, C. A., and Champoux, J. J. (1994). The use of DNA and RNA oligonucleotides in hybrid structures with longer polynucleotide chains to probe the structural requirements for Moloney murine leukemia virus plus strand priming. *J. Biol. Chem.* **269,** 19207–19215.

214. Götte, M., Maier, G., Gross, H. J., and Heumann, H. (1998). Localization of the active site of HIV-1 reverse transcriptase-associated RNase H domain on a DNA template using site-specific generated hydroxyl radicals. *J. Biol. Chem.* **273,** 10139–10146.
215. DeStefano, J. J., Mallaber, L. M., Fay, P. J., and Bambara, R. A. (1994). Quantitative analysis of RNA cleavage during RNA-directed DNA synthesis by human immunodeficiency and avian myeloblastosis virus reverse transcriptases. *Nucleic Acids Res.* **22,** 3793–3800.
216. Champoux, J. J. (1993). Roles of ribonuclease H in reverse transcription. *In* "Reverse Transcriptase" (A. M. Skalka and S. P. Goff, Eds.), pp. 103–117. Cold Spring Harbor Laboratory Press, Cold Spring Harbor, New York.
217. DeStefano, J. J., Buiser, R. G., Mallaber, L. M., Bambara, R. A., and Fay, P. J. (1991). Human immunodeficiency virus reverse transcriptase displays a partially processive 3′ to 5′ endonuclease activity. *J. Biol. Chem.* **266,** 24295–24301.
218. Wöhrl, B. M., Volkmann, S., and Moelling, K. (1991). Mutations of a conserved residue within HIV-1 ribonuclease H affect its exo- and endonuclease activities. *J. Mol. Biol.* **220,** 801–818.
219. Kati, W. M., Johnson, K. A., Jerva, L. F., and Anderson, K. S. (1992). Mechanism and fidelity of HIV reverse transcriptase. *J. Biol. Chem.* **267,** 25988–25997.
220. Powell, M. D. *et al*. (1999). Residues in the αH and αI helices of the HIV-1 reverse transcriptase thumb subdomain required for the specificity of RNase H-catalyzed removal of the polypurine tract primer. *J. Biol. Chem.* **274,** 19885–19893.
221. Schultz, S. J., Zhang, M., Kelleher, C. D., and Champoux, J. J. (1999). Polypurine tract primer generation and utilization by Moloney murine leukemia virus reverse transcriptase. *J. Biol. Chem.* **274,** 34547–34555.
222. Wisniewski, M., Balakrishnan, M., Palaniappan, C., Fay, P. J., and Bambara, R. A. (2000). Unique progressive cleavage mechanism of HIV reverse transcriptase RNase H. *Proc. Natl. Acad. Sci. USA* **97,** 11978–11983.
223. Wisniewski, M., Balakrishnan, M., Palaniappan, C., Fay, P. J., and Bambara, R. A. (2000). The sequential mechanism of HIV reverse transcriptase RNase H. *J. Biol. Chem.* **275,** 37664–37671.
224. Wisniewski, M. *et al*. (2002). Substrate requirements for secondary cleavage by HIV-1 reverse transcriptase RNase H. *J. Biol. Chem.* **277,** 28400–28410.
225. Palaniappan, C., Fuentes, G. M., Rodríguez-Rodríguez, L., Fay, P. J., and Bambara, R. A. (1996). Helix structure and ends of RNA/DNA hybrids direct the cleavage specificity of HIV-1 reverse transcriptase RNase H. *J. Biol. Chem.* **271,** 2063–2070.
226. DeStefano, J. J. (1995). The orientation of binding of human immunodeficiency virus reverse transcriptase on nucleic acid hybrids. *Nucleic Acids Res.* **23,** 3901–3908.
227. DeStefano, J. J., Cristofaro, J. V., Derebail, S., Bohlayer, W. P., and Fitzgerald-Heath, M. J. (2001). Physical mapping of HIV reverse transcriptase to the 5′ end of RNA primers. *J. Biol. Chem.* **276,** 32515–32521.
228. Gao, H. Q., Sarafianos, S. G., Arnold, E., and Hughes, S. H. (2001). RNase H cleavage of the 5′ end of the human immunodeficiency virus type 1 genome. *J. Virol.* **75,** 11874–11880.
229. Cameron, C. E., Ghosh, M., Le Grice, S. F. J., and Benkovic, S. J. (1997). Mutations in HIV reverse transcriptase which alter RNase H activity and decrease strand transfer efficiency are suppressed by HIV nucleocapsid protein. *Proc. Natl. Acad. Sci. USA* **94,** 6700–6705.
230. Lener, D., Tanchou, V., Roques, B. P., Le Grice, S. F. J., and Darlix, J.-L. (1998). Involvement of HIV-I nucleocapsid protein in the recruitment of reverse transcriptase into nucleoprotein complexes formed *in vitro*. *J. Biol. Chem.* **273,** 33781–33786.
231. Druillennec, S., Caneparo, A., de Rocquigny, H., and Roques, B. P. (1999). Evidence of interactions between the nucleocapsid protein NCp7 and the reverse transcriptase of HIV-1. *J. Biol. Chem.* **274,** 11283–11288.

232. Berkhout, B., van Wamel, J., and Klaver, B. (1995). Requirements for DNA strand transfer during reverse transcription in mutant HIV-1 virions. *J. Mol. Biol.* **252,** 59–69.
233. Lobel, L. I., and Goff, S. P. (1985). Reverse transcription of retroviral genomes: Mutations in the terminal repeat sequences. *J. Virol.* **53,** 447–455.
234. Ramsey, C. A., and Panganiban, A. T. (1993). Replication of the retroviral terminal repeat sequence during *in vivo* reverse transcription. *J. Virol.* **67,** 4114–4121.
235. Klaver, B., and Berkhout, B. (1994). Premature strand transfer by the HIV-1 reverse transcriptase during strong-stop DNA synthesis. *Nucleic Acids Res.* **22,** 137–144.
236. Kulpa, D., Topping, R., and Telesnitsky, A. (1997). Determination of the site of first strand transfer during Moloney murine leukemia virus reverse transcription and identification of strand transfer-associated reverse transcriptase errors. *EMBO J.* **16,** 856–865.
237. Yin, P. D., Pathak, V. K., Rowan, A. E., Teufel, R. J., II, and Hu, W.-S. (1997). Utilization of nonhomologous minus-strand DNA transfer to generate recombinant retroviruses. *J. Virol.* **71,** 2487–2494.
238. Ohi, Y., and Clever, J. L. (2000). Sequences in the 5′ and 3′ R elements of human immunodeficiency virus type 1 critical for efficient reverse transcription. *J. Virol.* **74,** 8324–8334.
239. Dang, Q., and Hu, W.-S. (2001). Effects of homology length in the repeat region on minus-strand DNA transfer and retroviral replication. *J. Virol.* **75,** 809–820.
240. Pfeiffer, J. K., and Telesnitsky, A. (2001). Effects of limiting homology at the site of intermolecular recombinogenic template switching during Moloney murine leukemia virus replication. *J. Virol.* **75,** 11263–11274.
241. Roda, R. H. *et al.* (2002). Strand transfer occurs in retroviruses by a pause-initiated two-step mechanism. *J. Biol. Chem.* **277,** 46900–46911.
242. Derebail, S. S., and DeStefano, J. J. (2004). Mechanistic analysis of pause site dependent and independent recombinogenic strand transfer from structurally diverse regions of the HIV genome. *J. Biol. Chem.* **279,** 47446–47454.
243. Negroni, M., and Buc, H. (2000). Copy-choice recombination by reverse transcriptases: Reshuffling of genetic markers mediated by RNA chaperones. *Proc. Natl. Acad. Sci. USA* **97,** 6385–6390.
244. Moumen, A. *et al.* (2003). Evidence for a mechanism of recombination during reverse transcription dependent on the structure of the acceptor RNA. *J. Biol. Chem.* **278,** 15973–15982.
245. Galetto, R. *et al.* (2004). The structure of HIV-1 genomic RNA in the gp120 gene determines a recombination hot spot *in vivo*. *J. Biol. Chem.* **279,** 36625–36632.
246. Roda, R. H. *et al.* (2003). Role of the reverse transcriptase, nucleocapsid protein, and template structure in the two-step transfer mechanism in retroviral recombination. *J. Biol. Chem.* **278,** 31536–31546.
247. Berkhout, B., Vastenhouw, N. L., Klasens, B. I. F., and Huthoff, H. (2001). Structural features in the HIV-1 repeat region facilitate strand transfer during reverse transcription. *RNA* **7,** 1097–1114.
247a. Heath, M. J., and DeStefano, J. J. (2005). A complementary single-stranded docking site is required for enhancement of strand exchange by human immunodeficiency virus nucleocapsid protein on substrates that model viral recombination. *Biochemistry* **44,** 3915–3925.
248. Zuker, M., Mathews, D. H., and Turner, D. H. (1999). Algorithms and thermodynamics for RNA secondary structure prediction: A practical guide. *In* "RNA Biochemistry and Biotechnology" (J. Barciszewski and B. F. C. Clark, Eds.), pp. 11–43. Kluwer Academic Publishers, Dordrecht, The Netherlands.
249. Mathews, D. H., Sabina, J., Zuker, M., and Turner, D. H. (1999). Expanded sequence dependence of thermodynamic parameters improves prediction of RNA secondary structure. *J. Mol. Biol.* **288,** 911–940.

250. South, T. L., and Summers, M. F. (1993). Zinc- and sequence-dependent binding to nucleic acids by the N-terminal zinc finger of the HIV-1 nucleocapsid protein: NMR structure of the complex with the Psi-site analog, dACGCC. *Protein Sci.* **2,** 3–19.
251. Morellet, N. *et al*. (1998). Structure of the complex between the HIV-1 nucleocapsid protein NCp7 and the single-stranded pentanucleotide d(ACGCC). *J. Mol. Biol.* **283,** 419–434.
252. Balakrishnan, M., Fay, P. J., and Bambara, R. A. (2001). The kissing hairpin sequence promotes recombination within the HIV-I 5′ leader region. *J. Biol. Chem.* **276,** 36482–36492.
253. Balakrishnan, M., Roques, B. P., Fay, P. J., and Bambara, R. A. (2003). Template dimerization promotes an acceptor invasion-induced transfer mechanism during human immunodeficiency virus type 1 minus-strand synthesis. *J. Virol.* **77,** 4710–4721.
254. Telesnitsky, A., and Goff, S. P. (1993). RNase H domain mutations affect the interaction between Moloney murine leukemia virus reverse transcriptase and its primer-template. *Proc. Natl. Acad. Sci. USA* **90,** 1276–1280.
255. Guo, J. *et al*. (1995). Defects in primer-template binding, processive DNA synthesis, and RNase H activity associated with chimeric reverse transcriptases having the murine leukemia virus polymerase domain joined to *Escherichia coli* RNase H. *Biochemistry* **34,** 5018–5029.
256. Dudding, L. R., Nkabinde, N. C., and Mizrahi, V. (1991). Analysis of the RNA- and DNA-dependent DNA polymerase activities of point mutants of HIV-1 reverse transcriptase lacking ribonuclease H activity. *Biochemistry* **30,** 10498–10506.
257. DeStefano, J. J., Mallaber, L. M., Rodríguez-Rodríguez, L., Fay, P. J., and Bambara, R. A. (1992). Requirements for strand transfer between internal regions of heteropolymer templates by human immunodeficiency virus reverse transcriptase. *J. Virol.* **66,** 6370–6378.
258. Klarmann, G. J., Schauber, C. A., and Preston, B. D. (1993). Template-directed pausing of DNA synthesis by HIV-1 reverse transcriptase during polymerization of HIV-1 sequences *in vitro*. *J. Biol. Chem.* **268,** 9793–9802.
259. Suo, Z., and Johnson, K. A. (1997). Effect of RNA secondary structure on RNA cleavage catalyzed by HIV-1 reverse transcriptase. *Biochemistry* **36,** 12468–12476.
260. Suo, Z., and Johnson, K. A. (1997). RNA secondary structure switching during DNA synthesis catalyzed by HIV-1 reverse transcriptase. *Biochemistry* **36,** 14778–14785.
261. Harrison, G. P., Mayo, M. S., Hunter, E., and Lever, A. M. (1998). Pausing of reverse transcriptase on retroviral RNA templates is influenced by secondary structures both 5′ and 3′ of the catalytic site. *Nucleic Acids Res.* **26,** 3433–3442.
262. Post, K. *et al*. (2003). Human immunodeficiency virus type 2 reverse transcriptase activity in model systems that mimic steps in reverse transcription. *J. Virol.* **77,** 7623–7634.
263. Messer, L. I. *et al*. (1985). Functional analysis of reverse transcription by a frameshift *pol* mutant of murine leukemia virus. *Virology* **146,** 146–152.
264. Fuentes, G. M., Rodríguez-Rodríguez, L., Fay, P. J., and Bambara, R. A. (1995). Use of an oligoribonucleotide containing the polypurine tract sequence as a primer by HIV reverse transcriptase. *J. Biol. Chem.* **270,** 28169–28176.
265. Powell, M. D., and Levin, J. G. (1996). Sequence and structural determinants required for priming of plus-strand DNA synthesis by the human immunodeficiency virus type 1 polypurine tract. *J. Virol.* **70,** 5288–5296.
266. Götte, M. *et al*. (1999). Temporal coordination between initiation of HIV (+)-strand DNA synthesis and primer removal. *J. Biol. Chem.* **274,** 11159–11169.
267. Schultz, S. J., Zhang, M., Kelleher, C. D., and Champoux, J. J. (2000). Analysis of plus-strand primer selection, removal, and reutilization by retroviral reverse transcriptases. *J. Biol. Chem.* **275,** 32299–32309.

268. Schultz, S. J., Zhang, M., and Champoux, J. J. (2003). Specific cleavages by RNase H facilitate initiation of plus-strand RNA synthesis by Moloney murine leukemia virus. *J. Virol.* **77,** 5275–5285.
269. Rausch, J. W., and Le Grice, S. F. J. (2004). "Binding, bending, and bonding": Polypurine tract-primed initiation of plus-strand DNA synthesis in human immunodeficiency virus. *Int. J. Biochem. Cell. Biol.* **36,** 1752–1766.
270. Powell, M. D. *et al.* (1997). Alanine-scanning mutations in the "primer grip" of p66 HIV-1 reverse transcriptase result in selective loss of RNA priming activity. *J. Biol. Chem.* **272,** 13262–13269.
271. Ghosh, M., Williams, J., Powell, M. D., Levin, J. G., and Le Grice, S. F. J. (1997). Mutating a conserved motif of the HIV-1 reverse transcriptase palm subdomain alters primer utilization. *Biochemistry* **36,** 5758–5768.
272. Fedoroff, O. Y., Salazar, M., and Reid, B. R. (1993). Structure of a DNA:RNA hybrid duplex. Why RNase H does not cleave pure RNA. *J. Mol. Biol.* **233,** 509–523.
273. Sarafianos, S. G. *et al.* (2001). Crystal structure of HIV-1 reverse transcriptase in complex with a polypurine tract RNA:DNA. *EMBO J.* **20,** 1449–1461.
274. Kvaratskhelia, M., Budihas, S. R., and Le Grice, S. F. J. (2002). Pre-existing distortions in nucleic acid structure aid polypurine tract selection by HIV-1 reverse transcriptase. *J. Biol. Chem.* **277,** 16689–16696.
275. Charneau, P., and Clavel, F. (1991). A single-stranded gap in human immunodeficiency virus unintegrated linear DNA defined by a central copy of the polypurine tract. *J. Virol.* **65,** 2415–2421.
276. Hungnes, O., Tjøtta, E., and Grinde, B. (1991). The plus strand is discontinuous in a subpopulation of unintegrated HIV-1 DNA. *Arch. Virol.* **116,** 133–141.
277. Charneau, P., Alizon, M., and Clavel, F. (1992). A second origin of DNA plus-strand synthesis is required for optimal human immunodeficiency virus replication. *J. Virol.* **66,** 2814–2820.
278. Hungnes, O., Tjøtta, E., and Grinde, B. (1992). Mutations in the central polypurine tract of HIV-1 result in delayed replication. *Virology* **190,** 440–442.
279. Klarmann, G. J., Yu, H., Chen, X., Dougherty, J. P., and Preston, B. D. (1997). Discontinuous plus-strand DNA synthesis in human immunodeficiency virus type 1-infected cells and in a partially reconstituted cell-free system. *J. Virol.* **71,** 9259–9269.
280. Roth, M. J., Schwartzberg, P. L., and Goff, S. P. (1989). Structure of the termini of DNA intermediates in the integration of retroviral DNA: Dependence on IN function and terminal DNA sequence. *Cell* **58,** 47–54.
281. Renda, M. J. *et al.* (2001). Mutation of the methylated $tRNA_3^{Lys}$ residue A58 disrupts reverse transcription and inhibits replication of human immunodeficiency virus type 1. *J. Virol.* **75,** 9671–9678.
282. Ben-Artzi, H. *et al.* (1996). Molecular analysis of the second template switch during reverse transcription of the HIV RNA template. *Biochemistry* **35,** 10549–10557.
283. Burnett, B. P., and McHenry, C. S. (1997). Posttranscriptional modification of retroviral primers is required for late stages of DNA replication. *Proc. Natl. Acad. Sci. USA* **94,** 7210–7215.
284. Adachi, A. *et al.* (1986). Production of acquired immunodeficiency syndrome-associated retrovirus in human and nonhuman cells transfected with an infectious molecular clone. *J. Virol.* **59,** 284–291.
285. Smith, C. M., Smith, J. S., and Roth, M. J. (1999). RNase H requirements for the second strand transfer reaction of human immunodeficiency virus type 1 reverse transcription. *J. Virol.* **73,** 6573–6581.
286. Yusupova, G. *et al.* (1996). Primer selection by HIV-1 reverse transcriptase on RNA-$tRNA_3^{Lys}$ and DNA-$tRNA_3^{Lys}$ hybrids. *J. Mol. Biol.* **261,** 315–321.

287. Kulkosky, J., Katz, R. A., and Skalka, A. M. (1990). Terminal nucleotides of the preintegrative linear form of HIV-1 DNA deduced from the sequence of circular DNA junctions. *J. Acquir. Immune Defic. Syndr.* **3,** 852–858.
288. Smith, J. S., Kim, S. Y., and Roth, M. J. (1990). Analysis of long terminal repeat circle junctions of human immunodeficiency virus type 1. *J. Virol.* **64,** 6286–6290.
289. Whitcomb, J. M., Kumar, R., and Hughes, S. H. (1990). Sequence of the circle junction of human immunodeficiency virus type 1: Implications for reverse transcription and integration. *J. Virol.* **64,** 4903–4906.
290. Hong, T., Drlica, K., Pinter, A., and Murphy, E. (1991). Circular DNA of human immunodeficiency virus: Analysis of circle junction nucleotide sequences. *J. Virol.* **65,** 551–555.
291. Pullen, K. A., Ishimoto, L. K., and Champoux, J. J. (1992). Incomplete removal of the RNA primer for minus-strand DNA synthesis by human immunodeficiency virus type 1 reverse transcriptase. *J. Virol.* **66,** 367–373.
292. Smith, J. S., and Roth, M. J. (1992). Specificity of human immunodeficiency virus-1 reverse transcriptase-associated ribonuclease H in removal of the minus-strand primer, $tRNA^{Lys3}$. *J. Biol. Chem.* **267,** 15071–15079.
293. Schultz, S. J., Whiting, S. H., and Champoux, J. J. (1995). Cleavage specificities of Moloney murine leukemia virus RNase H implicated in the second strand transfer during reverse transcription. *J. Biol. Chem.* **270,** 24135–24145.
294. Smith, C. M., Potts, W. B., III, Smith, J. S., and Roth, M. J. (1997). RNase H cleavage of $tRNA^{Pro}$ mediated by M-MuLV and HIV-1 reverse transcriptases. *Virology* **229,** 437–446.
295. Omer, C. A., and Faras, A. J. (1982). Mechanism of release of the avian retrovirus $tRNA^{Trp}$ primer molecule from viral DNA by ribonuclease H during reverse transcription. *Cell* **30,** 797–805.
296. Schatz, O., Cromme, F. V., Grüninger-Leitch, F., and Le Grice, S. F. J. (1989). Point mutations in conserved amino acid residues within the C-terminal domain of HIV-1 reverse transcriptase specifically repress RNase H function. *FEBS Lett.* **257,** 311–314.
297. Kelleher, C. D., and Champoux, J. J. (1998). Characterization of RNA strand displacement synthesis by Moloney murine leukemia virus reverse transcriptase. *J. Biol. Chem.* **273,** 9976–9986.
298. Fuentes, G. M., Fay, P. J., and Bambara, R. A. (1996). Relationship between plus strand DNA synthesis removal of downstream segments of RNA by human immunodeficiency virus, murine leukemia virus, and avian myeloblastoma virus reverse transcriptases. *Nucleic Acids Res.* **24,** 1719–1726.
299. Lanciault, C., and Champoux, J. J. (2004). Single unpaired nucleotides facilitate HIV-1 reverse transcriptase displacement synthesis through duplex RNA. *J. Biol. Chem.* **279,** 32252–32261.
300. Egelé, C. *et al*. (2004). HIV-1 nucleocapsid protein binds to the viral DNA initiation sequences and chaperones their kissing interactions. *J. Mol. Biol.* **342,** 453–466.
301. Bebenek, K., Abbotts, J., Roberts, J. D., Wilson, S. H., and Kunkel, T. A. (1989). Specificity and mechanism of error-prone replication by human immunodeficiency virus-1 reverse transcriptase. *J. Biol. Chem.* **264,** 16948–16956.
302. Huber, H. E., McCoy, J. M., Seehra, J. S., and Richardson, C. C. (1989). Human immunodeficiency virus 1 reverse transcriptase. Template binding, processivity, strand displacement synthesis, and template switching. *J. Biol. Chem.* **264,** 4669–4678.
303. Williams, K. J., Loeb, L. A., and Fry, M. (1990). Synthesis of DNA by human immunodeficiency virus reverse transcriptase is preferentially blocked at template oligo(deoxyadenosine) tracts. *J. Biol. Chem.* **265,** 18682–18689.
304. Ratner, L. *et al*. (1985). Complete nucleotide sequence of the AIDS virus, HTLV-III. *Nature* **313,** 277–284.

305. Shinnick, T. M., Lerner, R. A., and Sutcliffe, J. G. (1981). Nucleotide sequence of Moloney murine leukaemia virus. *Nature* **293,** 543–548.
306. Bendinelli, M. *et al.* (1995). Feline immunodeficiency virus: An interesting model for AIDS studies and an important cat pathogen. *Clin. Microbiol. Rev.* **8,** 87–112.
307. Shank, P. R. *et al.* (1978). Mapping unintegrated avian sarcoma virus DNA: Termini of linear DNA bear 300 nucleotides present once or twice in two species of circular DNA. *Cell* **15,** 1383–1395.
308. Collett, M. S., Leis, J. P., Smith, M. S., and Faras, A. J. (1978). Unwinding-like activity associated with avian retrovirus RNA-directed DNA polymerase. *J. Virol.* **26,** 498–509.
309. Matson, S. W., Fay, P. J., and Bambara, R. A. (1980). Mechanism of inhibition of the avian myeloblastosis virus deoxyribonucleic acid polymerase by adriamycin. *Biochemistry* **19,** 2089–2096.
310. Boone, L. R., and Skalka, A. M. (1981). Viral DNA synthesized *in vitro* by avian retrovirus particles permeabilized with melittin. II. Evidence for a strand displacement mechanism in plus-strand synthesis. *J. Virol.* **37,** 117–126.
311. Hottiger, M., Podust, V. N., Thimmig, R. L., McHenry, C., and Hübscher, U. (1994). Strand displacement activity of the human immunodeficiency virus type 1 reverse transcriptase heterodimer and its individual subunits. *J. Biol. Chem.* **269,** 986–991.
312. Fuentes, G. M., Rodríguez-Rodríguez, L., Palaniappan, C., Fay, P. J., and Bambara, R. A. (1996). Strand displacement synthesis of the long terminal repeats by HIV reverse transcriptase. *J. Biol. Chem.* **271,** 1966–1971.
313. Stetor, S. R. *et al.* (1999). Characterization of (+) strand initiation and termination sequences located at the center of the equine infectious anemia virus genome. *Biochemistry* **38,** 3656–3667.
314. Hsu, T. W., and Taylor, J. M. (1982). Single-stranded regions on unintegrated avian retrovirus DNA. *J. Virol.* **44,** 47–53.
315. Taylor, J. M., Cywinski, A., and Smith, J. K. (1983). Discontinuities in the DNA synthesized by an avian retrovirus. *J. Virol.* **48,** 654–659.
316. Boone, L. R., and Skalka, A. M. (1993). *In* "Reverse Transcriptase" (A. M. Skalka and S. P. Goff, Eds.), pp. 119–133. Cold Spring Harbor Laboratory Press, Cold Spring Harbor, New York.
317. Charneau, P. *et al.* (1994). HIV-1 reverse transcription. A termination step at the center of the genome. *J. Mol. Biol.* **241,** 651–662.
318. Hameau, L. *et al.* (2001). Human immunodeficiency virus type 1 central DNA flap: Dynamic terminal product of plus-strand displacement DNA synthesis catalyzed by reverse transcriptase assisted by nucleocapsid protein. *J. Virol.* **75,** 3301–3313.
319. Fuentes, G. M., Palaniappan, C., Fay, P. J., and Bambara, R. A. (1996). Strand displacement synthesis in the central polypurine tract region of HIV-1 promotes DNA to DNA strand transfer recombination. *J. Biol. Chem.* **271,** 29605–29611.
320. Whiting, S. H., and Champoux, J. J. (1994). Strand displacement synthesis capability of Moloney murine leukemia virus reverse transcriptase. *J. Virol.* **68,** 4747–4758.
321. Whiting, S. H., and Champoux, J. J. (1998). Properties of strand displacement synthesis by Moloney murine leukemia virus reverse transcriptase: Mechanistic implications. *J. Mol. Biol.* **278,** 559–577.
322. Winshell, J., and Champoux, J. J. (2001). Structural alterations in the DNA ahead of the primer terminus during displacement synthesis by reverse transcriptases. *J. Mol. Biol.* **306,** 931–943.
323. Berg, J. M., and Shi, Y. (1996). The galvanization of biology: A growing appreciation for the roles of zinc. *Science* **271,** 1081–1085.

324. Zhang, Y., and Barklis, E. (1995). Nucleocapsid protein effects on the specificity of retrovirus RNA encapsidation. *J. Virol.* **69,** 5716–5722.
325. Méric, C., and Spahr, P. F. (1986). Rous sarcoma virus nucleic acid-binding protein p12 is necessary for viral 70S RNA dimer formation and packaging. *J. Virol.* **60,** 450–459.
326. Méric, C., Gouilloud, E., and Spahr, P. F. (1988). Mutations in Rous sarcoma virus nucleocapsid protein p12 (NC): Deletions of Cys-His boxes. *J. Virol.* **62,** 3328–3333.
327. Méric, C., and Goff, S. P. (1989). Characterization of Moloney murine leukemia virus mutants with single-amino-acid substitutions in the Cys-His box of the nucleocapsid protein. *J. Virol.* **63,** 1558–1568.
328. Gorelick, R. J., Henderson, L. E., Hanser, J. P., and Rein, A. (1988). Point mutants of Moloney murine leukemia virus that fail to package viral RNA: Evidence for specific RNA recognition by a "zinc finger-like" protein sequence. *Proc. Natl. Acad. Sci. USA* **85,** 8420–8424.
329. Dupraz, P., Oertle, S., Méric, C., Damay, P., and Spahr, P. F. (1990). Point mutations in the proximal Cys-His box of Rous sarcoma virus nucleocapsid protein. *J. Virol.* **64,** 4978–4987.
330. Gorelick, R. J. *et al.* (1990). Noninfectious human immunodeficiency virus type 1 mutants deficient in genomic RNA. *J. Virol.* **64,** 3207–3211.
331. Gorelick, R. J. *et al.* (1996). Genetic analysis of the zinc finger in the Moloney murine leukemia virus nucleocapsid domain: Replacement of zinc-coordinating residues with other zinc-coordinating residues yields noninfectious particles containing genomic RNA. *J. Virol.* **70,** 2593–2597.
332. Gorelick, R. J. *et al.* (1999). Strict conservation of the retroviral nucleocapsid protein zinc finger is strongly influenced by its role in viral infection processes: Characterization of HIV-1 particles containing mutant nucleocapsid zinc-coordinating sequences. *Virology* **256,** 92–104.
333. Gorelick, R. J., Chabot, D. J., Rein, A., Henderson, L. E., and Arthur, L. O. (1993). The two zinc fingers in the human immunodeficiency virus type 1 nucleocapsid protein are not functionally equivalent. *J. Virol.* **67,** 4027–4036.
334. Dorfman, T., Luban, J., Goff, S. P., Haseltine, W. A., and Göttlinger, H. G. (1993). Mapping of functionally important residues of a cysteine-histidine box in the human immunodeficiency virus type 1 nucleocapsid protein. *J. Virol.* **67,** 6159–6169.
335. Mizuno, A. *et al.* (1996). Mutational analysis of two zinc finger motifs in HIV type 1 nucleocapsid proteins: Effects on proteolytic processing of Gag precursors and particle formation. *AIDS Res. Hum. Retroviruses* **12,** 793–800.
336. Bowles, N. E., Damay, P., and Spahr, P. F. (1993). Effect of rearrangements and duplications of the Cys-His motifs of Rous sarcoma virus nucleocapsid protein. *J. Virol.* **67,** 623–631.
337. Yovandich, J. L. *et al.* (2001). Alteration of zinc-binding residues of simian immunodeficiency virus $p8^{NC}$ results in subtle differences in gag processing and virion maturation associated with degradative loss of mutant NC. *J. Virol.* **75,** 115–124.
338. Tanchou, V. *et al.* (1998). Role of the N-terminal zinc finger of human immunodeficiency virus type 1 nucleocapsid protein in virus structure and replication. *J. Virol.* **72,** 4442–4447.
339. Buckman, J. S., Bosche, W. J., and Gorelick, R. J. (2003). Human immunodeficiency virus type 1 nucleocapsid Zn^{2+} fingers are required for efficient reverse transcription, initial integration processes, and protection of newly synthesized viral DNA. *J. Virol.* **77,** 1469–1480.
340. Berthoux, L., Pechoux, C., Ottmann, M., Morel, G., and Darlix, J. L. (1997). Mutations in the N-terminal domain of human immunodeficiency virus type 1 nucleocapsid protein affect virion core structure and proviral DNA synthesis. *J. Virol.* **71,** 6973–6981.
341. Yu, Q., and Darlix, J.-L. (1996). The zinc finger of nucleocapsid protein of Friend murine leukemia virus is critical for proviral DNA synthesis *in vivo*. *J. Virol.* **70,** 5791–5798.

342. Gorelick, R. J. *et al.* (1999). Characterization of the block in replication of nucleocapsid protein zinc finger mutants from Moloney murine leukemia virus. *J. Virol.* **73,** 8185–8195.
343. Huang, Y. *et al.* (1998). The role of nucleocapsid and U5 stem/A-rich loop sequences in $tRNA_3^{Lys}$ genomic placement and initiation of reverse transcription in human immunodeficiency virus type 1. *J. Virol.* **72,** 3907–3915.
344. Remy, E. *et al.* (1998). The annealing of $tRNA_3^{Lys}$ to human immunodeficiency virus type 1 primer binding site is critically dependent on the NCp7 zinc fingers structure. *J. Biol. Chem.* **273,** 4819–4822.
345. Lee, N., Gorelick, R. J., and Musier-Forsyth, K. (2003). Zinc finger-dependent HIV-1 nucleocapsid protein-TAR RNA interactions. *Nucleic Acids Res.* **31,** 4847–4855.
346. Ramboarina, S., Druillennec, S., Morellet, N., Bouaziz, S., and Roques, B. P. (2004). Target specificity of human immunodeficiency virus type 1 NCp7 requires an intact conformation of its CCHC N-terminal zinc finger. *J. Virol.* **78,** 6682–6687.
347. Manning, G. S. (1975). On the application of polyelectrolyte limiting laws to the helix-coil transition of DNA. V. Ionic effects on renaturation kinetics. *Biopolymers* **15,** 1333–1343.
348. Frank-Kamenetskii, M. D., Anshelevich, A. A., and Lukashin, A. V. (1987). Polyelectrolyte model of DNA. *Sov. Phys. Uspekhi* **151,** 595–618.
349. Rouzina, I., and Bloomfield, V. A. (1999). Heat capacity effects on the melting of DNA. 1. General aspects. *Biophys. J.* **77,** 3242–3251.
350. Williams, M. C., and Rouzina, I. (2002). Force spectroscopy of single DNA and RNA molecules. *Curr. Opin. Struct. Biol.* **12,** 330–336.
351. Wenner, J. R., Williams, M. C., Rouzina, I., and Bloomfield, V. A. (2002). Salt dependence of the elasticity and overstretching transition of single DNA molecules. *Biophys. J.* **82,** 3160–3169.
352. Williams, M. C., Rouzina, I., and Bloomfield, V. A. (2002). Thermodynamics of DNA interactions from single molecule stretching experiments. *Acc. Chem. Res.* **35,** 159–166.
353. Williams, M. C., Wenner, J. R., Rouzina, I., and Bloomfield, V. A. (2001). Entropy and heat capacity of DNA melting from temperature dependence of single molecule stretching. *Biophys. J.* **80,** 1932–1939.
354. Williams, M. C., Wenner, J. R., Rouzina, I., and Bloomfield, V. A. (2001). Effect of pH on the overstretching transition of double-stranded DNA: Evidence of force-induced DNA melting. *Biophys. J.* **80,** 874–881.
355. Smith, S. B., Cui, Y., and Bustamante, C. (1996). Overstretching B-DNA: The elastic response of individual double-stranded and single-stranded DNA molecules. *Science* **271,** 795–799.
356. Rouzina, I., and Bloomfield, V. A. (2001). Force-induced melting of the DNA double helix. 2. Effect of solution conditions. *Biophys. J.* **80,** 894–900.
357. Rouzina, I., and Bloomfield, V. A. (2001). Force-induced melting of the DNA double helix 1. Thermodynamic analysis. *Biophys. J.* **80,** 882–893.
358. Azoulay, J., Clamme, J. P., Darlix, J. L., Roques, B. P., and Mély, Y. (2003). Destabilization of the HIV-1 complementary sequence of TAR by the nucleocapsid protein through activation of conformational fluctuations. *J. Mol. Biol.* **326,** 691–700.
359. Beltz, H. *et al.* (2004). Role of the structure of the top half of HIV-1 cTAR DNA on the nucleic acid destabilizing activity of the nucleocapsid protein NCp7. *J. Mol. Biol.* **338,** 711–723.
360. Cosa, G. *et al.* (2004). Secondary structure and secondary structure dynamics of DNA hairpins complexed with HIV-1 NC protein. *Biophys. J.* **87,** 2759–2767.
361. Kim, H. D. *et al.* (2002). Mg^{2+}-dependent conformational change of RNA studied by fluorescence correlation and FRET on immobilized single molecules. *Proc. Natl. Acad. Sci. USA* **99,** 4284–4289.

362. Alberts, B. M., and Frey, L. (1970). T4 bacteriophage gene 32: A structural protein in the replication and recombination of DNA. *Nature* **227,** 1313–1318.
363. Christiansen, C., and Baldwin, R. L. (1977). Catalysis of DNA reassociation by the *Escherichia coli* DNA binding protein: A polyamine-dependent reaction. *J. Mol. Biol.* **115,** 441–454.
364. Herschlag, D., Khosla, M., Tsuchihashi, Z., and Karpel, R. L. (1994). An RNA chaperone activity of non-specific RNA binding proteins in hammerhead ribozyme catalysis. *EMBO J.* **13,** 2913–2924.
365. Pant, K., Karpel, R. L., Rouzina, I., and Williams, M. C. (2004). Mechanical measurement of single-molecule binding rates: Kinetics of DNA helix-destabilization by T4 gene 32 protein. *J. Mol. Biol.* **336,** 851–870.
366. Wetmur, J. G., and Davidson, N. (1968). Kinetics of renaturation of DNA. *J. Mol. Biol.* **31,** 349–370.
367. Wetmur, J. G. (1976). Hybridization and renaturation kinetics of nucleic acids. *Annu. Rev. Biophys. Bioeng.* **5,** 337–361.
368. Wetmur, J. G. (1991). DNA probes: Applications of the principles of nucleic acid hybridization. *CRC Crit. Rev. Biochem. Mol. Biol.* **26,** 227–259.
369. Reynaldo, L. P., Vologodskii, A. V., Neri, B. P., and Lyamichev, V. I. (2000). The kinetics of oligonucleotide replacements. *J. Mol. Biol.* **297,** 511–520.
370. Pontius, B. W., and Berg, P. (1990). Renaturation of complementary DNA strands mediated by purified mammalian heterogeneous nuclear ribonucleoprotein A1 protein: Implications for a mechanism for rapid molecular assembly. *Proc. Natl. Acad. Sci. USA* **87,** 8403–8407.
371. Pontius, B. W., and Berg, P. (1991). Rapid renaturation of complementary DNA strands mediated by cationic detergents: A role for high-probability binding domains in enhancing the kinetics of molecular assembly processes. *Proc. Natl. Acad. Sci. USA* **88,** 8237–8241.
372. Pontius, B. W., and Berg, P. (1992). Rapid assembly and disassembly of complementary DNA strands through an equilibrium intermediate state mediated by A1 hnRNP protein. *J. Biol. Chem.* **267,** 13815–13818.
373. Kumar, A., and Wilson, S. H. (1990). Studies of the strand-annealing activity of mammalian hnRNP complex protein A1. *Biochemistry* **29,** 10717–10722.
374. Homann, M., Nedbal, W., and Sczakiel, G. (1996). Dissociation of long-chain duplex RNA can occur via strand displacement *in vitro*: Biological implications. *Nucleic Acids Res.* **24,** 4395–4400.
375. Nedbal, W., Frey, M., Willemann, B., Zentgraf, H., and Sczakiel, G. (1997). Mechanistic insights into p53-promoted RNA–RNA annealing. *J. Mol. Biol.* **266,** 677–687.
376. Nedbal, W., Homann, M., and Sczakiel, G. (1997). The association of complementary ribonucleic acids can be strongly increased without lowering Arrhenius activation energies or significantly altering structures. *Biochemistry* **36,** 13552–13557.
377. Windbichler, N., Werner, M., and Schroeder, R. (2003). Kissing complex-mediated dimerization of HIV-1 RNA: Coupling extended duplex formation to ribozyme cleavage. *Nucleic Acids Res.* **31,** 6419–6427.
378. Lai, E., and van Zanten, J. H. (2001). Monitoring DNA/poly-L-lysine polyplex formation with time-resolved multiangle laser light scattering. *Biophys. J.* **80,** 864–873.
379. Nguyen, T. T., and Shklovskii, B. I. (2002). Kinetics of macroion coagulation induced by multivalent counterions. *Phys. Rev. E. Stat. Nonlin. Soft Matter Phys.* **65,** 1–7.
380. Craig, M. E., Crothers, D. M., and Doty, P. (1971). Relaxation kinetics of dimer formation by self complementary oligonucleotides. *J. Mol. Biol.* **62,** 383–401.
381. Kozyavkin, S. A., Mirkin, S. M., and Amirikyan, B. R. (1987). The ionic strength dependence of the cooperativity factor for DNA melting. *J. Biomolec. Struct. Dynam.* **5,** 119–126.

382. Kallenbach, N. R., Crothers, D. M., and Mortimer, R. G. (1963). Interpretation of the kinetics of helix formation. *Biochem. Biophys. Res. Commun.* **11,** 213–216.
383. Sikorav, J. L., and Church, G. M. (1991). Complementary recognition in condensed DNA: Accelerated DNA renaturation. *J. Mol. Biol.* **222,** 1085–1108.
384. Gabus, C. *et al*. (2001). The prion protein has DNA strand transfer properties similar to retroviral nucleocapsid protein. *J. Mol. Biol.* **307,** 1011–1021.
385. Gabus, C. *et al*. (2001). The prion protein has RNA binding and chaperoning properties characteristic of nucleocapsid protein NCp7 of HIV-1. *J. Biol. Chem.* **276,** 19301–19309.
386. Matulis, D., Rouzina, I., and Bloomfield, V. A. (2002). Thermodynamics of cationic lipid binding to DNA and DNA condensation: Roles of electrostatics and hydrophobicity. *J. Am. Chem. Soc.* **124,** 7331–7342.
387. Pontius, B. W. (1993). Close encounters: Why unstructured, polymeric domains can increase rates of specific macromolecular association. *Trends Biochem. Sci.* **18,** 181–186.
388. Rouzina, I., and Bloomfield, V. A. (1996). Macroion attraction due to electrostatic correlation between screening counterions. 1. Mobile surface-adsorbed ions and diffuse ion cloud. *J. Phys. Chem.* **100,** 9977–9989.
389. Nguyen, T. T., Rouzina, I., and Shklovskii, B. I. (2000). Reentrant condensation of DNA induced by multivalent counterions. *J. Chem. Phys.* **112,** 2562–2568.
390. Heilman-Miller, S. L., Thirumalai, D., and Woodson, S. A. (2001). Role of counterion condensation in folding of the Tetrahymena ribozyme. I. Equilibrium stabilization by cations. *J. Mol. Biol.* **306,** 1157–1166.
391. Heilman-Miller, S. L., Pan, J., Thirumalai, D., and Woodson, S. A. (2001). Role of counterion condensation in folding of the Tetrahymena ribozyme. II. Counterion-dependence of folding kinetics. *J. Mol. Biol.* **309,** 57–68.
392. Koculi, E., Lee, N. K., Thirumalai, D., and Woodson, S. A. (2004). Folding of the Tetrahymena ribozyme by polyamines: Importance of counterion valence and size. *J. Mol. Biol.* **341,** 27–36.
393. Jeeninga, R. E., Huthoff, H. T., Gultyaev, A. P., and Berkhout, B. (1998). The mechanism of actinomycin D-mediated inhibition of HIV-1 reverse transcription. *Nucleic Acids Res.* **26,** 5472–5479.
394. Imamichi, T. *et al*. (2003). Actinomycin D induces high-level resistance to thymidine analogs in replication of human immunodeficiency virus type 1 by interfering with host cell thymidine kinase expression. *J. Virol.* **77,** 1011–1020.
395. Rice, W. G. *et al*. (1995). Inhibitors of HIV nucleocapsid protein zinc fingers as candidates for the treatment of AIDS. *Science* **270,** 1194–1197.
396. Gabbara, S., Davis, W. R., Hupe, L., Hupe, D., and Peliska, J. A. (1999). Inhibitors of DNA strand transfer reactions catalyzed by HIV-1 reverse transcriptase. *Biochemistry* **38,** 13070–13076.
397. Davis, W. R. *et al*. (2000). Inhibition of HIV-1 reverse transcriptase-catalyzed DNA strand transfer reactions by 4-chlorophenylhydrazone of mesoxalic acid. *Biochemistry* **39,** 14279–14291.
398. Lifson, J. D. *et al*. (2004). Evaluation of the safety, immunogenicity, and protective efficacy of whole inactivated simian immunodeficiency virus (SIV) vaccines with conformationally and functionally intact envelope glycoproteins. *AIDS Res. Hum. Retroviruses* **20,** 772–787.